



HELSINKI UNIVERSITY OF TECHNOLOGY
Department of Electrical and Communications Engineering

Jaakko Kauramäki

Effect of attention on neural tuning

In partial fulfillment of the requirements for the degree of Master
of Science, Espoo 25th February 2005.

Supervisor: Academy Professor Mikko Sams

Instructor: Professor Iiro Jääskeläinen

| | | |
|--|--|----------------------|
| Tekijä: | Jaakko Kauramäki | |
| Otsikko: | Tarkkaavaisuuden vaikutus hermosolujen ärsykepiirreviritykseen | |
| Päivämäärä: | 25. helmikuuta 2005 | Sivumäärä: 91 |
| Osasto: | Sähkö- ja tietoliikennetekniikan osasto | |
| Professori: | S-114, Kognitiivinen teknologia | |
| Työn valvoja: | Akatemiaprofessori Mikko Sams | |
| Työn ohjaaja: | Professor Iiro Jääskeläinen | |
| Tiivistelmäteksti: | | |
| <p>Tarkkaavaisuuden avulla valikoimme kulloisellakin hetkellä tärkeimmät ärsykkeet. Tässä kokeessa tutkittiin tarkkaavaisuuden vaikutuksia ihmisen kuuloaivokuorella käyttäen sekä elektroenkefalografiaa (EEG) että magnetoenkefalografiaa (MEG) tutkimusmenetelminä. Tutkimusoletuksenamme oli, että tarkkaavaisuus terävöittää hermosolujen reaktioiden viritystä ärsykkeen tarkkailtavien piirteiden osalta.</p> <p>Työn yhteydessä tehtiin psykofyysinen koe käyttäen ääniärsykeitä ja mitaten samalla joko EEG:tä tai MEG:tä. Kokeessa esitettiin 1000 Hz siniääniä jatkuvan kohinapeiton kanssa. Kohina luotiin kaistanestosuodattamalla valkoista kohinaa vaihtelevilla suotimen leveyksillä ($\pm 500 \dots 0$) 1000 Hz ympäriltä. Suodatettu kaista pidettiin vakiona kunkin herätepotentiaalilin ja herätekentän nauhoituksen ajan. Kokeessa oli kolme tilannetta: kaksi tarkkaavaisuutta vaativaa tehtävää, jossa koehenkilön piti kiinnittää huomiota joko äänen korkeuseroon tai äänen keston eroon, sekä yksi passiivinen tilanne, jossa koehenkilö katsoi hiljaista animaatiofilmiä siten, että kokeessa käytetyt äänet kuuluivat taustalla.</p> <p>Kokeen tulokset osoittivat, että tarkkaavaisuus muuttaa hermosolujen vasteiden suuruutta. Ääniärsykkeen herätepotentiaalilin komponentit (P50, N100 ja P200) muuttuivat siten, että erityisesti N100:n amplitudi oli suurempi tarkkaavaisuutta vaativissa tilanteissa kuin passiivisessa tilanteessa. Tämä tapahtui kuitenkin vain muutamilla kapeimmilla kaistanestosuotimen leveyksillä. Tämä viittaisi siihen, että vaikutus ei ole ainoastaan hermosolujen aktiivatiota ja herätepotentiaalilin komponenttien amplitudeja kautta linjan lisäävä, vaan että tarkkaavaisuustilanteessa N100-komponentin synnyttäneet hermosolut ovat myös tarkemmin virittyneet tarkkaillun äänen taajuudelle.</p> <p>Tuloksia voi hyödyntää esimerkiksi tarkkaavaisuushäiriöiden, kuten Alzheimerin taudin, skitsofrenian tai ADHD-oireyhtymän kliinisissä tutkimuksissa tai taudinmäärityksessä. Suuntaa-antavia tuloksia tarkkaavaisuushäiriön suuruudesta voidaan saada siten, että käytetään sopivia ääniärsykeitä, ja ärsykeisiin liittyviä hermosolujen vasteita verrataan terveiltä ihmisiltä saatuihin vasteisiin.</p> | | |
| Avainsanat: | elektroenkefalografia, magnetoenkefalografia, herätepotentiaali, äänen havaitseminen, hermosolujen ärsykepiirreviritys | |

| | | |
|-----------------------|--|----------------------------|
| Author: | Jaakko Kauramäki | |
| Title: | Effect of attention on neural tuning | |
| Date: | 25th February 2005 | Number of pages: 91 |
| Department: | Department of Electrical and Communications Engineering | |
| Professorship: | S-114, Cognitive Technology | |
| Supervisor: | Academy Professor Mikko Sams | |
| Instructor: | Professor Iiro Jääskeläinen | |
| Abstract: | <p>Attention refers to our amazing ability to focus on the relevant bits of information amongst the vast inflow of sensory information. Here, we studied the effect of attention in the human auditory cortex using both electroencephalography (EEG) and magnetoencephalography (MEG). We specifically hypothesized that attention sharpens the tuning of neural responses, as opposed to a simple increase in gain.</p> <p>A psychophysical experiment using auditory stimuli was conducted, measuring simultaneously either EEG or MEG. In the experiment, sine tones of 1000 Hz were presented with a continuous noise masker. The masker was generated by bandstop filtering white noise with a varying notch width ($\pm 500 \dots 0$) around 1000 Hz. The notch width was kept constant during the acquisition of each event-related potential and event-related field. The experiment included three different conditions: two attended conditions where subject was instructed to pay attention either to frequency or duration difference, and one passive condition where the subject watched a silent movie, with the auditory stimuli in the background.</p> <p>The results suggest that attention modulates the amplitudes of the neural responses. Amplitudes of the auditory evoked potential components (P50, N100 and P200) were modulated so that especially the N100 amplitude was significantly higher in the attended conditions than in the passive condition. However, this happened only when the notch widths were relatively small, suggesting that the effect was not only gain-based, causing an overall stronger neural activation, but also involved sharpening of sound frequency tuning of the auditory cortex neurons.</p> <p>This information can be adapted to clinical attention deficiency studies or diagnoses, where e.g. Alzheimer's disease, schizophrenia or ADHD-syndrome patients are involved. By using a suitable set of auditory stimuli and comparing the neural responses linked to stimulus to ones from healthy people, an indicative measure of the gravity of attention deficiency could be obtained.</p> | |
| Keywords: | electroencephalography, magnetoencephalography, attention, event-related potentials, auditory perception, neural tuning | |

Foreword

This work was done in the Laboratory of Computational Engineering (LCE) in the Helsinki University of Technology (TKK). The supervisor of this work was Academy Professor Mikko Sams and the instructor was Professor Iiro Jääskeläinen.

I would like to thank both my instructor Prof. Iiro Jääskeläinen and my supervisor Academy Prof. Mikko Sams for the opportunity to work in the LCE and for the expertise and encouragement they have given me throughout this period. Especially the valuable comments and directions from my instructor have given much to the final form of this work. Additional thanks go to Dr. Vasily Klucharev, Dr. Riikka Möttönen and all the other colleagues in the laboratory that have helped and assisted me with the practical things.

Finally, I would like to thank my parents and my family members for the support they have given me throughout my studies. I would like to thank my fiancée Jaana for her love and patience especially during the last months of the thesis writing. Special thanks to our new furry "member of the family" who in her own way made me forget the stress of graduating when needed. Thanks go out also to all my friends, you know who you are.

In Espoo, 5th January 2006

Jaakko Kauramäki

Contents

| | | |
|----------|--|----------|
| 1 | Introduction | 1 |
| 2 | Background | 3 |
| 2.1 | The human auditory system | 3 |
| 2.1.1 | Range of hearing | 3 |
| 2.1.2 | Structure of ear | 4 |
| 2.1.3 | Auditory masking | 11 |
| 2.1.4 | Auditory pathway | 12 |
| 2.1.5 | Auditory cortex | 13 |
| 2.1.6 | Feedback mechanisms | 14 |
| 2.1.7 | Frequency discrimination | 16 |
| 2.1.8 | Duration discrimination | 17 |
| 2.2 | Electric signals of the brain | 17 |
| 2.2.1 | Field potentials and neural sources of EEG and MEG signals . . . | 20 |
| 2.2.2 | Event-related potentials | 22 |
| 2.2.3 | The forward and the inverse problem | 24 |
| 2.3 | Electroencephalography (EEG) | 26 |
| 2.3.1 | Equipment | 26 |
| 2.3.2 | Problems | 28 |
| 2.4 | Magnetoencephalography (MEG) | 28 |
| 2.4.1 | Measuring magnetic fields | 29 |
| 2.4.2 | Equipment | 30 |
| 2.4.3 | Problems | 31 |
| 2.5 | How attention works at the neural level | 32 |

| | | |
|----------|---|-----------|
| 2.5.1 | Neural changes in vision and other modalities induced by attention | 33 |
| 2.5.2 | Attentional effects in the auditory system | 34 |
| 2.5.3 | Attentional dysfunctions | 36 |
| 2.5.4 | Specific hypothesis for the present study | 38 |
| 3 | Methods | 39 |
| 3.1 | Experimental subjects | 39 |
| 3.2 | Instrumentation | 40 |
| 3.2.1 | EEG equipment | 40 |
| 3.2.2 | MEG equipment | 42 |
| 3.3 | Test setup | 42 |
| 3.3.1 | Stimuli details | 43 |
| 3.3.2 | Description of the test run | 45 |
| 3.4 | EEG and MEG data analysis | 48 |
| 3.4.1 | Data quantification and statistical analysis | 49 |
| 3.4.2 | MEG data analysis | 49 |
| 3.5 | Simulating the effects of attention | 50 |
| 4 | Results | 54 |
| 4.1 | Pilot study results | 54 |
| 4.2 | Results of the EEG study | 56 |
| 4.2.1 | ERP calculation | 56 |
| 4.2.2 | EEG contour maps | 60 |
| 4.3 | Results of the MEG study | 60 |
| 4.4 | Behavioral task | 62 |
| 4.4.1 | Hit rate vs. N100 peak amplitude | 64 |
| 4.4.2 | Reaction time vs. N100 latency | 65 |
| 4.5 | Simulation results | 66 |
| 4.5.1 | Simulation results vs. the actual data | 67 |
| 5 | Discussion | 70 |
| 5.1 | Neural response amplitude suppression by the masker stimuli | 70 |
| 5.2 | Attentional modulation of the neural responses | 71 |

| | | |
|----------|--|-----------|
| 5.3 | Behavioral task results and other notes | 73 |
| 5.4 | Final notes and ideas for further experiments | 75 |
| | Bibliography | 78 |
| A | Presentation scripts used in study | 85 |
| A.1 | Example main presentation script for one stimulus type (d_1.sce) | 85 |
| A.2 | Supplementary file for main script (noise_stim.sce) | 86 |
| A.3 | Supplementary file for main script (read_volume.pcl) | 87 |
| A.4 | Volume adjust part, main script (adjust_volume.sce) | 88 |
| A.5 | Supplementary file for volume adjust script (adjust_volume.pcl) | 89 |

List of Figures

| | | |
|------|---|----|
| 2.1 | The audibility curve and equal loudness curves | 4 |
| 2.2 | The structure of ear | 5 |
| 2.3 | Cochlea | 7 |
| 2.4 | Cross section of cochlea | 7 |
| 2.5 | Organ of Corti | 8 |
| 2.6 | Frequency tuning curves of the cat auditory nerve fibers | 10 |
| 2.7 | Diagram of functional areas of the brain and Brodmann areas | 12 |
| 2.8 | Auditory pathway | 13 |
| 2.9 | Organization of the auditory cortex | 14 |
| 2.10 | Inner ear block diagram | 15 |
| 2.11 | Diagram of a nerve cell | 18 |
| 2.12 | Potential generation on the scalp by current summation | 21 |
| 2.13 | ERP signal quality as the number of averages increases | 23 |
| 2.14 | Basic principles of differential amplifier | 27 |
| 2.15 | Idealized magnetic and electrical field patterns generated by tangential dipole | 30 |
| 2.16 | An axial and a planar gradiometer | 31 |
| 2.17 | Examples of effect of attention on tuning curves. | 35 |
| 3.1 | The international 10-20 system | 41 |
| 3.2 | Diagram of the stimuli used in the experiment | 44 |

| | | |
|------|---|----|
| 3.3 | An example of experiment presentation order | 44 |
| 3.4 | An example of volume adjust part in the beginning of trial | 46 |
| 3.5 | Tuning curves approximated by rounded-exponential filter shape | 51 |
| 3.6 | Modeling the probability of neuron firing when CF is 1000 Hz | 52 |
| 3.7 | Envelope functions used for modeling stimuli set #1 | 52 |
| 3.8 | Examples of simulated activation of neurons | 53 |
| 4.1 | Grand average ERPs from electrode Cz in pilot subjects | 55 |
| 4.2 | Grand average ERPs from electrode Cz in pilot subjects (alternate view) | 55 |
| 4.3 | Behavioral task data from the pilot subjects | 56 |
| 4.4 | Grand average ERPs from electrode Cz | 57 |
| 4.5 | Averaged ERP peak values from electrode Cz | 57 |
| 4.6 | Latency of the N100 and P200 peaks | 58 |
| 4.7 | EEG contour maps of different conditions at N100 peak latency of electrode Cz | 61 |
| 4.8 | Average MEG dipole moments | 62 |
| 4.9 | MEG dipole moments of individual subjects | 62 |
| 4.10 | Behavioral task results (hit rate) from the EEG study | 63 |
| 4.11 | Reaction times from the EEG study | 63 |
| 4.12 | N100 peak amplitude from electrode Cz vs. behavioral task hit rate | 64 |
| 4.13 | Scatterplot of hit rate and N100 peak amplitude | 65 |
| 4.14 | Scatterplot of N100 latency and the reaction time | 65 |
| 4.15 | Modeling the effect of tuning curve sharpness change | 66 |
| 4.16 | Modeling the effect of gain change | 67 |
| 4.17 | Best fit results of the actual data vs. simulation | 68 |

List of Tables

| | | |
|-----|--|----|
| 3.1 | Types of tones used | 43 |
| 3.2 | Used noise maskers | 45 |
| 3.3 | Up-down rule table used | 46 |
| 4.1 | F values for different stimulus types, unattended (UD) vs. attended conditions (DD and FD) | 59 |
| 4.2 | Results of fitting the simulation results to the real data | 69 |

Abbreviations and notations

| | |
|----------------|---|
| \overline{B} | magnetic field density |
| \overline{E} | electric field density |
| f | frequency |
| I | electric current |
| \overline{J} | current density |
| p | probability or parameter of <i>Roex(p)</i> filter |
| t | time |
| V | voltage |
| ϵ_0 | electric permittivity of free space |
| λ | length constant of the membrane |
| μ_0 | magnetic permeability |
| ρ | free electric charge density |
| A1 | auditory cortical area |
| AC | auditory cortex |
| AEP | auditory evoked potential |
| AN | auditory nerve |
| ANOVA | analysis of variance |
| AP | action potential |
| BF | best frequency (a.k.a. CF) |
| BM | basilar membrane |

| | |
|--------|---|
| CF | characteristic frequency (a.k.a. BF) |
| CMRR | common mode rejection ratio |
| dB | decibel |
| DC | direct current |
| DD | duration discrimination task in this experiment |
| EEG | electroencephalography |
| ERP | event-related potential |
| FD | frequency discrimination task in this experiment |
| fMRI | functional magnetic resonance imaging |
| Hz | Hertz, 1/s |
| IHC | inner hair cell |
| ISI | interstimuli interval |
| JND | just noticeable difference |
| MANOVA | multivariate analysis of variance |
| MEG | magnetoencephalography |
| MGB | medial geniculate body |
| MMN | mismatch negativity |
| N100 | negative peak in the ERP approximately 100 ms from the stimulus onset |
| OHC | outer hair cell |
| P300 | positive peak in the ERP approximately 300 ms from the stimulus onset |
| P50 | positive peak in the ERP approximately 50 ms from the stimulus onset |
| PAC | primary auditory cortex |
| SEM | standard error of the mean |
| SNR | signal-to-noise ratio |
| SPL | sound pressure level |
| SQUID | superconducting quantum interference device |
| UD | unattended (passive) task in this experiment |
| V1, V4 | visual cortical areas |
| VEP | visual evoked potential |

Chapter 1

Introduction

Attention is invaluable in our everyday life. What is attention then? How does it work? A closer inspection reveals that our common definition is quite vague. Most of us have first-hand experience on how attention, or especially the lack of it, can change our perception of the outside world. Famous 19th century psychologist William James defined attention in "*The Principles of Psychology*" (1890) as follows:

"Everyone knows what attention is. It is the taking possession by the mind, in clear and vivid form, of one out of what seem several simultaneously possible objects or trains of thought. [...] It implies withdrawal from some things in order to deal effectively with others, and is a condition which has a real opposite in the confused, dazed, scatterbrained state."

Attention, then, makes it possible to select only the relevant part of all the sensory information we receive. As an example, auditory selective attention refers to our ability to select relevant information from the surrounding acoustic events. "Cocktail party effect" describes the ability to focus our attention only on one specific speaker, understand his or her speech, while we efficiently filter out the surrounding background noise and the other speakers.

Attention is a pre-requisite for survival. For example, driving a car is a complicated process, where much visual information has to be filtered out so that we can act coherently in traffic. Attention can also reshape our perceptual system as needed, for the effects of attention can be noted at many different levels of our perceptual system, based on our actions. Further, attentional dysfunctions can be found in a number of clinical conditions, including Alzheimer's disease, schizophrenia and attention-deficit hyperactivity disorder (ADHD). These dysfunctions, in addition to attention-induced changes in healthy people, can be seen even with non-invasive brain imaging methods, such as EEG and MEG.

In this thesis, the neural mechanisms underlying selective attention in the auditory system were studied. We specifically asked whether the selective attention can be explained by changes in neural gain, i.e. do we perceive the attended sounds better because the neural responses are stronger and augmented, or can the effects of attention be explained by a special modulation of the neural populations towards the attended sound frequency.

Chapter 2

Background

2.1 The human auditory system

The human auditory system converts sound in a physical form to neural signals. Hearing has a very important function in survival, as it functions as a signaling system for events that we can't see. For a review of human auditory system and its functions, see e.g. Goldstein (2002) or Karjalainen (1999).

2.1.1 Range of hearing

Threshold of hearing is about 0 dB SPL, where the sound pressure level (SPL) refers to pressure of the sound which is often represented as decibels (dB). The dynamic range of the human hearing is about 120 dB. Loudness is a term very closely related to SPL, it only takes into account the compressive nature and the frequency dependency of the human hearing system. Just noticeable difference (JND) in SPL is about 1 dB. Also sound duration influences the perceived loudness for sounds lasting under about 200 ms. This effect is stronger with even shorter sounds, loudness being perceived higher the shorter the duration of the sound is (see e.g. Buus et al., 1997).

The human hearing range extends in the frequency domain from about 20 Hz to 20 kHz. This range diminishes with age. However, the human ear does not perceive different frequencies with the same sound pressure level (SPL) with equal loudness. As can be seen in Figure 2.1, the ear is most sensitive to the middle frequencies of 2–4 kHz. Importantly, this range of frequencies is most essential for understanding speech.

The audibility curve, as seen in Figure 2.1, shows the threshold of hearing for different frequencies. Auditory response area refers to the area over the audibility curve. Tones played with intensities that fall below the curve are not audible. For example, 40 dB SPL tone at 30 Hz is not audible, but at 1 kHz we can hear it well (Goldstein, 2002).

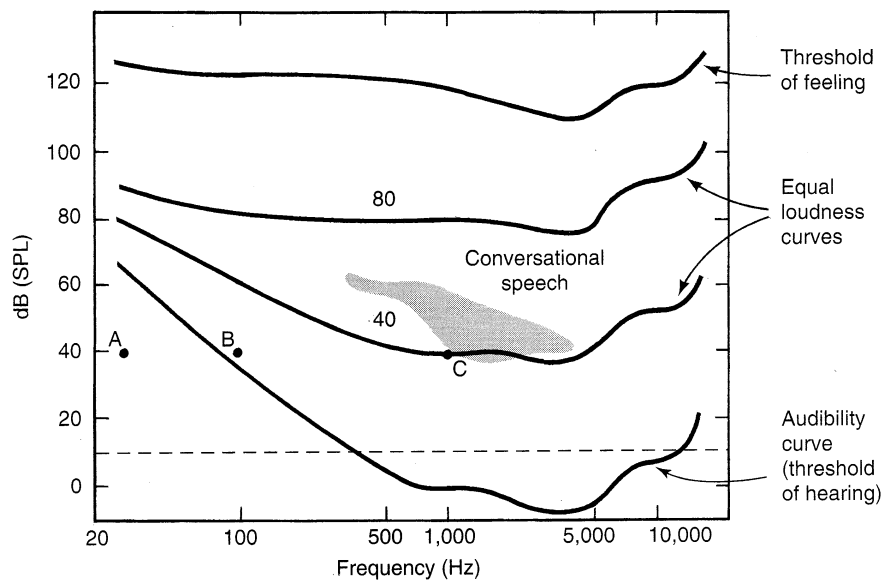


Figure 2.1: The audibility curve and equal loudness curves (adapted from Goldstein, 2002).

2.1.2 Structure of ear

Sound enters the ear through the outer ear (Figure 2.2). The middle ear transduces the sound to a suitable range of pressure changes. The sound is finally converted to neural signals inside the inner ear, in the cochlea. The following section describes the structure of the ear in little more detail. Especially the inner ear structure and functionality is emphasized, as it is most important concerning this study.

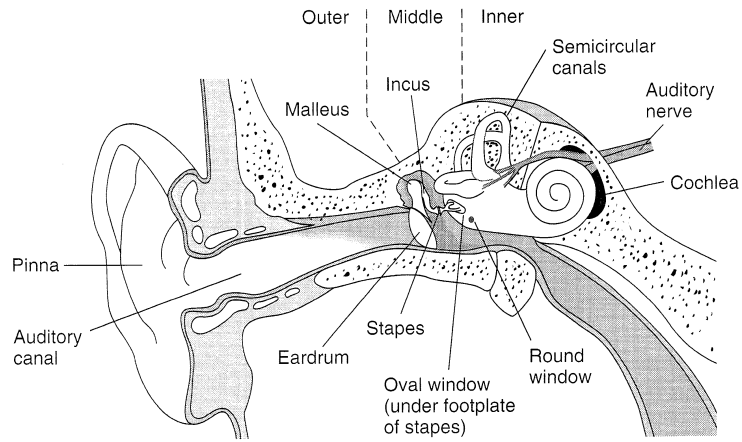


Figure 2.2: The structure of ear (adapted from Goldstein, 2002)

The Outer Ear

The part of ear that sticks out of the head is called *pinnae*. Due to its structure, it helps us determine the location of the sound, but the most important parts of the ear are found inside the head.

Sound passes through the outer ear, which consists of the *pinna* and the *auditory canal*. The auditory canal is a short, tube-like structure that basically protects the middle ear from the outside world. It is about 3 cm in length and is covered with wax. In the end of the auditory canal there is a *tympanic membrane*, or *eardrum*. Tympanic membrane vibrates when the sound wave enters the auditory canal.

Besides the protection of inner structures, the outer ear also enhances intensities of some sounds by means of resonance. Resonance occurs when sound waves reflect back from closed end of the auditory canal, and interact with sounds entering the auditory canal. Resonance is highest at the *resonant frequency* of the canal, which is determined by the length of the canal. Measurements inside the ear indicate that resonance has a slight amplifying effect on frequencies between about 2 kHz and 5 kHz (compare to Figure 2.1). This range is most important in perceiving and recognizing auditory speech stimuli.

The middle ear

The *middle ear* is a small cavity of about 2 cm² in volume. It consists of the *ossicles*, three smallest bones of the human body. Ossicles are called the *malleus*, the *incus* and the *stapes* (Figure 2.2).

Malleus is attached to tympanic membrane that sets it into vibration when sound enters the auditory canal. Malleus passes the vibrations to the second bone, incus, which in turn passes them to the last bone, stapes. The stapes finally delivers the vibrations to the *oval window* by pushing against the membrane covering the window.

Most important function of the middle ear is to work as a transducer. It amplifies the vibrations in the air to be suitable to move the dense cochlear fluid behind the oval window. Vibrations would otherwise pass very poorly from air to the liquid. Amplifying is accomplished in two ways: (1) concentrating the vibration of the large tympanic membrane to much smaller stapes, and (2) ossicles being hinged to create a lever.

Middle ear also contains small muscles, the *middle-ear muscles*. These muscles are attached to the ossicles, and function as a protection to the inner ear at high sound intensities. At high intensities these muscles contract to dampen the ossicles vibration. Otherwise, a powerful vibration would pass to the inner ear, possibly causing pain and damage. This automatic contraction is called the *stapedius reflex*. Dampening occurs mainly on the lower frequencies (0–2 kHz). Middle-ear muscles take some time to function (from tens to few hundred milliseconds), so they do not provide protection against a sudden high-intensity sound (Karjalainen, 1999).

From the middle ear there is also a connection to the nose, called the *eustachian tube*. Most important function of this is to balance the air pressure inside the ear to the pressure of the surrounding environment, so that the tympanic membrane can vibrate freely.

The Inner Ear

Main structure of the *inner ear* is the *cochlea* (Figure 2.2 and 2.3). It is filled with a liquid called the cochlear fluid. Cochlea can be realized by thinking about a narrow tube which is tightly coiled as a spiral-like structure.

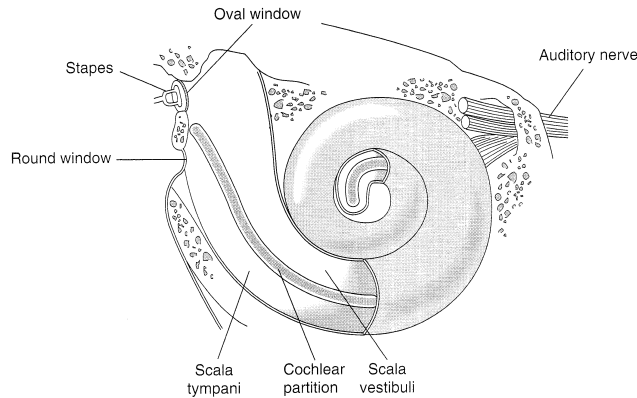


Figure 2.3: Cochlea (adapted from Goldstein, 2002).

Upper half of the cochlea is called the scala vestibuli and the lower part is called the scala tympani. These parts are separated by a cochlear partition, which contains the basilar membrane and the organ of Corti. Cochlear cross section (Figure 2.4) shows also the tectorial membrane and the organ of Corti.

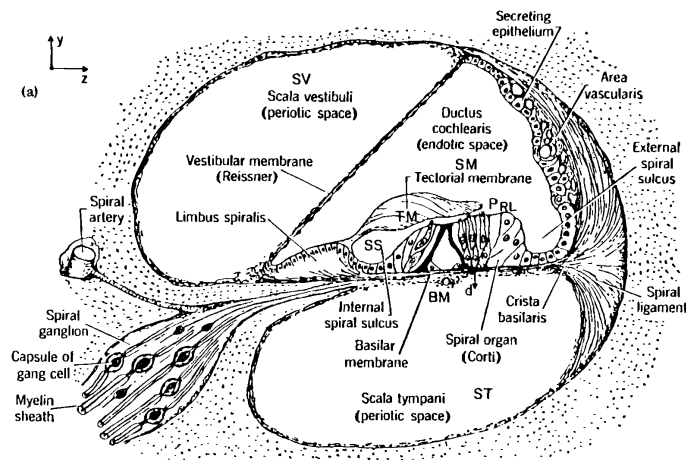


Figure 2.4: Cross section of cochlea (adapted from Allen, 2001).

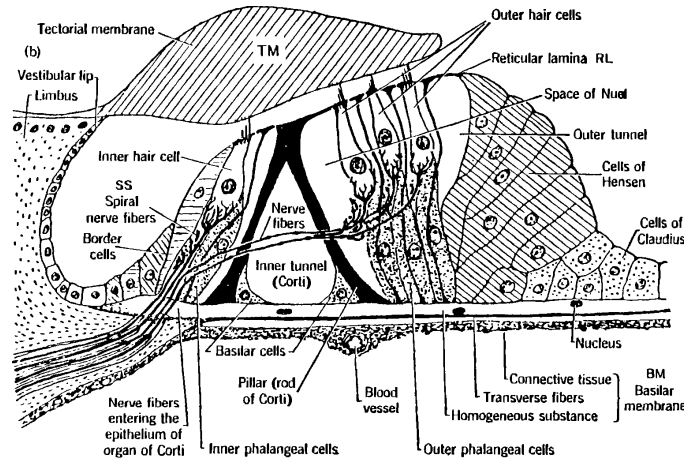


Figure 2.5: Organ of Corti (adapted from Allen, 2001).

Organ of Corti lies on top of the basilar membrane and below the tectorial membrane (Figure 2.5). It contains the auditory receptors called the *hair cells*. There are, in total, about 20 000–30 000 hair cells, which are scattered approximately evenly on the basilar membrane. They are divided into two groups, the inner and the outer hair cells, depending on their location in the organ of Corti. Also the structure of the inner and outer hair cells differ. Hair cells have very fine *cilia*, or hairs, which respond to vibration. Vibration of the cilia causes an electrical signal, which releases a chemical transmitter that finally generates a response in nerve fibers. In other words, hair cells work as mechanotransducers, converting mechanical energy into neural signals.

Sound travels through the middle ear and causes movement of the cochlear fluid. Fluid movement causes the basilar membrane to vibrate. This in turn causes up-and-down movement of the organ of Corti and also back-and-forth movement of the tectorial membrane relative to the hair cells. Both movements contribute to the very fine bending of the cilia in the hair cells. At the threshold of hearing, cilia movements can be as small as 100 picometers ($100 \times 10^{-15} \text{ m}$).

The basilar membrane is *tonotopically* organized, meaning that nearby frequencies cause activation to nearby hair cells. Each frequency has its unique place in the structure. High frequencies are coded by the hair cells located in the beginning of the membrane (base), and low frequencies are coded in the end of membrane (apex), near the round window.

The basilar membrane is three or four times narrower in the beginning than in the end. This gives a physical basis for the place coding. The traveling wave on the basilar membrane has a certain frequency. It starts from the base, near the oval window, and peaks at some point in the membrane. This is the place where the basilar membrane has the maximal displacement due to the vibration, and also the place where most hair cells are activated. Other hair cells in different loci can also be activated due to the membrane vibration, but their activation is smaller. Place theory of hearing was originally proposed by Georg von Békésy in 1928 (see Goldstein, 2002). This so-called tonotopic organization (also sometimes referred as *cochleotopy*) is maintained throughout the auditory pathway (Ashmore and Gale, 2000). Similar organization is found in the visual and somatosensory pathways, where it is called either *retinotopy* or *somatotopy*, respectively (Goldstein, 2002).

In addition to place-coding, the timing of the auditory nerve firing is used to encode frequency information. A mechanism called *phase locking* refers to a neuron firing when the amplitude of the sound is at its peak point or near it. As a result, high frequencies cause firing bursts more often than low frequencies, because the sound waves reach their peak more often (Goldstein, 2002).

Hair cells are not just simple receptors, but they also contribute as a regulator or an inducer of movement. This is modulated by feedback mechanism from higher parts of cortex (Karjalainen, 1999).

Human hearing also has a larger dynamic range (about 120 dB) than should be possible based on the structure of the ear. The cochlear detectors, inner hair cells, have a dynamic range of less than 65 dB (acquired by analyzing IHC voltage SNR). Studies have shown that outer hair cells have an important role in the large dynamic range of our hearing, providing mechanical nonlinear signal compression. OHCs also cause distortion in the frequency when using combination tones, e.g. $2f_1 - f_2$. This distortion is nonlinear at low intensities (Allen, 2001).

More precise results for place coding have been obtained using microelectrodes placed in individual hair cells and in auditory nerve fibers. Frequency tuning curves (see Fig-

ure 2.6) can then be obtained by playing tones of different frequencies and plotting the sound intensity (in dB SPL) to elicit minimal neural response. The tip of of the tuning curve is called the *best frequency* (BF), a.k.a. the *characteristic frequency* (CF). This is the acoustical frequency that the hair cell or the neuron is most sensitive to. Peripheral tuning curves of neurons for example in mammalian A1 can also be multipeaked, having multiple best frequencies (see e.g. Kadia and Wang, 2003). These kind of neurons can show complex interactions in their firing rate, when presenting combination of tones including frequency components of these several CFs.

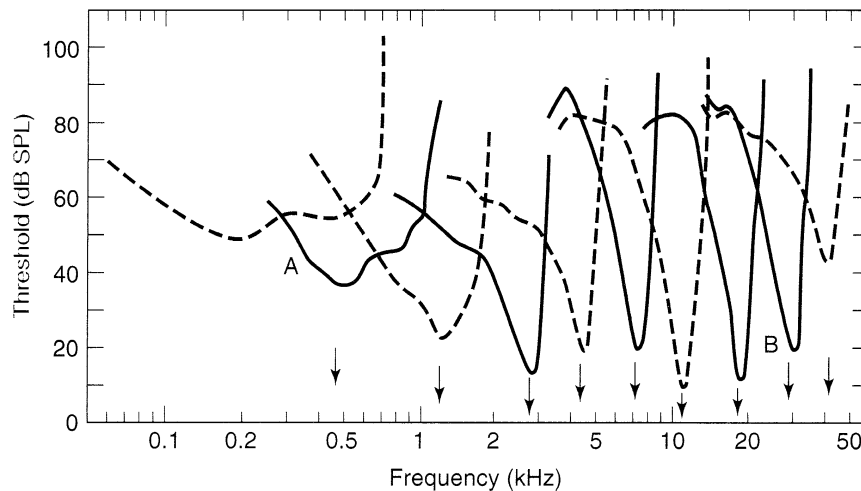


Figure 2.6: Frequency tuning curves of the cat auditory nerve fibers. The characteristic frequency of each fiber is shown by an arrow (adapted from Goldstein, 2002).

Tuning curves can also be measured in psychophysical experiments (e.g., Moore, 1978). Psychophysical or psychoacoustical tuning curves can be measured by presenting a test tone with low SPL intensity, and then finding out the masking tone level needed to eliminate the perception of the test tone. The resulting narrow tuning curves are similar to those obtained from auditory nerve fibers using microelectrodes, which suggests that our perception of frequencies is largely based on the activation of these neurons (Goldstein, 2002).

2.1.3 Auditory masking

Auditory masking means that the existence of intense enough a tone can decrease our perception of another tone. That is, the threshold of hearing a normal tone increases because of the presence of a masker. This can occur in time domain, if the tones are presented almost simultaneously (temporal masking), and in frequency domain, if the tones are sufficiently near to each other in pitch (frequency masking) (Goldstein, 2002; Karjalainen, 1999).

Frequency masking causes biggest increase in threshold near the masker frequency. Masking effect spreads more to higher frequencies than to lower frequencies. This has a substrate in the travelling wave patterns of the basilar membrane (see Section 2.1.2, p. 7).

The critical band

The critical band refers to the frequency width, which excites effectively the same place on the basilar membrane. The approximate equation for critical band width around the frequency f is

$$df = 25 + 75 \times (1 + 1.4f^2)^{0.69} \quad (2.1)$$

where df is in Hz, and f in kHz (Zwicker and Terhardt, 1980). In low frequencies the width of the critical band is small, and the width progressively grows with higher frequencies (Karjalainen, 1999). Modeling the human auditory system as a series of *auditory filters* is a relatively new concept, and this is basically an expansion to the critical band concept, with multiple interacting and hierarchically organized levels.

For instance, in the present study, 20 Hz difference was used (1000 Hz and 1020 Hz sine tones, see Chapter 3, p. 39 for more details). Even though this difference is only about a third of a musical semitone, it was still found to be detectable for clear majority of test subjects, even with a noise masker. The critical band around the 1000 Hz test tone is about 160 Hz (Karjalainen, 1999). The just noticeable difference (JND) of sound pitch at certain frequency is related to the width of the critical band. Two tones with different frequencies

that fall within the same critical band are generally not easily detectable from each other (Allen, 2001). The observed ability to distinguish such a small difference in pitch would suggest that we have some kind of specific attention-related mechanisms, which tune our perception towards the attended sound frequency.

2.1.4 Auditory pathway

The brain receives and processes information from our senses. The outer layer of the brain, *cortex*, is divided to areas and regions in several different ways. Functional division tells which cortex regions respond mostly to specific senses (hearing, vision, somatosensory information like touch) or, for example, participate in planning of our actions (premotor and motor areas). Figure 2.7 shows this division with color-coding, and also displays the numbered Brodmann areas. The cortical area which handles first the incoming sounds in humans (the *primary auditory cortex*) is in Brodmann area 41.

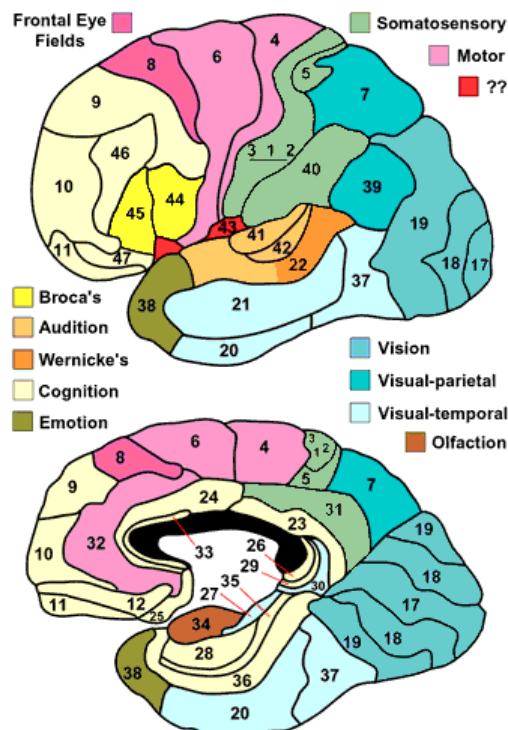


Figure 2.7: Diagram of functional areas of the brain and Brodmann areas (adapted from Dubin, 2001).

The auditory pathway starts from the cochlea (Figure 2.8). Auditory nerve carries the signal first to the *cochlear nucleus*. From there, the signal synapses in the *superior olivary nucleus* in the brain stem, in the *inferior colliculus* of the midbrain and in the *medial geniculate nucleus* of the thalamus (MGN). From MGN, the fibers go to the *primary auditory cortex* (PAC, or in non-human primates also known as A1), in the temporal lobe of the cortex.

Auditory structures are bilateral, meaning that they exist in both parts of the brain. Input can be either ipsi- or contralateral (i.e., from cochlea in the same side or the opposite side, respectively), even though most of the afferent fibers are to the contralateral auditory cortex.

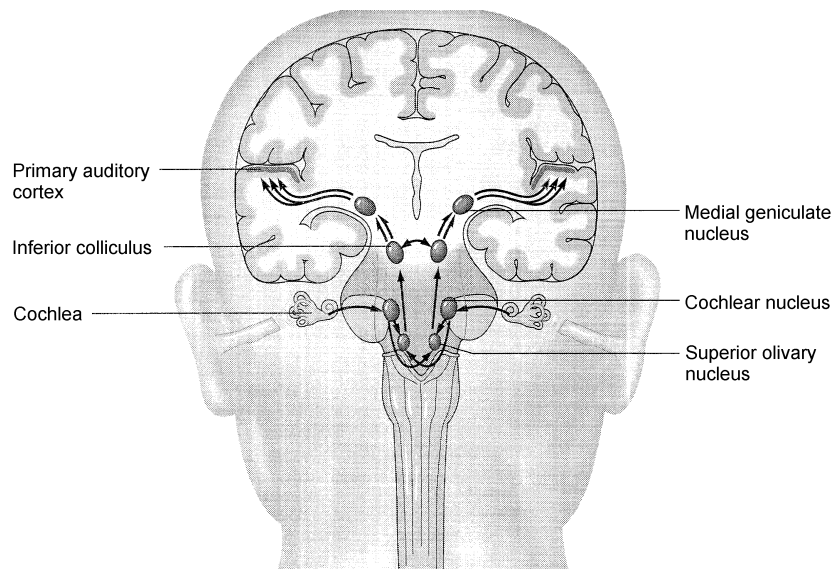


Figure 2.8: Auditory pathway (adapted from Goldstein, 2002).

2.1.5 Auditory cortex

Auditory cortex (AC) refers to the temporal region of the cerebral cortex that contains neurons responsive to auditory stimuli. It receives afferent input from the medial geniculate nucleus (MGN) of the thalamus. Studies have shown that the AC is not a homogenic receptive field. It is a complex structure containing different fields: primary field (the primary auditory cortex) and several surrounding areas (Brugge and Reale, 1985).

The organization of the AC fields has been studied microelectronically with cats and monkeys (Brugge and Reale, 1985). First the input is received in the *core area*, which includes A1 and some nearby areas (Figure 2.9). Signals are then sent to areas surrounding the core, called the *secondary auditory cortex* and after that, to the *auditory association cortex* (Goldstein, 2002).

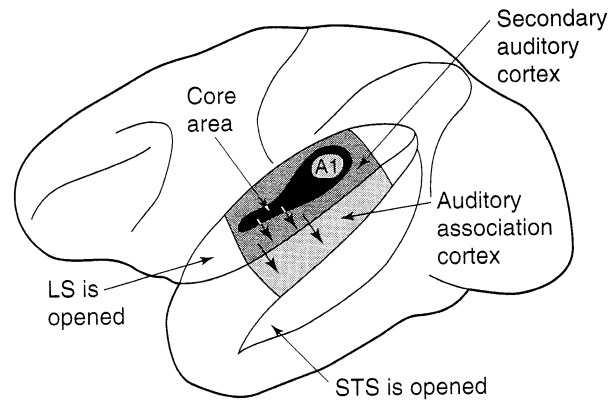


Figure 2.9: Organization of the auditory cortex. LS stands for lateral sulcus and STS for superior temporal sulcus. In this picture both the LS and STS are "opened" to expose part of the auditory cortex not visible from the surface (adapted from Goldstein, 2002).

Timing information due to phase locking is not as important as a frequency encoding mechanism in AC as it is in the earlier processing stages. Neurons in A1 phase lock only up to about 500 Hz, in contrast to the auditory nerves that phase lock up to about 5000 Hz (Goldstein, 2002).

2.1.6 Feedback mechanisms

Frequency selectivity has been extensively studied in animals. Studies have documented feedback mechanisms that increase the frequency selectivity and sharpen the tuning of the auditory system neurons. Interestingly, both amphibians and reptiles use each hair cell as an electrical resonant filter. This causes neural activation to be elicited only if the frequency of the stimulus matches the electrical resonant frequency. This mechanism is modulated in hair cells by calcium-activated potassium channels and calcium currents (Ashmore and Gale, 2000).

Also, the outer hair cells change the basilar membrane impedance (see Figure 2.10), and this causes changes in the "best frequency" places of the basilar membrane. This process is modulated by both place on the basilar membrane (fast feedback loop) and by the efferent neurons connected to OHCs (slow feedback loop) (Allen, 2001).

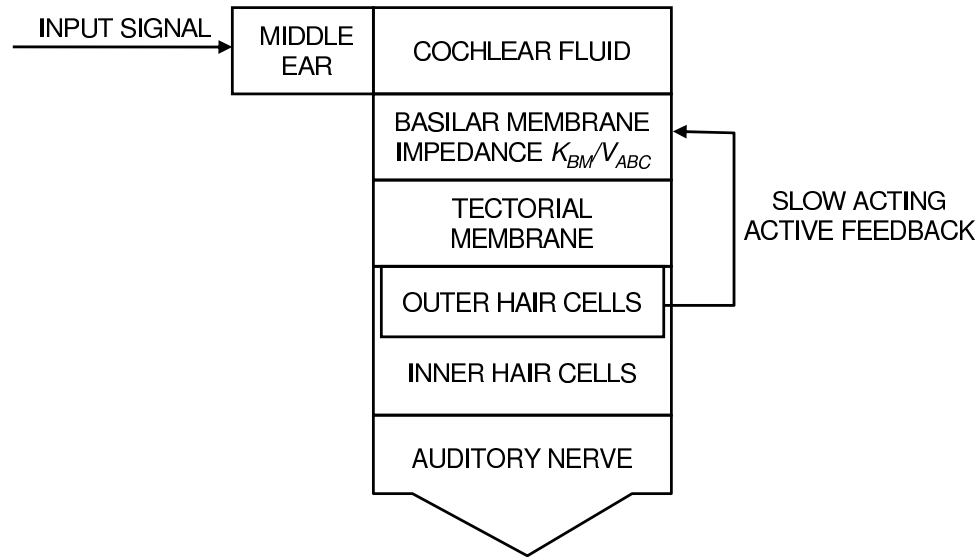


Figure 2.10: Inner ear block diagram (adapted from Allen, 2001).

The tuning curves of the auditory nerves are very narrow, but this cannot be fully explained by the vibration patterns of the basilar membrane. Studies have shown that the frequency-tuned movement of the outer hair cells sharpens the response to a certain frequency. This movement, called the electromotile response, mechanically amplifies the vibration of the membrane at certain point (Goldstein, 2002). Outer hair cells do not send large electrical signals to the auditory nerve, but destroying them from cochlea also significantly reduces the responses of the inner hair cells. Motile response of OHC is modulated by a slow active feedback mechanism (Allen, 2001).

Increased frequency selectivity in cochlea can be explained by an micromechanical theory called the *cochlear amplifier* hypothesis. This explains a hypothetical mechanism, which increases the sensitivity of BM to low level sounds and, at the same time, increases frequency selectivity of the BM vibrations. This is done by drawing or adding electrical and mechanical energy to outer hair cells in cochlear partition, depending on frequency

(Allen, 2001). Feedback refines and tunes the resonant frequency location in BM, either by amplifying hair cell bundle movements, or by amplifying the BM motion in the specified location.

Recently, a gene named *pres* and especially a protein called *prestin*, operating only in OHCs, have been found to be a likely requisites of this kind of fast, active feedback. Prestin has been demonstrated to be necessary for OHC electromotility, and deletion of *pres* has been noted to cause hundred-fold loss of hearing sensitivity (Liberman et al., 2002; Géléoc and Holt, 2003). Whether *prestin* is then both necessary and sufficient for the OHC electromotility, or if it requires some other substances, still requires further studies.

There has been quite a lot of evidence of different active feedback mechanisms that work already at the level of BM. As an alternative, the passive BM model, where no new mechanical energy is added to system, is also able to explain the measured neural responses (Allen, 2001). Liberman et al. (2002) also suggests the possibility that no additional active feedback mechanisms are required besides the *prestin* protein for the high cochlear sensitivity. In summary, the function of outer hair cells seems very important for the sharp frequency tuning properties of our hearing system.

2.1.7 Frequency discrimination

The primary auditory cortex (PAC) is crucial for the fine-grained frequency discrimination. There is physiological evidence from AC lesions indicating that neurons in PAC are required to maintain finely tuned frequency discrimination capabilities of human (Tramo et al., 2002). Weber fractions for the frequency discrimination (fraction between just noticeable difference in frequency and base frequency, $W = \Delta F / F_c$) in a patient having AC lesion was about 8-fold compared to other neurological patients, and 20-fold compared to normal control subjects. Further, monkey studies support the involvement of primary auditory areas in frequency discrimination capabilities. Studies have found that neurons in the surrounding areas of the A1 (equivalent to human PAC) are not as narrowly tuned

to sound frequency as the primary auditory areas of AC (Kosaki et al., 1997; Rauschecker et al., 1995). Surrounding regions seem to exhibit preference to more complex sounds than pure tones.

2.1.8 Duration discrimination

Neural substrate of sound duration discrimination has been discussed in Belin et al. (2002). There appears to be two cerebral processes involved in this discrimination task: a supramodal right fronto-parietal cortical network and a network of regions such as basal ganglia, cerebellum and right prefrontal cortex. At the level of human AC, the right temporal lobe seems to be specifically important for the precise duration discrimination, based on MEG studies that have found mismatch negativity (MMN) to duration changes to be stronger over the right temporal areas (Giard et al., 1995).

Similar to the frequency specificity of AC neurons, there is physiological evidence from bats that some AC neurons have preference to a narrow range of stimulus durations, or alternatively either to a short or long duration (Galazyuk and Feng, 1997). Again, similar to the corticofugal modulation of the frequency-tuned neurons, the "duration-tuned" neurons of the bat AC have been shown to change their best duration with various feedback-induced mechanisms (Ma and Suga, 2001).

2.2 Electric signals of the brain

The basis of all bioelectric signals is the transformation of a non-electric signal to an electrical signal in the active cellular membrane. A chemical process involving both the influx and outflux of potassium (K^+) and sodium (Na^+) ions through a cellular membrane starts an *action potential* (AP) in a single *nerve cell* (Figure 2.11). Signal arrives to a neuron through a chemical mechanism in its *dendrites*. If a neuron should fire, the action potential travels down an *axon* to the end terminals in order to signal to other neurons. The junction between an axon and the adjacent cell is called the *synapse*. This is the

channel that neurons use to communicate with each other. Information from the cell body goes along the axon as an electrical action potential, then across the synapse to the next nerve cell or muscle cell as a release of specific transmitter substances (Malmivuo and Plonsey, 1995; Lang et al., 1994).

The part of the synapse on the axon side is called the *presynaptic terminal*, and the part on the receiving side is called the *postsynaptic terminal*. The gap between these sides, the *synaptic cleft*, and its chemical properties are responsible for that the information in synapse goes only in one direction (Malmivuo and Plonsey, 1995).

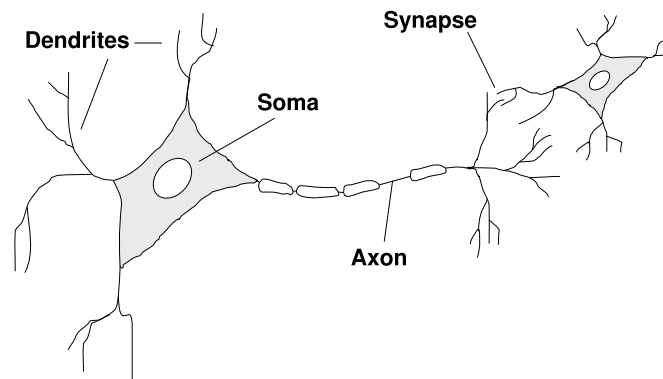


Figure 2.11: Diagram of a nerve cell.

Action potentials alone cannot be measured using EEG or MEG. Postsynaptic potentials (PSP) are thought to be the primary source of the extracellular field potentials, i.e., the potentials that are measurable with non-invasive methods (Speckmann and Elger, 1999). In an ideal dendrite, the postsynaptic potential causes an intracellular current that can be approximated with a current dipole. The density of this current diminishes quickly as the distance from the synapse grows (Malmivuo and Plonsey, 1995). While postsynaptic potentials are also relatively short in time, they are an order of magnitude longer potentials, lasting from milliseconds to even tens of seconds (depending on the transmitter), whereas action potential lasts only for about 1 ms (Malmivuo and Plonsey, 1995). Thus, PSPs are summable which makes it possible to detect them even from the scalp (Lang et al., 1994).

Postsynaptic potentials are either excitatory (EPSP) and inhibitory (IPSP). EPSP occurs in a so-called excitatory synapse, and IPSP in an inhibitory synapse. Several action po-

tentials that travel along the same fiber within a short period of time cause summation of EPSP in the synapse, which again can trigger a new action potential in the postsynaptic neuron if the AP firing threshold is reached (superthreshold potential). IPSP causes hyperpolarization in the postsynaptic neuron, i.e., change of the resting potential to an even more negative value (Speckmann and Elger, 1999).

EPSP causes a net inflow of *cations* (i.e., ions that have positive charge) on the postsynaptic membrane. This causes an increase in the potential, depolarization. IPSP has the opposite effect, causing an outflow of cations from the nerve and/or inflow of the *anions* (ions with negative charge) into the nerve cell (Speckmann and Elger, 1999). Each PSP causes an elementary dipole moment of

$$Q = I\lambda \quad (2.2)$$

in the end of dendrite, where I is the intracellular current and λ is the length constant of the membrane, typically 0.1–0.2 mm for cortical neuron. Calculation of the current I can be done using change of voltage ΔV during a PSP. This is done using equation

$$I = \Delta V / (\lambda r_x) \quad (2.3)$$

where r_s is the resistance of the intracellular fluid per unit length. Evaluating this with typical values gives $Q \approx 20$ fAm for a single PSP. Usually the current-dipole moments have to be in an order of 10 nAm to be measurable outside the head. Thus, synchronous activation of hundreds of thousands or possibly even millions of synapses is required (Hämäläinen et al., 1993).

Both the action potentials and postsynaptic potentials cause electric fields, and by Ohm's law also intra- and extracellular currents. Resistance of the cellular membrane is low compared to the intra- and extracellular space (Lang et al., 1994). As said before, activity of single neurons, action potentials, can't be measured by noninvasive methods, like EEG (Section 2.3) or MEG (Section 2.4). Whether the brain activity can be measured outside the head depends both on the number of activated neurons and the synchrony of activation. Neurons that are activated in synchrony cause the largest responses. Other factors include

geometry of activated neuron groups and their relation to each other. To cause summable activation, a large number of neurons have to be oriented in the same direction. Random orientation of cells would cause them to cancel each others potentials out due to the vector summation.

Open fields, that are caused e.g. by pyramidal cells in the cortex, are visible even far away from the source. *Closed fields*, that are generated e.g. in nuclei, are measurable only in close vicinity of the source (Lang et al., 1994). Pyramidal cells form 70% of the neocortical cells. Pyramidal cells oriented parallel to surface contribute to most of the magnetic field that extends outside the skull.

2.2.1 Field potentials and neural sources of EEG and MEG signals

Activation of the synapses generates postsynaptic potentials, and further cause neural currents to flow. This can be seen in both EEG and MEG, as the neural currents cause electromagnetic fields. Negative electrical field potentials in the scalp are generated when superficial excitatory synapses, or more deeply located inhibitory synapses, are activated in synchrony. Electric potentials with positive polarity, on the other hand, are similarly generated by superficial inhibitory synapses or deeply located excitatory synapses (Speckmann and Elger, 1999).

Synaptic activity thus causes small potential differences in the extracellular space, that again, lead to extracellular currents $I_1 \dots I_n$. After a large-scale summation, these currents can cause large field potentials that are measurable from outside the head. Basics of this process are shown in Figure 2.12. The strongest signals are generated by large pyramidal cells, oriented perpendicular to the cortical surface.

The potential distribution changes over time and place, depending on the neural activity source location and strength, and these small electric potential differences are the signals that are recorded using *electroencephalography* (EEG). In traditional EEG, the potentials are measured from outer layer of the head (scalp) using an array of *electrodes*. EEG can be used to measure *spontaneous activity* and *event-related (evoked) potentials* (ERP or just

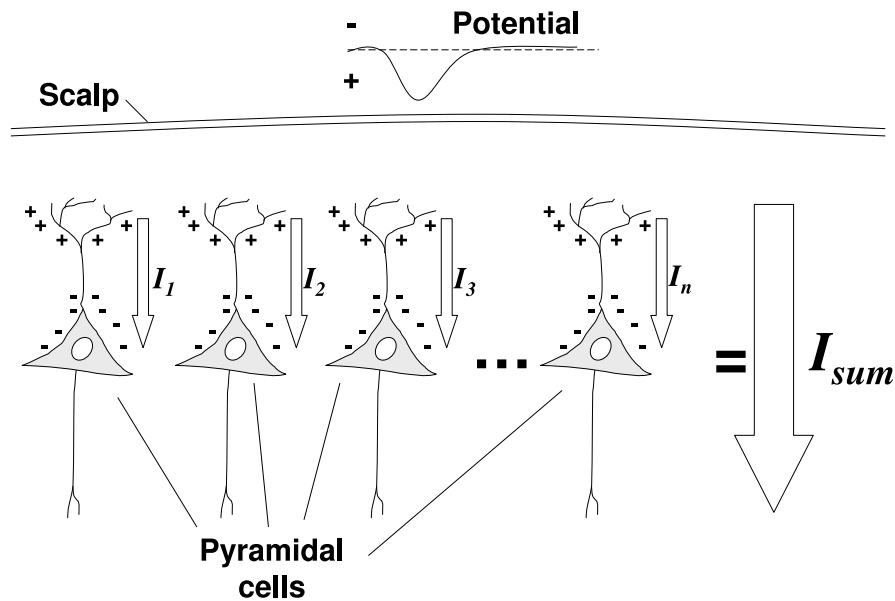


Figure 2.12: Potential generation on the scalp by current summation.

EP). Spontaneous activity of the brain, when measured from the scalp, is about $\pm 100 \mu V$ (Malmivuo and Plonsey, 1995). If using a DC amplifier, even wider range of potentials can be measured. These are generally known as *DC potentials*, which corresponds to oscillations of about 0.01–0.1 Hz. Due to many kinds of technical problems, DC potentials are rarely measured from the scalp. DC measurements, however, may show better and more accurately the actual functions of neural cells (Speckmann and Elger, 1999).

Regularly occurring rhythmic activity in EEG are traditionally divided to different bands, which are called the *delta band* (< 4 Hz), the *theta band* (4–8 Hz), the *alpha band* (8–13 Hz) and the *beta band* (>13 Hz) (Lang et al., 1994). EEG activity that occurs within these bands are called with corresponding names, e.g. *delta rhythm*. In addition to these bands, also so called *gamma band* activity at about 40–100 Hz can be detected from EEG signal. Some additional ways of using even more Greek letters to divide EEG activity to frequency bands has also been proposed, but they have not been very successful (Niedermeyer, 1999).

2.2.2 Event-related potentials

Basic idea in an event-related potential (ERP) measurement is to take short segments (epochs) of EEG data time-locked to stimuli, and average them across all identical stimuli. With this kind of method, the spontaneous changes, DC offset drifts and other typical changes in EEG signal are averaged out, and the signal-to-noise ratio (SNR) is better than analyzing only single segments. Signal quality is basically the better the more averages there is (Figure 2.13). ERPs are in magnitude smaller than of the spontaneous activity, as the averaging decreases the level of background activity. ERPs consist of both negative and positive fluctuations during a short period of time right before and after the stimulus onset. This period is usually in the order of a few hundred milliseconds in neurophysiological studies. Naturally the period can be shorter or longer, for example in the order of only milliseconds when studying brainstem responses.

Event-related potentials can be elicited by for many kinds of stimuli, for example a flash of light. This kind of potential is called the *visual evoked potential* (VEP). *Auditory evoked potentials* (AEP) are studied in a similar fashion, by presenting a sound stimulus and investigating what happens right after the onset of sound. Also neural response to a touch stimulus (*somatosensory evoked potential*, SSEP) can be studied with this research method.

The auditory responses

The neural responses to auditory stimuli can be measured at different levels and time scales of the auditory pathway. Electrocochleogram (ECoChG) is measured with an electrode near the round window. These responses are very early, having latencies of 1–4 ms. Brainstem auditory evoked potentials (BAEP) stand for a set of seven positive waves during the first 12 ms following sound onset. Middle latency potentials (MLP) occur between 12–50 ms after the stimulation. Late responses mean any evoked potentials after 50 ms. Late auditory evoked potentials have given much insight to human cognitive neuropsychology, and they are an area of great interest (Niedermeyer, 1999).

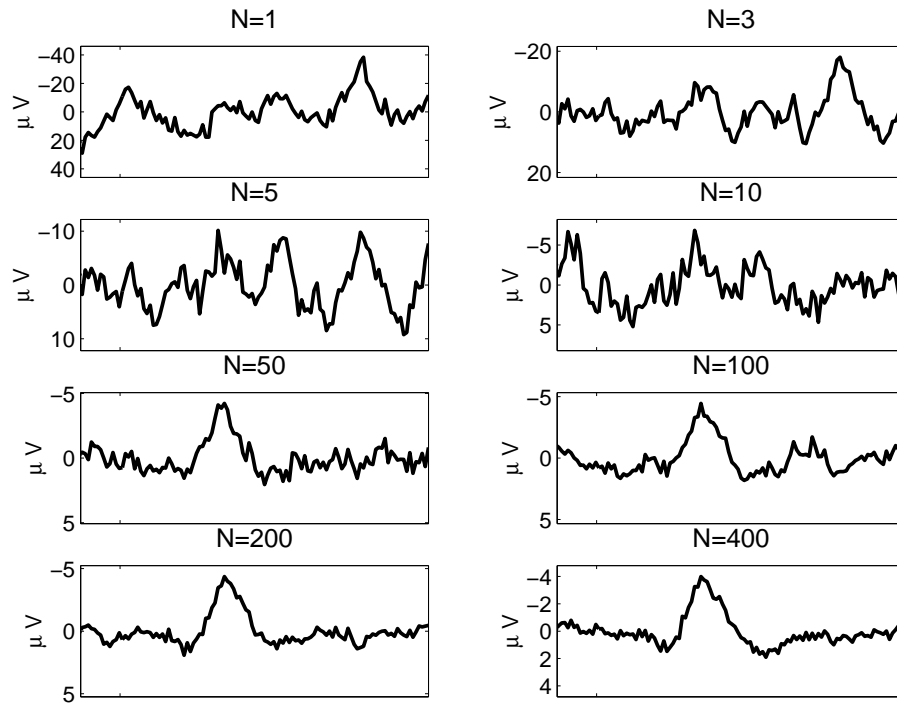


Figure 2.13: ERP signal quality as the number of averages increases. Notice the smaller vertical scale in subfigures as N progresses.

Using ERP studies to study auditory stimulus processing, different late components can be pointed out from the ERP. *P50* refers to positive peak at about 50 ms from stimulus onset. *N100* (or just *N1*) means the negative peak at around 100 ms. This is usually one of the most prominent of the auditory responses. *N200*, *P200* and *P300* are similarly defined. An additional *m* can be added to response name (e.g. *N100m*) to clarify that the response is obtained using MEG, i.e., it is an average of the magnetic response. In MEG, the averaged responses are called *evoked response fields* or *event-related fields* (ERF).

The amplitude of *N100* depends on the amplitude of the stimuli and the uniqueness of the presented sound. By presenting successive identical stimuli with a short interstimulus interval (ISI), the *N100* peak amplitude is decreased. This is often explained to be caused by synaptic depression (e.g., Budd et al., 1998). Basically the longer the ISI, the higher the *N100* peak (Hari et al., 1982). Using for example the oddball experiment paradigm, the amount of difference between the standard stimuli and the deviant stimuli affects the amplitude and latency of the *N100* elicited by the deviant stimuli (Jääskeläinen et al.,

2004). This automatic difference in neural responses is called the MMN (mismatch negativity). By exploiting information about amplitude changes of N100 in successive trials, the neural generators of N100 (or in general the whole N100 wave) have been found to be both frequency and location specific (Näätänen et al., 1988). However, in that study, the frequency specificity of N100 was found to be much more robust than the location specificity.

There are of course several other factors that affect the neural responses to auditory stimuli, but the N100 changes were discussed here most as they are discussed later in this thesis. Additionally, for example P300 increases in latency and decreases in amplitude under light drowsiness (Koshino et al., 1993). During sleep deprivation, N200 is found to increase in latency and decrease in amplitude besides just P300. However, no significant change in N100 was found in a similar experiment (Lee et al., 2004).

In general, to be able to measure the relatively small changes in auditory responses induced by e.g. attention, the stimulus intensity should be kept as low as possible. Otherwise no change in responses might be visible, because the neurons or neural populations can e.g. reach their maximal firing rate or be in their refractory period during the presentation of stimuli. In this study, we hypothesized that the frequency selectivity would be higher with a low stimulus intensity. Additionally, the location specificity of the active neural populations will be lower with loud auditory stimuli, as activation of nearby populations will lead to poorer spatial SNR in noninvasive brain imaging methods.

2.2.3 The forward and the inverse problem

In the *forward problem*, electromagnetic fields outside the head are calculated when neural source location and strength are known. The problem can be defined also as the calculation of any electromagnetic field outside the head, given the current distribution inside.

Noninvasive methods of recording activity of the brain have their limitations. The basic question of interest in studies is what kind of activity of the brain the measurements correspond to, and where are the sources of these activations. Estimating the source

currents using only the measurements on the scalp is called the *inverse problem*. The source localization accuracy depends on the number of independent measurement points, the more the better (Malmivuo and Plonsey, 1995).

The inverse problem is generally ill-posed, meaning that there is no unique solution to the problem. Several different dipole configurations can in principle yield the same potential distribution. With some constraints concerning e.g. the number of sources or their shape, a unique solution can be found. For this, there has to be a model for both volume conductor (the head) and for the source.

The model of the source can lead to systematic errors, if it does not correspond to reality. If no extra information about the source(s) is available, one solution is to estimate an *equivalent current dipole* (ECD) on each time point. ECD is allowed to change position, rotate and to change amplitude. Traditionally dipole fitting has been done using least-squares fitting technique, minimizing the error function with respect to the location and orientation of the dipoles. This has some problems, e.g., the function could get stuck in local minima, so various other algorithms have been developed to overcome these problems (Mosher et al., 1999).

Exact localization of neural sources needs simultaneous information from several channels. Thus, multi-channel MEG data is a good choice for ECD estimation. In MEG, the localization is most accurate for cortical sources that are perpendicular to the scalp. Radial source dipoles are problematic, as they generate little external magnetic field that could be measured. Also, the deeper the sources are located, the more inaccuracies occur in dipole location and magnitude estimation (Mosher et al., 1999).

2.3 Electroencephalography (EEG)

2.3.1 Equipment

Electrodes

EEG electrodes can be either bipolar or unipolar. In bipolar electrodes, the potential difference between a pair of electrodes is used. In unipolar electrodes, potential of each electrode is compared to either a neutral electrode (reference) or to the average of all electrodes (common average) (Malmivuo and Plonsey, 1995). Time-course display from a single electrode is also referred as a *channel*.

Surface electrodes are metallic rings, with diameter of about 1 cm. When using surface electrodes, the material of the electrodes is important. Electrode should provide stable values, i.e., the electric properties should not change over time. Also the electrode should provide good and long-lasting electric contact, making it insensitive to electrode movements. Good surface electrode materials are noble metals (gold, platinum, silver) and electrodes coated with salt, like Ag-AgCl.

Electric wires and amplifiers

Signal from the scalp goes from the electrode in a wire to an amplifier. These wires are exposed to electromagnetic disturbance, so their length should be kept at minimum. From the amplifier the signal is transferred away for further processing using a shielded cable, like a coaxial or twisted pair cable, or as recently is often done via an optic fiber.

To reduce the effects of outside disturbances, a differential amplifier is often used to amplify EEG signals. Differential amplifier only amplifies the difference between two electrodes, thus losing the common noise (often the 50 Hz power line). In practice this is not completely possible, as the amplifier is not able to separate only the common voltage V_c from the differential voltage $V_1 - V_2$ (see Figure 2.14). The difference between the

gains A and C is called the Common Mode Rejection Ratio (CMRR). It is often defined in decibels as $CMRR=20*\log(A/C)$. Most modern amplifiers have CMRR value of over 100 dB.

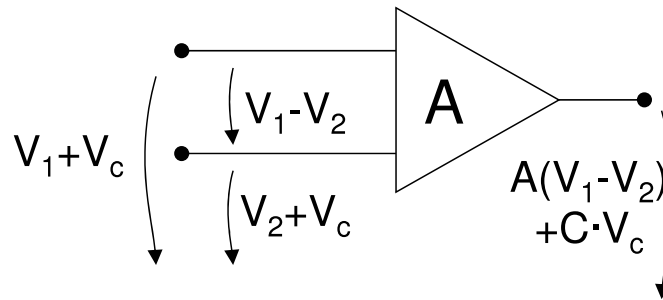


Figure 2.14: Basic principles of differential amplifier (adapted from Lang et al., 1994).

Electrode configuration

The most widely used international standard of electrode placement is called the *10-20 system*. In this system, the electrode positions are determined by four reference points: the *nasion* (delle at the top of the nose), the *inion* (lump at the base of the skull in the back of the head) and the outer edges of auditory canals on both ears. After measuring the distance between these points (center-line and ear-to-ear), the lines are divided to 10% and 20% intervals and this information is then used when placing other electrodes. Figure 3.1 (p. 41) demonstrates this system in practice and shows common names of the electrodes as well. The advantages of using 10-20 system is that the results from different laboratories and across subjects are comparable.

Electrode attachment

EEG measurement from the scalp is prone to various artifacts and noise. To maximize the quality of the signal, impedance for every electrode should be adjusted to equal level, preferably as low as possible. Typically impedance is set to 5–10 k Ω . Impedance can be minimized by preparing the skin before attaching electrodes to it. Skin underlying

the electrode should be first cleaned up. Scrubbing the skin with a special paste during preparation and using a conductive paste between the electrode and the skin is a common practice.

2.3.2 Problems

EEG is very prone to electric disturbance. This can be reduced by good placement of wires. EEG and in general the electric field potentials that are measured from the scalp do not directly correspond to brain activity. Signal is both attenuated and distorted on its path to the surface. The strongest attenuator is the skull, but also the electrode and its impedance attenuate the signal. Tissue outside the brain attenuates the signal depending on the frequency. Slow delta-band activity might pass through almost intact, but beta activity can be attenuated by a significant amount (Lang et al., 1994).

EEG has good temporal resolution, about 1 ms, but spatial resolution is poor, thus making source estimation inaccurate. Spatial accuracy can be increased by adding more electrodes and by using a Laplacian estimate. This way EEG can reach almost the spatial accuracy of MEG. This improvement has its limits, because tissues underlying the scalp both attenuate and blur the signal together (Lang et al., 1994). The skull smears the potential distribution, which makes solving of the inverse problem problematic.

2.4 Magnetoencephalography (MEG)

For a comprehensive review, see e.g. Hämäläinen et al. (1993), on which this section is largely based.

2.4.1 Measuring magnetic fields

MEG is closely related to EEG. The generator for both signals is same, our brain, and the electrical and magnetic fields are coupled by Maxwell's equations. MEG measures only the magnetic fields on the scalp. EEG has more sources of artifacts, e.g. due to the head and other muscle movements and sweating. Additionally, as the EEG signals are recorded from the scalp, the electrical properties of skin, like conductivity, should stay identical throughout the recording, which is rarely realistic. If EEG source modeling is attempted, an accurate multi-layer volume conductor model is required. Magnetic fields, on the other hand, are not affected by tissue the same way as electric fields, so MEG offers often in practice less distorted signal than EEG and thus also better spatial resolution (Lang et al., 1994). MEG recordings are also reference-free, whereas EEG field maps largely depend on the type of reference used (Hari, 1999).

As said, electric and magnetic fields are coupled by Maxwell's equations, which are in non-dispersive, isotropic material as follows

$$\nabla \cdot \bar{E} = \frac{\rho}{\epsilon_0} \quad (2.4)$$

$$\nabla \times \bar{E} = \frac{-\partial \bar{B}}{-\partial t} \quad (2.5)$$

$$\nabla \cdot \bar{B} = 0 \quad (2.6)$$

$$\nabla \times \bar{B} = \mu_0(\bar{J} + \epsilon_0 \partial \frac{\bar{E}}{\partial t}) \quad (2.7)$$

where \bar{E} is the electrical field density [V/m], ρ free electric charge density [C/m^3], ϵ_0 electrical permittivity for free space [F/m], \bar{B} magnetic flux density [Wb/m^2], t time [s], μ_0 magnetic permeability [H/m] and \bar{J} current density [A/m^2]. A quasistatic approximation, ignoring terms $\partial E/\partial t$ and $\partial B/\partial t$, can be made as frequencies involved in brain activity are generally below 100 Hz (Hämäläinen et al., 1993).

Basically this means that change in the magnetic flux causes an electric field, and a electrical current or a change in the electric field induces a magnetic field. Magnetic and electric fields are orthogonal, i.e., their field differs by 90° . This causes different type of field patterns for EEG and MEG (Figure 2.15).

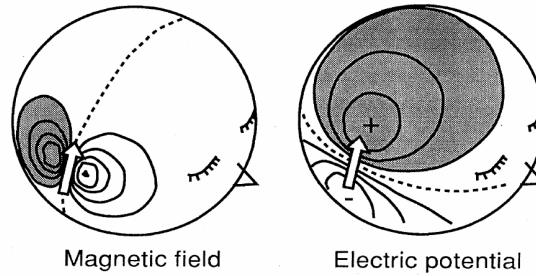


Figure 2.15: Idealized magnetic and electrical field patterns generated by tangential dipole (adapted from Hämäläinen et al., 1993).

2.4.2 Equipment

Most MEG measurements are done utilizing *SQUID* (Superconducting QUantum Interference Device) gradiometers, introduced in the early 1970s (Hari, 1999). Alternating magnetic fields generated by the brain induce current to SQUID sensors through the superconducting flux transformers. To retain their SQUID properties, the sensors are located in a dewar containing liquid helium at -269°C . Container including the sensors is then brought to as close to the head as possible.

A gradiometer basically picks up the magnetic flux only from a certain spatial location. This is more sophisticated than using a single pick-up loop magnetometer. Problem with this kind of magnetometers is, that they measure both the signal and the noise, noise meaning here magnetic fields not caused by neuronal sources, e.g. the magnetic field of the earth. By using two pick-up coils in series, wound in opposite directions, it is possible to overcome the problem of constant magnetic field and design sensors sensitive only to nearby neural sources. Two most widely used types of gradiometers are the *axial* and the *planar gradiometer* (Figure 2.16). First order axial gradiometer is most sensitive to B_r , the radial magnetic field component. The axial gradiometer detects maximum signals in both sides of a dipole. The lower loop is called the *pick-up coil* and it detects most of the signal as it's closer to the neural source. The upper loop, the *compensation coil*, is identical in area but wound in opposition. The planar gradiometer measures essentially the tangential derivate of the magnetic field, $\partial B_r / \partial x$ or $\partial B_r / \partial y$, and it detects maximum

signal right above the dipole (Hämäläinen et al., 1993; Hari, 1999)

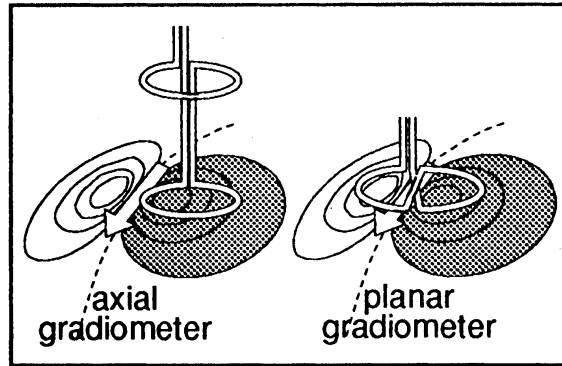


Figure 2.16: An axial and a planar gradiometer (adapted from Hari, 1999).

The pioneering MEG studies used only single-channel magnetometers, which meant that the magnetometer had to be moved to a different location to measure field map for the whole head (Hari, 1999). Nowadays multi-channel equipment, covering the whole head, has made MEG recording much faster and less prone to noise.

2.4.3 Problems

Magnetic field of the earth is in order of tens or even hundreds of millions higher than the magnetic field generated by our brain (Hari, 1999). This puts much pressure on the sensitivity of the measurement devices. MEG has to be measured in a magnetically shielded room, utilizing e.g. several layers of aluminum and μ -metal. Even small metallic objects can interfere with the recordings, if they are brought into too close vicinity of the magnetometer. MEG is most sensitive to the axial (tangential) cortical sources, generated in the fissures, and only a little signal is generated by radial sources located in the gyri (Hämäläinen et al., 1993).

2.5 How attention works at the neural level

Attentional mechanisms are known to operate within all sensory modalities, and also across modalities. In this short overview, only within-modality changes are handled in more detail.

Attentional processes involving integrating information from many modalities are controlled by both bottom-up and top-down mechanisms. Loci for these types of multimodal control circuits appear to be the superior colliculus (SC) in the midbrain and the pulvinar nucleus of the thalamus, which are both known to be operative at least in spatial attention tasks (Shipp, 2004). In addition to these structures, superior frontal, inferior parietal and superior temporal cortex have been found to exhibit changes in the neural activity during attentional cues, suggesting that these structures are involved in voluntary attentional control (Hopfinger et al., 2000). Additionally, both the dorsolateral prefrontal and anterior cingulate cortex seem to be involved in cognitive attentional task, with both areas having different roles for control (MacDonald et al., 2000). Thus, frontal areas seem to be important for attentional control. This is also supported by lesion studies, where especially right frontal lesion patients showed deficits in sustained attention (e.g., Wilkins et al., 1987; Rueckert and Grafman, 1996). The right frontal area has also been dominant in normal attentional task, as shown e.g. by the EEG topography maps in García-Larrea et al. (1992). However, it is likely that no single brain area dominates all the attentional effects. A possible explanation could be that there exists some kind of complex network for the top-down attentional control (Hopfinger et al., 2001), for which neuroimaging methods like functional magnetic resonance imaging (fMRI) could be used to study further.

Attention is classically thought to function within the sensory memory, where the incoming stimuli is compared to a template in the sensory memory (for a review, see Cowan, 1988). This "attentional trace" is a cortical representation of the relevant features needed to discriminate the attended stimuli from the other stimuli (Näätänen, 1982). The sensory store is called the *iconic memory* for vision, the *echoic memory* for hearing, and the *haptic memory* for the sense of touch. The capacity of the sensory memory is limited for all modalities, lasting only for seconds and having capacity of only few objects.

2.5.1 Neural changes in vision and other modalities induced by attention

Attention has been shown to induce direct neural changes in the visual cortex of a monkey. For example, attention was found to both enhance behavioral performance in a visual discrimination task and to selectively increase the neural responses in V4 area of rhesus monkeys (Spitzer et al., 1988), via attenuation of neural response to unattended visual stimuli just outside the receptive field of the attended stimuli in V4. In subsequent studies, the main effect of attention in the visual system of a monkey appeared to be an increase in gain of orientation-selective neurons in both V1 and V4 areas of the visual cortex (Treue and Trujillo, 1999; McAdams and Maunsell, 1999). In these two studies, attention did not appear to induce selective changes in the preferred orientation that the neurons responded to. There have been some studies where neuronal shifts towards attended location are notable, measured as changes of the receptive fields (e.g., Connor et al., 1996, 1997). In addition, McAdams and Maunsell (1999) found some neurons in V4 that would show proper orientation tuning only in the attended task, but none in the unattended task (16% of all neurons included in that study).

Both attentional modulation mechanisms, increase in gain (change in neurons firing threshold) and increase in selectivity (change in tuning curves of feature-specific neurons), could be used to explain the enhanced behavioral performance. A recent fMRI study in humans (Murray and Wojciulik, 2004) found evidence that visual attention causes such changes in the neuronal population level that cannot be explained by gain effect only. Increased selectivity of the orientation-specific areas was suggested as the cause for this.

Attention has also been shown to modulate the somatosensory system in neural level. In addition to ERP changes, attention has been e.g. shown to have direct changes in neuronal firing patterns of the somatosensory cortex of a monkey (Steinmetz et al., 2000).

2.5.2 Attentional effects in the auditory system

The effects of attention on visual processing has been much more thoroughly studied than the effects of attention on auditory perception. Similar to visual system, attention to auditory stimuli can also (1) increase the neural selectivity or (2) increase the gain of the neural responses. Neuronal mechanisms of attention in the auditory system have been reviewed in Giard et al. (2000). Here, the attentional effects especially in ERP studies involving auditory stimuli are reviewed.

So, then, how does attention modulate the neural responses that are measured by EEG? When attending a stimuli, the ERP component P300 is elicited due to cognitive processing. It is most clear in discrimination tasks, where infrequent (deviant) objects have to be differentiated from the frequent ones. The P300 is induced by voluntary attentional control, when attention is focused to objects within one modality. It has no single source inside the primary sensory cortex, like some other ERP components, but it has multiple distributed generators across the scalp (for a review, see Herrmann and Knight, 2001).

The attentional effect on earlier ERP components (P50 and N100) are not as clear as the P300, as their amplitudes are mostly affected by physical properties of the stimuli, like brightness of the visual stimulus or loudness of the auditory stimulus. Attention has been thought to involve cognitive processes, which often do not take place within tens of milliseconds after the stimulus onset. Enhancement of both the P50 and N100 amplitude due to selective attention has still been widely shown to take place in various experiments, which would suggest that attention *can* operate also in a very early stage of sensory processing (Herrmann and Knight, 2001). As an alternative to the direct, often described as a gain-based effect of attention on the early ERP component amplitudes, an idea of additional processing due to attention has been proposed. This would be seen as stimuli-specific *processing negativity* in the neural responses, when the ERP recorded in the unattended condition is subtracted from the ERP of the attended condition (Näätänen, 1982; Alho et al., 1987). This is similar to the *mismatch negativity* (MMN) of the neural responses in experiments using oddball paradigm, only MMN seems to be attention-independent process (Näätänen et al., 1993).

The underlying mechanism causing these changes in the neural responses could be e.g. shift of the frequency tuning curve (characteristic frequency change), sharpening of the tuning curves or a positive gain effect, i.e., the threshold for single response gets generally lower and the whole tuning curve shifts down (Figure 2.17). How these kind of specific changes might be reflected in large-scale neuronal activity are discussed later in this work under Section 3.5. Sharpening of the frequency tuning might occur due to inhibitory mechanisms as well, as reported in bat MGB by Suga et al. (1997).

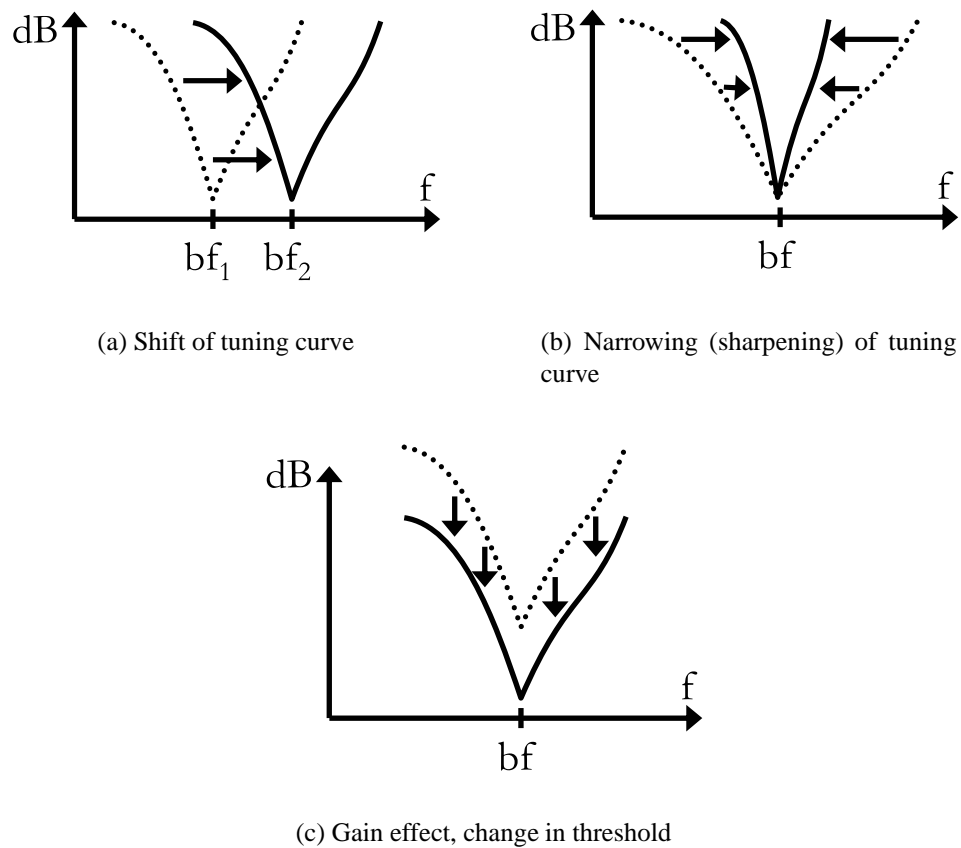


Figure 2.17: Examples of effect of attention on tuning curves.

Already the classic study by Hillyard et al. (1973) showed the effect of selective attention on the N100 amplitude in a binaural pitch discrimination task, where the attended sounds were presented only to the other ear. Early attentional modulation in the auditory system, starting as early as 20 ms from stimulus onset and being often present at around 100 ms, has been reported later e.g. in Rif et al. (1991) and in Woldorff et al. (1993).

The effect they found was basically gain-based: the evoked magnetic brain responses to attended sound were larger than the responses to unattended sound. Additionally, both studies were able to locate the source for this attentional effect to the auditory cortex on the supratemporal plane, suggesting that the attention modulates directly the neural generators of the auditory N100. Enlargement of both the early and later ERP components like N100 has been supported in several subsequent studies (e.g., Lange et al., 2003).

Monkey studies have shown that long-lasting training can reshape the tonotopic organization of A1 towards the attended sound frequency (Recanzone et al., 1993). The changes in A1 were also reflected in the performance of the behavioral task, i.e., in perceptual acuity. On the other hand, by classical conditioning, AC receptive field changes happened already after 5–10 trials in a study by Weinberger et al. (1993), so cortical remapping of the AC can in some cases be very rapid.

2.5.3 Attentional dysfunctions

All people do not possess normal attention network in their brain, i.e. they do not perform in selective attention tasks as well as healthy people and possibly have some attention-related problems in their everyday life. Attentional dysfunctions are very common in neurological diseases, typically including cognitive disorders as well (see Kuikka et al., 2001). Often the patients feel that their attention is somehow limited, and that they can concentrate on one task at a time. Focusing on the main task is impossible if there are even small distractors. Additionally slowing down of information processing is often evident.

The cause of the attentional dysfunction can be damage to a certain area of the brain or changes in the function of neural transmitters. For example, both mild closed head injury (MHI) and frontal lobe lesion patients have shown dysfunctions in attentional tasks, where especially the MHI patients had smaller negativity difference of ERP amplitudes than the controls in a dichotic listening task (Solbakk et al., 1999). This would suggest that the "attentional trace" mechanism worked less efficiently, and thus impaired their ability to detect deviant sounds. Many brain damage patients also constantly feel fatigue and

sleepiness, leading to reduced alertness and, thus, poorer performance in tasks involving attention.

Additionally, there are number of clinical conditions where persons attention is somehow dysfunct, e.g. Alzheimer's disease, schizophrenia and attention-deficit hyperactivity disorder (ADHD). For a review on ERP changes in ADHD, see Barry et al. (2003). ADHD-related changes in ERPs have been found especially in the auditory modality, from the earliest brain-stem responses to the late ERP components, where especially the reduced P300 is apparent. Typical ERP studies of ADHD involve auditory or visual selective attention tasks. However, many studies have also suggested that the reduced-capacity attention is not the cause of ADHD symptoms, even though the ERP studies have shown abnormalities in different stages of sensory processing. This is, people with ADHD might perform in the selective attention task as well as healthy people (no difference in reaction times or errors), but the ERP amplitudes, latencies or topographies differ from healthy people (even though these findings can sometimes be contradictory). Further, schizophrenic patient perform worse in the Stroop test, where efficient color-naming requires selective attention (for a review, see Henik and Salo, 2004). The anterior cingulate gyrus dysfunction has been proposed as one cause for this (Carter et al., 1997). Deep down, all of the mentioned clinical conditions may reduce to abnormalities in the structure or the wiring of the brain.

The latency of the ERP peaks in attention-related tasks can also be studied, along with the ERP component amplitudes and topographies. In a study having schizophrenic patients, the later peaking of the difference wave Nd (negative difference, a.k.a. processing negativity) was reported with patients, compared to healthy control subjects (Higashima et al., 2004). However, as the original authors commented, the patients were under medication during the tests, so the patients' attention might've been affected by this. On the other hand, a study with children having attention-deficit (ADHD) and tourette/tic syndrome has shown earlier peak latencies in the early ERP components with ADHD patients (Oades et al., 1996). In the same study, both patient groups with impaired attention had modified ERP topographies compared to healthy controls.

In summary, deficits in attention can impair or otherwise modify already the early sensory processing phases. With a suitable set of stimuli and experimental paradigm, the differences can be noted with ERP recordings. The earlier the diagnose is done, the better the treatment is to help the patient.

2.5.4 Specific hypothesis for the present study

Here, our aim was to show attentional modulation in the early auditory pathway, which would be seen as ERP changes to a simple auditory stimulus. We specifically hypothesized that during the frequency discrimination task, the attentional effect would be more evident than during the duration discrimination task. Additionally, it was tested whether either one of the mechanisms (sharpening vs. gain increase) better explains the changes induced by attention. The shift of tuning curves (CF change) was thought to be unlikely to happen in a relatively short period of time, such as during an half an hour experiment block. For example, in Recanzone et al. (1993), it took several weeks to show changes in A1.

The decision on which mechanism (sharpening vs. gain) is more likely to happen during the attentional task was done by comparing the simulation results to the empirical data. The simulation was done on how the frequency tuning curve changes could be reflected in large-scale neuronal activity level. Also a "best-fit" solution was calculated, using combination of both mechanisms, to roughly fit the real experimental data to the values given by the simulation model with a minimal error.

Chapter 3

Methods

3.1 Experimental subjects

Test subjects of the EEG experiment included in the data analysis (N=20) were healthy right-handed university students, aged 18–28 (mean±stdev=23.0±2.6), both male and female (N=13 / 65% male, N=7 / 35% female). All of the subjects had normal hearing. Some had previous experience as subjects in EEG, but most were naive. Subjects were paid to participate in the experiment.

Two of the EEG subjects were also selected to the MEG experiment. In addition, two extra subjects were selected, so that in total, N=4 people were measured in the MEG part. The MEG subjects were aged 22–31 years (mean±stdev=25.3±3.9), 1 female and 3 males.

3.2 Instrumentation

3.2.1 EEG equipment

The vast majority of modern EEG devices are digital, utilizing analog-to-digital (AD) conversion. The digital EEG equipment currently used in the Helsinki University of Technology, Laboratory of Computational Engineering, has been obtained from Brain Products GmbH (München, Germany).

Measurement system in this study consisted of two elastic EEG caps (Easy Cap, both 64-channel) of different sizes, and two BrainAmp 32-channel EEG amplifiers, of which only one was used in this study since 32 EEG channels were used. Either one of the caps was used in each study, depending on the diameter of the test subjects head. Amplifiers were connected with an optic fiber to a computer, that was equipped with a special PCI interface card.

The EEG channels that were used according to the extended 10-20 system were Fp1, Fp2, F3, F4, C3, C4, P3, P4, O1, O2, F7, F8, T7, T8, P7, P8, Fz, Cz, Pz, FC1, FC2, CP1, CP2, FC5, FC6, CP5, CP6, TP9 and TP10 (see Figure 3.1 for locations). In addition to these, two electro-oculogram (EOG) electrodes Eog1 and Eog2 were placed around the eyes to detect blink artifacts, and one electrode was attached to the tip of the nose in order to provide a common reference channel (here called the Ref_bi). In the beginning of each measurement, all electrode impedances were set below 10 k Ω .

EEG recording setting

EEG raw data were recorded using Vision Recorder software (Brain Products GmbH). Data postprocessing was done with Vision Analyzer software, also from Brain Products GmbH. EEG data were recorded with a sampling frequency of 500 Hz. In the analysis part, the tip of the nose was first selected as a new reference (Ref_bi). Afterwards, filtering was done using a passband of 0.5–40 Hz (attenuation 24 dB/octave) and 50 Hz notch filter.

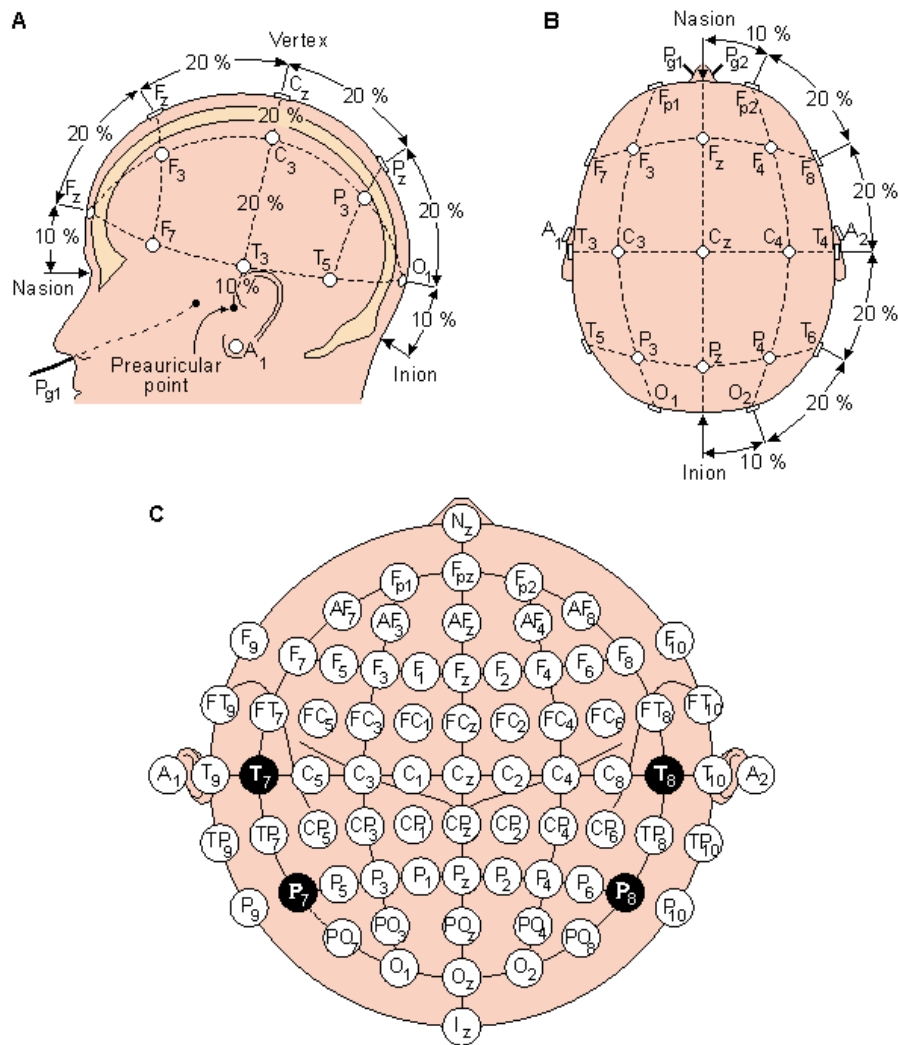


Figure 3.1: The international 10-20 system (adapted from Malmivuo and Plonsey, 1995).

The data were then segmented, with time course of -200–600 ms relative to the stimulus onset (standard tone). Artifact rejection was done using $>\pm 75 \mu\text{V}$ as the rejection criteria. Further, a so called gradient criterion was used, maximum voltage step per sampling point being $50 \mu\text{V}$. After that, the segments were baseline corrected for -200–0 ms and averaged.

The required number of good segments to be included in the averaged signal was 100. If the number of artifacts was too high, the experiment was continued manually and EEG recorded for an extra minute or two until a sufficient number of averages were collected. Initial number of standard tones for each condition was 119, which allowed at maximum 16% of segments to be bad. If the single subject data still failed to show enough good

averages, the subject was dropped out of further analysis. This happened for 2 subjects, either because of fatigue or excess number of blinks. For one subject measurement had to be redone on another day because of excessive sweat artifacts. Also there were 3 experimental test runs using a shorter ISI, but as the signals of interest were not as robust as with the original settings, these subjects were excluded from the analysis to keep the experiment settings homogeneous for all the subjects. Shorter ISI leads to smaller N100 amplitude (as explained e.g. in Budd et al., 1998), and in this case, the amplitude was then too small to provide good enough SNR for the EEG data. All in all, the number of "good" subjects for both stimuli sets was N=10. Typically the number of averages was about 105–110 for every response type.

3.2.2 MEG equipment

Helsinki University of Technology, Low Temperature Laboratory, houses a 306-channel *Neuromag Vectorview* SQUID neuromagnetometer, with 102 sensor elements in a helmet array (two orthogonal planar gradiometers and one magnetometer in each). This device is located in a shielded room, covered with two layers of μ -metal and aluminum to attenuate the effects of outside magnetic fields. The recording and analysis software used was also provided by the equipment manufacturer, Neuromag Ltd (Espoo, Finland).

All MEG channels available were recorded. In addition to MEG channels, two EEG EOG electrodes were attached in order to detect blink artifacts. During the recording, MEG data were filtered with 0.1–40 Hz passband. Segments with over 3000 fT/cm (MEG) or $\pm 75\mu\text{V}$ amplitude were automatically rejected from the average. The number of segments in averaged response was typically 105–115 (out of 119).

3.3 Test setup

The test setup and stimuli used were highly similar to the ones used by Sams and Salmelin (1994). Originally, there was only a passive task, where the subjects were reading a book

and ignored the stimuli. In the current study there were two attentive discrimination tasks: of (1) the duration and (2) frequency difference of short sounds, in addition to the passive task. There were also some methodological differences, as the Sams and Salmelin (1994) experiment was done using MEG only. Here, two experiments were done, the first using 32-channel EEG, and a follow-up experiment with selected subjects using MEG.

3.3.1 Stimuli details

1 kHz sinusoidal sounds were presented with continuous noise maskers. White noise was bandstop filtered with varying notch width. The notch was symmetrically located around 1 kHz. One condition included unfiltered white noise. There was also one "silent" control condition where the tones were presented with no masker in background.

The "standard" sine tone was 1000 Hz, 100 ms. Infrequent, deviant, target tones were either longer in length (150 ms), higher in pitch (1020 Hz) or both. The probability for standard sound was 85% and for each deviant tone type 5%. All sine tones had 5 ms linear rise and fall times. The order of the tones was randomized. ISI for each tone (from onset to onset) was 1.5-2.5 s, varied randomly. In the beginning of each trial, five standard tones were presented in a row, but EEG segments during these first 5 tones were omitted (i.e., not included in calculation of the average ERP). See Table 3.1, Figure 3.2 and Figure 3.3 for details about stimuli and for a diagram of the stimuli presentation order.

Table 3.1: Types of tones used.

| Frequency (Hz) | Duration (ms) | Percentage of all tones |
|----------------|---------------|-------------------------|
| 1000 | 100 | 85% ("standard") |
| 1000 | 150 | 5% |
| 1020 | 100 | 5% |
| 1020 | 150 | 5% |

White noise was digitally bandstop filtered using a high order FIR filter in Matlab (R12.1, MathWorks Inc., Natick, USA). Attenuation in the stopband was high and transition band was very steep, minimum of 120 dB attenuation with transition band of 1 Hz. Stopband limits were symmetrically located in the frequency domain around 1000 Hz, although the

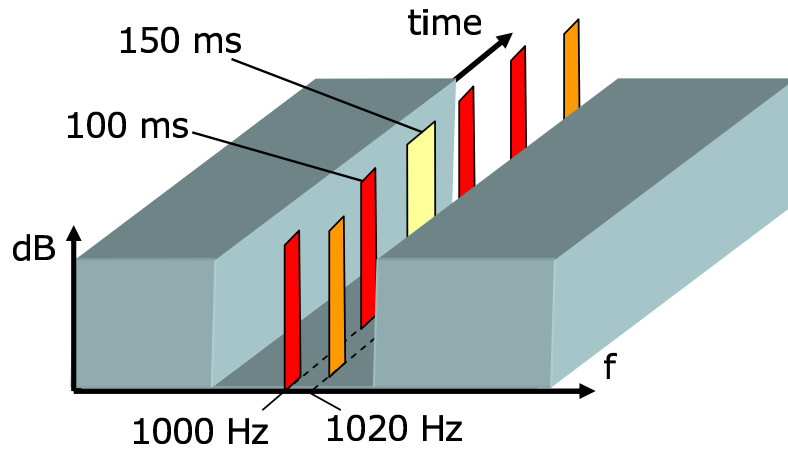


Figure 3.2: Diagram of the stimuli used in the experiment. The stimuli were presented with a continuous white noise masker in the background. The tones followed each other, the deviant tones were either longer in duration or higher in pitch or both.

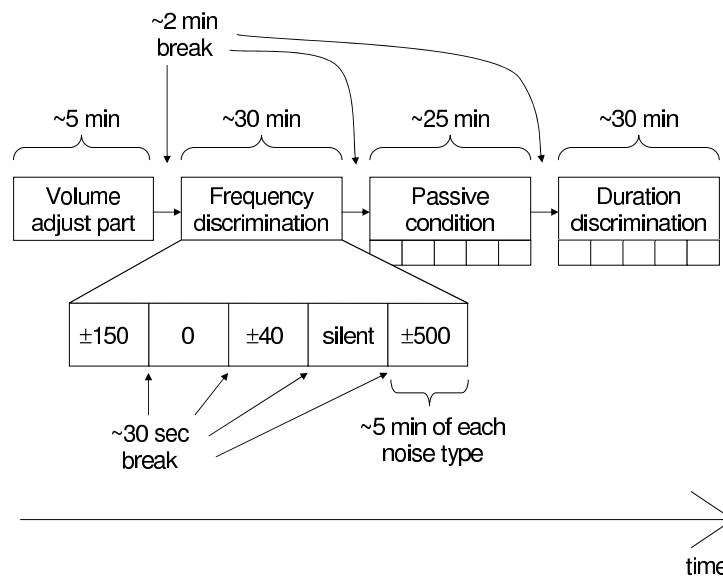


Figure 3.3: An example of experiment presentation order. Order of three different conditions and noise types were randomized.

symmetry was not then present in octave scale. For example, "±150 Hz" in Table 3.2 means limits of 1000 Hz±150 Hz (i.e., the white noise was bandstop filtered in range 850 Hz–1150 Hz). Notches were divided into two stimuli sets (Table 3.2) to make the experiment shorter for individual test subjects, while still collecting enough interesting data. For both stimuli sets, N=10 subjects were included in the data analysis.

Table 3.2: Used noise maskers. "±500 Hz" below means bandstop filtering white noise around 1000 Hz±500 Hz, i.e., 500–1500 Hz.

| Notches for stimuli set #1 | Notches for stimuli set #2 |
|-------------------------------|-------------------------------|
| silent (no masker) | silent (no masker) |
| ± 500 Hz | ± 400 Hz |
| ± 150 Hz | ± 250 Hz |
| ± 40 Hz | ± 80 Hz |
| 0 Hz (unfiltered white noise) | 0 Hz (unfiltered white noise) |

3.3.2 Description of the test run

Sound intensity level adjustment

Before the actual tests, the noise intensity level was adjusted so that the tones were barely audible (i.e., the 50% hearing threshold). Adjustment was done by the experiment instructor in 1 dB steps using simple up-down rules defined in Table 3.3. This procedure was explained in Levitt (1971). Basically the level of sound was adjusted depending on the answers the subject gave. The volume was not changed after each answer, but was based on the last 2–3 answers.

During the volume adjustment, the subjects were instructed to press a button whenever they heard a tone (sine-wave tone, 1000 Hz, 100 ms, 5 ms linear rise and fall times). Tones were played with an ISI of 2–8 seconds. Unfiltered white noise was played constantly in the background and the SPL of this noise that was changed by experiment instructor. Too late an answer (over 1 second from stimulus onset) was regarded as a miss ('-' in Table 3.3). See Figure 3.4 for an illustration of the volume adjustment. As the volume adjustments were done by hand, the up-down rules of Table 3.3 were not always followed vigorously. During the volume adjustment, subject was sitting inside the same room where the actual test took place as well.

Table 3.3: Up-down rule table used. – denotes no answer, + correct answer. Stimuli SNR was increased by adjusting noise volume to lower intensity.

| UP group, increase stimuli SNR | DOWN group, decrease stimuli SNR |
|--------------------------------|----------------------------------|
| -- | ++ |
| -+- | + - + |
| + -- | - + + |

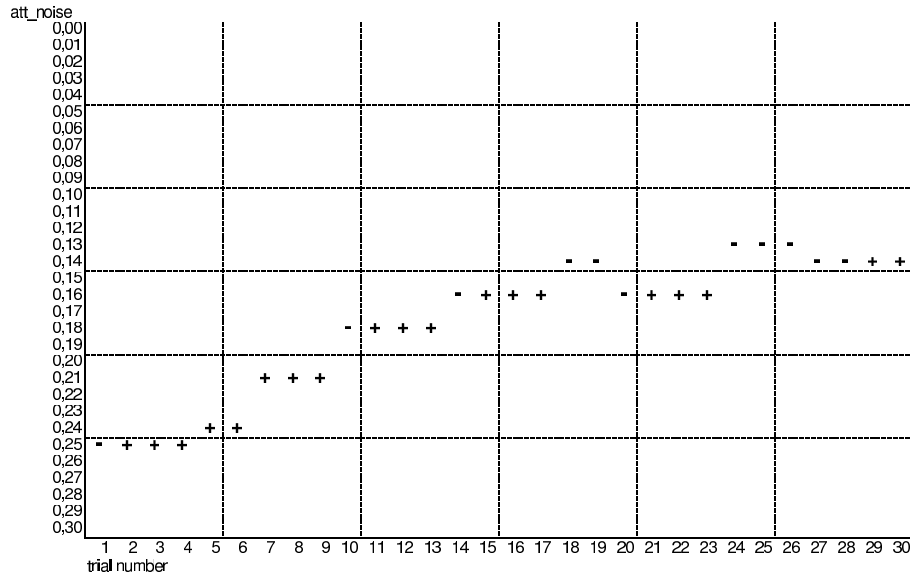


Figure 3.4: An example of volume adjust part in the beginning of trial.

Trial run

The whole test was divided into three conditions: (1) duration discrimination, (2) frequency discrimination, and (3) a passive task. Each condition was further divided into five shorter parts, each lasting approximately 5 minutes. Four parts out of five had different kind of white noise in the background (either bandstop filtered or unfiltered, plain white noise), while in one part only the tones were presented ("silent" condition). The sine tone stimuli were identical in all of the parts.

During all conditions, the subjects were sitting alone in front of a computer monitor in a soundproof and electrically shielded (RF shielded) room. The distance between subjects' head and computer screen was 90–100 cm. The room was equipped with a small

camera for subject monitoring and safety reasons. The computer which the stimuli were presented and the subjects' answers recorded, was located outside the shielded room. In the discrimination tasks, the subjects were instructed to press a button as fast as possible whenever he or she could hear a deviant tone. In the passive task, the subjects either watched a silent movie from computer screen (EEG) or read a book (MEG), and were instructed to disregard the sounds that were played in background.

The order of the three conditions was counterbalanced (randomized) across subjects. The order of the different noise types during one condition was also counterbalanced by randomization. After each noise type of about 5 minutes there was a short break. After five 5 minute blocks there was a longer break and during that the subject was disconnected from the EEG amplifier and was allowed to walk freely outside the shielded room.

The stimuli were presented with a dedicated computer (Pentium III, Windows 98) and Presentation Software (version 0.81/9.00, Neurobehavioral Systems Inc., Albany, USA). The script listings used for presentation are included in Appendix A. All of the sound files used in the experiment were in WAV format, using 44.1 kHz sampling frequency and 16-bit precision. Sounds were presented binaurally through two high quality speakers (Roland Stereo Micro Monitor MA-8), which were located symmetrically in both sides of the computer monitor (distance from subjects head 90–100 cm). Speakers were directly connected to Sound Blaster Live! card working as the sound source. During the discrimination tasks, a small fixation cross was shown on computer screen.

The MEG experiment

There were some differences between the EEG and MEG recording sessions. In MEG, the sounds were presented monaurally only to the left ear through a custom-made auditory tube, as external loudspeakers could not be brought to the shielded room. There was no computer monitor in the MEG room, as the fixation cross was only marked to the wall. The stimuli, the order of test runs etc. were otherwise identical. However, in MEG only the notch widths from the stimuli set #1 were used, i.e. no pooled set of stimulus types as in EEG. This was due to few number of experimental subjects.

3.4 EEG and MEG data analysis

EEG peak detection

The evoked response components P50, N100, and P200 were determined manually. Brain Vision Analyzer was used in EEG data display. In the marking phase, averaged responses from electrodes Fz, Cz, TP9 and TP10 were displayed simultaneously on screen. Time offset for component peak was selected subjectively on common criteria, with 2 ms resolution. If any component seemed to have multiple peaks, either the first or the global peak was selected, depending on the situation. In total, 900 time points were selected (10+10 subjects, for each subject 3 tasks with 5 stimuli types in each task, 3 evoked potential components => $20 \times 3 \times 5 \times 3 = 900$).

These hand-picked latencies were used to obtain amplitude values from all channels at that particular latency. Additionally, the standard error of the mean (SEM) and the P50-N100 peak-to-peak values were also calculated. The peak-to-peak values were thought to show the amplitude suppression effect more clearly, as the baseline for EEG data in averaged ERPs seemed to have some amount of DC shift in different conditions, even after baseline correction of -200–0 ms. However, the peak-to-peak values are not presented here.

For some test subjects, the AEP components were almost impossible to mark in conditions where the signal was strongly attenuated (i.e., smallest notch widths and plain white-noise masker). This was due to poor SNR in evoked EEG responses. Even the N100 component could not be clearly detected for some cases. These values were not excluded from calculation of average. Since the signal of interest was predicted *ad hoc* to be very weak in these conditions, the latency was marked by extrapolating from earlier and easier tasks (with larger notch width) to get even some descriptive latency and amplitude value for this condition.

3.4.1 Data quantification and statistical analysis

In most of the subsequent data analysis steps the two stimuli sets used were pooled together so that the masker window widths form a continuum. This is also reflected in the data figures. The two common stimulus types ("silent" and unfiltered white noise, "0") were simply averaged in some calculations, or in some cases where standard error calculation was involved, all the cases were included. This also means that $N=20$ for these two extremities, and $N=10$ for the stimulus types in between.

EEG data was quantified by taking the mean amplitude around the AEP peak. The time window selected for this was 8 ms, so given the sampling steps of 2 ms, two values before and two values after the absolute maximum peak value were included. These amplitudes were analyzed using a two-way repeated measures ANOVA, with *condition* (duration vs. frequency discrimination task vs. passive task) and *stimulus type* (silent, ± 500 , \dots , 0, see Figure 3.2, p. 45) as within-subjects factors. Similar analysis was done also on the N100 peak latencies.

A two-way repeated measures ANOVA was also used to analyze the reaction times. Analysis was done in Statistica (version 5.5, StatSoft Inc., Tulsa, USA) and in Excel (version 2002, Microsoft Corp, Redmond, USA). Same factors (*condition* and *stimulus type*) were used, but this time there was only two conditions, as in the passive task the subjects did not have to respond at all.

3.4.2 MEG data analysis

MEG data were modeled using equivalent current dipole (ECD) fitting. Dipole fitting (fixed dipole model) was done in Neuromag software, using a sphere as the conductor model for the head. Initially, one dipole was calculated in the silent condition (only sine tones), using a selection of 34 channels over the right hemisphere temporal areas. After that, the event-related fields (ERFs) from other conditions (stimuli set #1: ± 500 , ± 150 , ± 40 and 0) were used to fit a new dipole to the original dipole settings. ERF was baseline-

corrected for -50–0 ms before dipole fitting. Goodness-of-fit was generally >70% even for the conditions with the lowest notch widths.

3.5 Simulating the effects of attention

A relatively simple computer model was constructed to simulate the effects of attention in two ways: (1) increase in gain and (2) sharpening of tuning curves of auditory-cortex neurons. These changes were assumed to be reflected in the electric potential amplitude across the different experimental conditions. Modeling was done using Matlab (R13, MathWorks Inc., Natick, USA). The approximate shape of a single tuning curve was chosen to resemble single-parameter rounded-exponential $Roex(p)$ filter. Single-parameter $Roex(p)$ has a general form of

$$W(g) = (1 + pg)e^{-pg} \quad (3.1)$$

where p is the steepness of the filter and g the relative width of the frequency notch. Note that the rounded-exponential filter is not used here in traditional way to describe general auditory perception under notched-noise condition. In this model, the $Roex(p)$ filter was chosen to model the tuning curves of single neurons, and g is used as a factor to the frequency difference between each neurons characteristic frequency (CF) and the standard sound frequency. $Roex(p)$ was adopted for simplicity, even though there are more precise filter types for auditory system modeling, e.g., the *gammachirp* (Irino and Patterson, 1996, 2001) or the *gammatone* filter. The general shapes of these kind of simulated tuning curves are shown in Figure 3.5 for p values 5, 10, 15 and 20. As can be seen, the higher p is, the narrower the tuning curve is around the center frequency.

The frequency range around the region of interest was divided into equal spaces, each representing a characteristic frequency of a single tuning curve. Region-of-interest limits were based on the task with the largest notch width, 1000 ± 500 Hz. Frequency range 350–1850 Hz was then chosen to include the critical bands around the noise edges. This range was divided to 10 Hz steps (151 in total), and for each frequency 200 "neurons" were

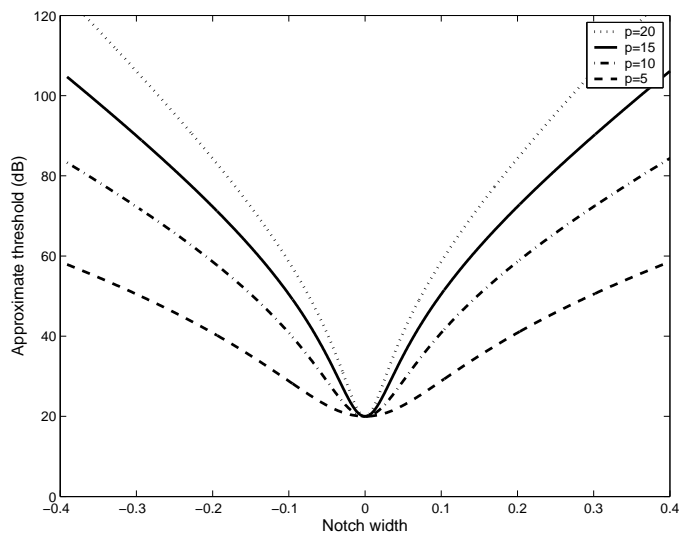


Figure 3.5: Tuning curves approximated by rounded-exponential filter shape.

simulated. The probability for each neuron to fire on the standard stimuli of 1000 Hz was inversely proportional to the shape of the $Roex(p)$ filter (see Figure 3.6), basically the closer the CF of "neuron" was to 1000 Hz the more probable the firing would be. Probability distribution was scaled to yield a total sum of 1. The probability curves highly resemble the normal curves with same mean and different variance. Additionally, if the neuron didn't fire on a certain time point, there was still $p=0.02$ chance it would fire on its own, corresponding to the spontaneous activity of neurons. This probability is not shown in the figure.

The probability distributions were additionally masked with a window function, trying to take into account the edges of the noise masker. This envelope was basically rectangular, with both edges following a raised-cosine function. The raised-cosine function width was based on the critical band width of the edge frequency (i.e. its width was $2df$, where the df is given by Equation 2.1). On the edge frequency, the value of the envelope function was thus initially $p=0.50$ before normalizing. As an example, envelope functions for stimuli set #1 (± 500 , ± 150 , ± 40 and 0) are shown in Figure 3.7. The envelope functions were not strictly symmetrical, as the frequency-dependent critical band determined the width of the rising or falling edge. To somehow model the "silent" condition, a completely rectangular window was used ($p=1.0$ for every frequency).

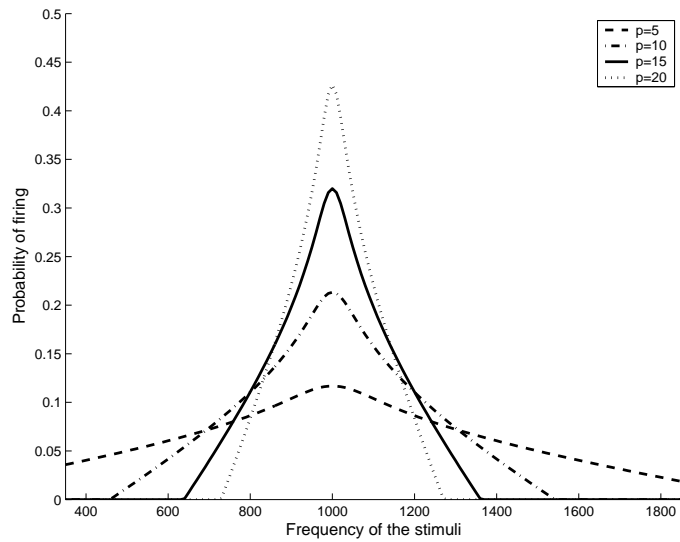


Figure 3.6: Modeling the probability of neuron firing when CF is 1000 Hz

Compression of the neural response based on the stimulus intensity was not taken into account, as the stimuli SPL stayed constant during all the actual tests.

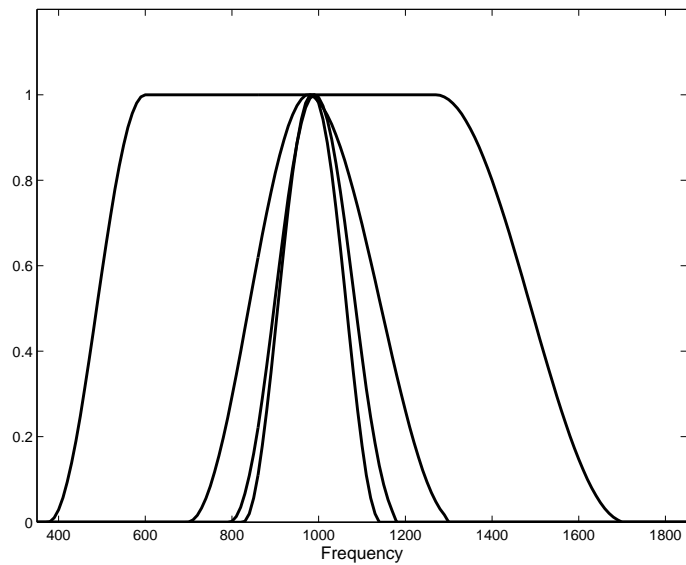


Figure 3.7: Envelope functions used for modeling stimuli set #1 (± 500 , ± 150 , ± 40 , 0).

After setting up the initial parameters, the modeling was started. Time course for model was -50–150 ms, with 1 ms steps. For each time point, the total number of activated neurons was recorded. After firing, each neuron had 5–13 ms refractory period. This relates to spike rate of about 65–200 spikes/second, which is quite reasonable value based on

neurophysiological data. The playing time of the stimuli was 0–100 ms, during which all the neurons were allowed to fire. When stimuli were not playing, only modeled spontaneous activity was taking place. Examples of time course data are shown in Figure 3.8.

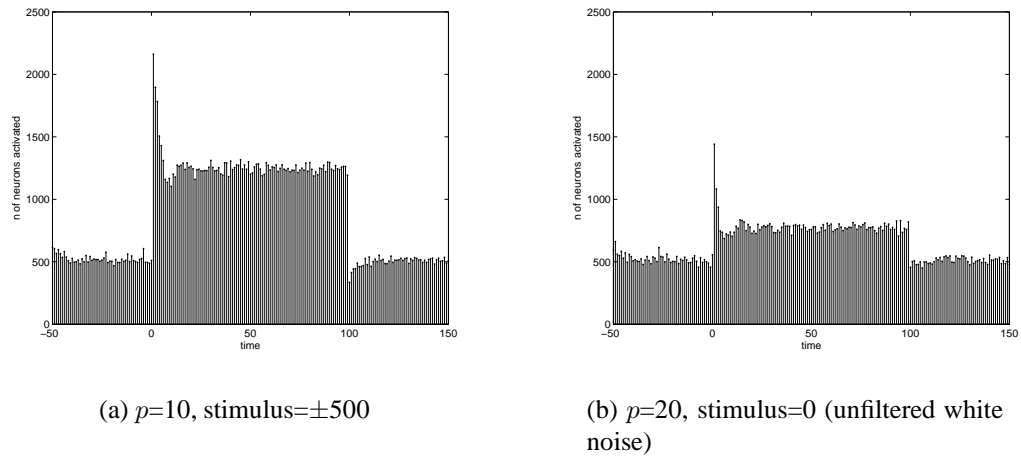


Figure 3.8: Examples of simulated activation of neurons.

The spontaneous activity level was calculated by taking the mean of neural firing rate during the time period of 120–150 ms (i.e., after the stimulus presentation). This was subtracted from the average firing rate during stimulus presentation (0–100 ms) to get some kind of estimate for the level of neural activity.

Additionally, it was tested what a gain-type change would cause to the amount of simulated neural activity with the given tuning curves. Increase in gain would cause downward-shift in the tuning curve, reducing the threshold of the sound stimuli SPL needed for neuronal activity. Similarly, a decrease in gain would shift the tuning curve upward. This effect was simulated with a constant coefficient in the probability curve of Figure 3.6. For studying this effect in approximate scale, p of $Roex(p)$ was chosen to be constant of 15. Gain values g of 0.8–1.4 were chosen for visualization, with step sizes of 0.2.

Chapter 4

Results

4.1 Pilot study results

In the pilot study the whole research paradigm was tested. In total $N=7$ subjects were measured. All were male, aged 20–23 ($\text{mean} \pm \text{stdev} = 22.2 \pm 1.3$), and 6 of them were right-handed. The experiment settings (Presentation scripts) were fine-tuned during these tests. For example ISI, the total number of averages in the ERP etc. changed from subject to subject, so the measured data for one subject were not directly comparable to the other.

Even though the setup was not identical to all the subjects, the ERPs were still averaged for $N=6$ subjects, and grand average ERPs are shown in Figures 4.1 and 4.2. The curves look different for the attended tasks and the passive task, which was the aim. No further statistical analysis was made due to the nature of the data.

The results of the behavioral task (Figure 4.3) looked good as well, as a clear reduction in the number of correct answers was evident as a function of narrowing the notch width. This reduction was roughly the same for both tasks, suggesting that the difficulty level of both tasks was similar. The response times were also increased inversely proportional to the notch width. The harder the task, the more time it took to answer and less correct answers were given.

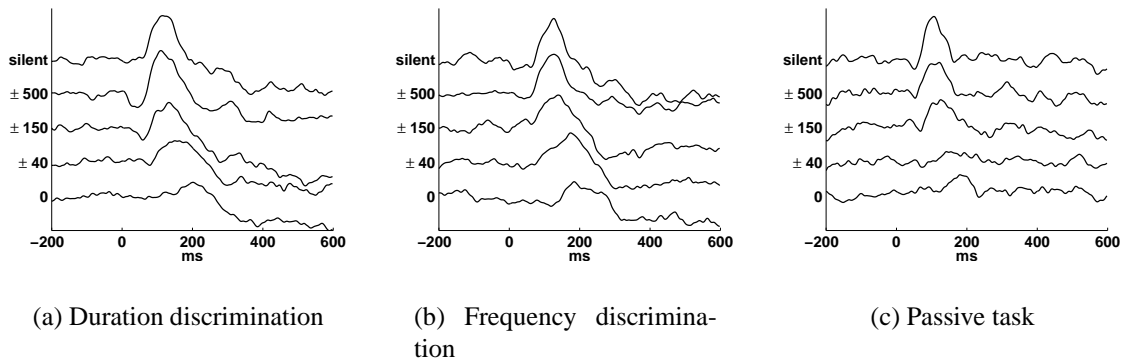


Figure 4.1: Grand average ERPs from electrode Cz in pilot subjects (N=6).

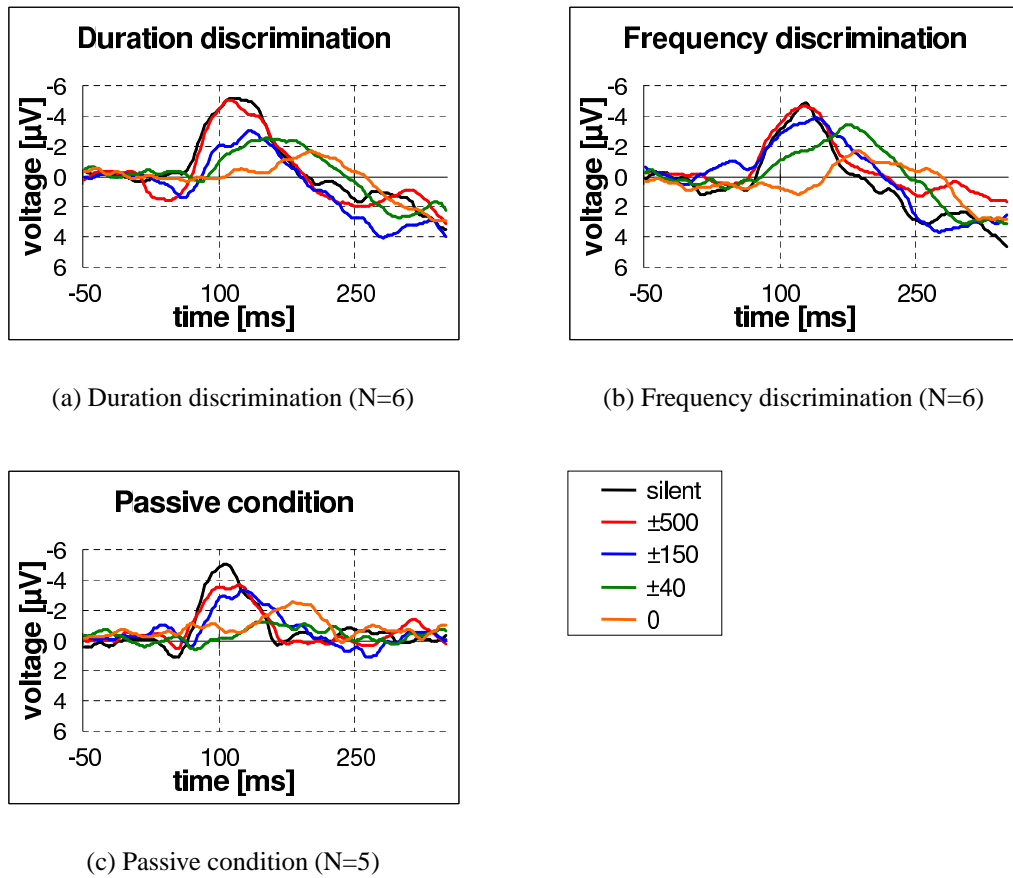


Figure 4.2: Grand average ERPs from electrode Cz in pilot subjects (alternate view).

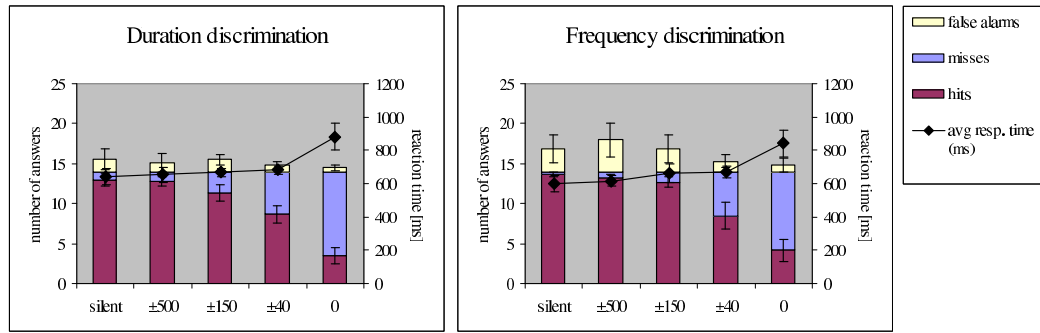


Figure 4.3: Behavioral task data from the pilot subjects (N=6). "False alarms" include answers to non-target stimuli and too long a response times (overlapping next stimulus). Standard error of the mean (SEM) of the response time is calculated from each subjects' average time, so the actual variance in response times is higher.

4.2 Results of the EEG study

4.2.1 ERP calculation

ERPs were plotted for all channels. As the N100 amplitude was most robust at electrode Cz, the resulting ERP from that channel is shown in Figure 4.4. The figure shows the gradual diminution of the ERP component amplitudes and increased peak latencies as the notch gets narrower. The averaged N100 peak values from individual subjects are shown in Figure 4.5.

Time resolution of the peak latencies was 2 ms, which was due to the 500 Hz sampling rate used in recording ($T_0 = \frac{1}{F_s}$, where T_0 is time interval and F_s the sampling rate). The EEG amplitude resolution was 0.1 μV

The latencies at which the auditory component peaks were found varied across the subjects and conditions, with a clear upward trend as the notch gets narrower. Mean latencies of the N100 peak and P200 peak are shown in Figure 4.6.

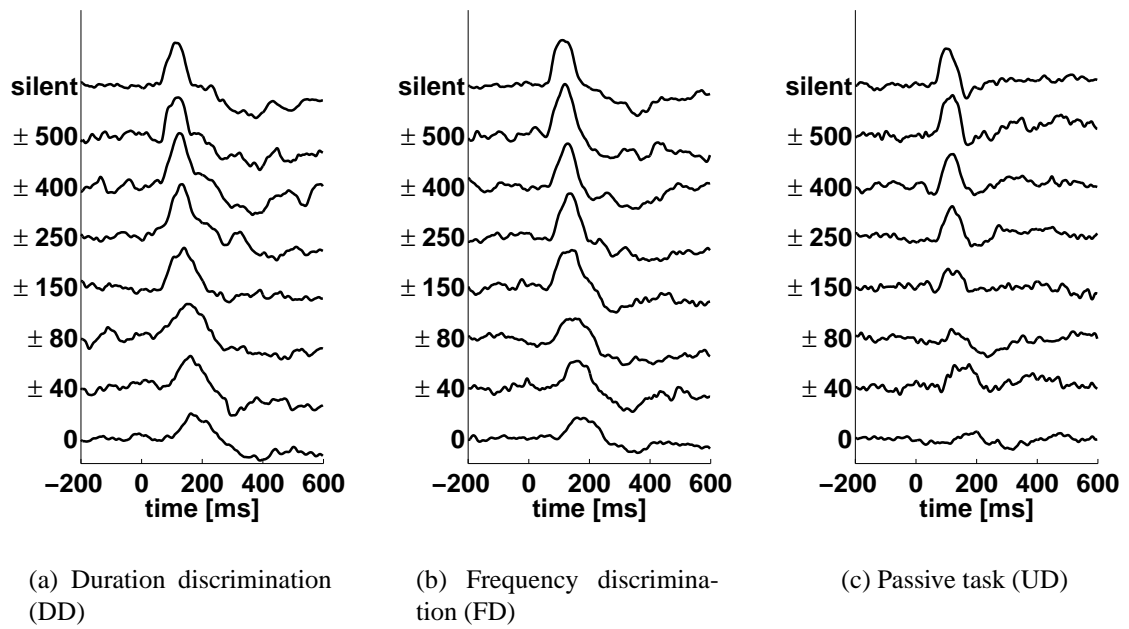


Figure 4.4: Grand average ERPs from electrode Cz (N=10).

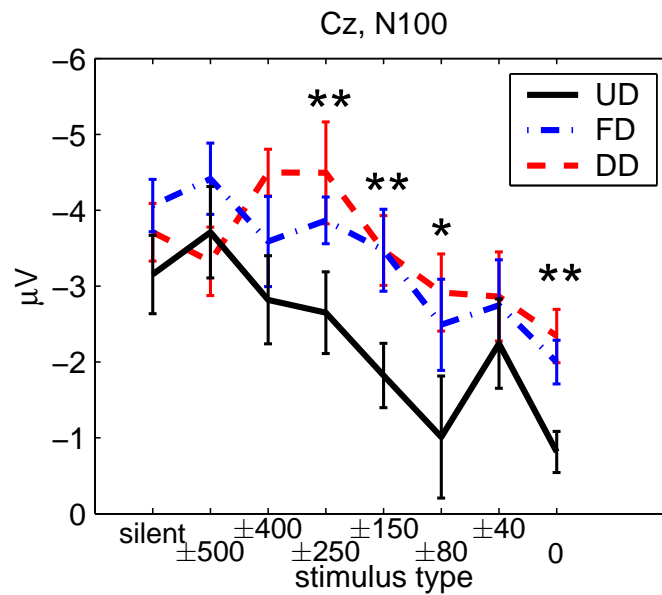


Figure 4.5: Averaged ERP peak values and SEM from electrode Cz (N=10). The conditions with statistically significant differences between the passive task (UD) and the attended tasks (DD and FD) are marked with * = $p < 0.05$ and ** = $p < 0.01$.

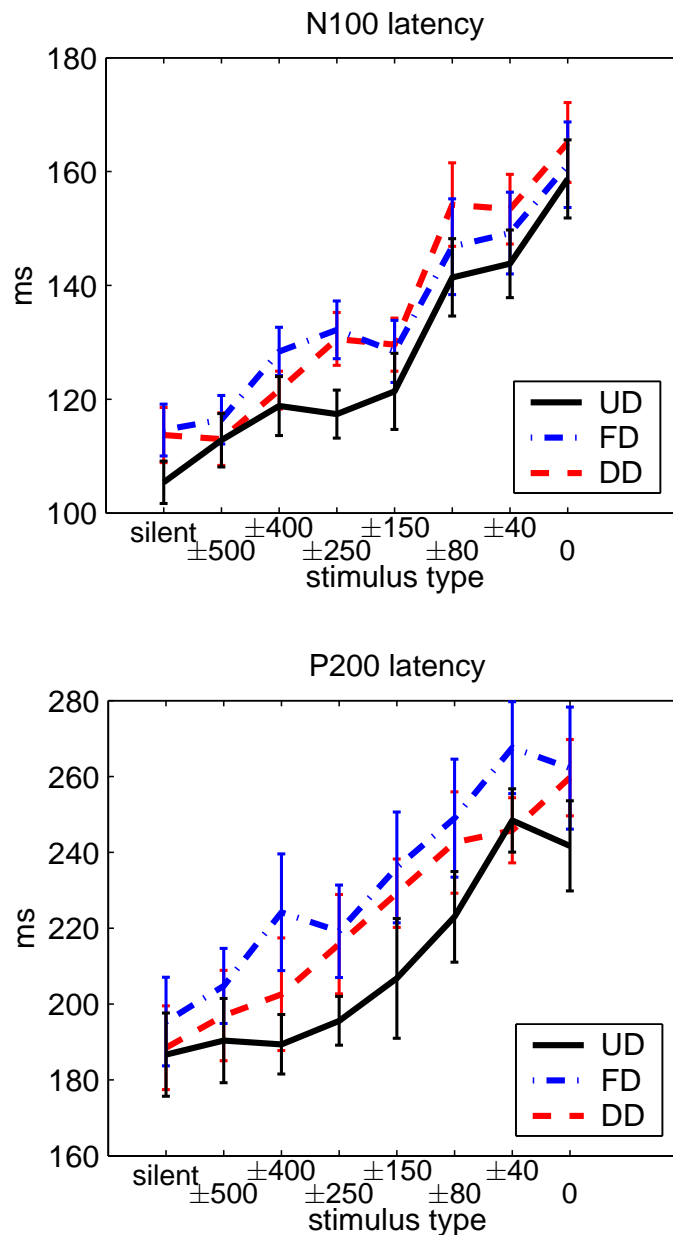


Figure 4.6: Latency of the N100 and P200 peaks (N=10).

Statistical analysis of the N100 peak amplitude and latency

ANOVA showed significant effect of both the *condition* ($F(2,18)=24.95$; $p<0.001$) and the *stimulus type* ($F(7,63)=4.17$; $p<0.001$) for the measured N100 peak amplitude at electrode Cz. However, the *condition* × *stimulus type* interaction of these factors was not significant other than in analysis done on stimuli set #1 values only ($F(8,72)=2.70$; $p<0.02$).

For the N100 peak latencies at Cz, a significant effect was found on both the *condition* ($F(2,18)=6.12$; $p<0.01$) and the *stimulus type* ($F(7,63)=26.88$; $p<0.001$), but not in their interaction.

After initial testing, an *a priori* planned comparison test (contrast analysis) was done to test the hypothesis if the two attended task differed from each other (contrast vector [1 -1 0], for DD, FD and UD, referring to the coefficients c_i used in comparison). No significant changes were found in N100 amplitude ($F(1,9)=0.35$; $p=0.57$) or in N100 latency ($F(1,9)=0.045$; $p=0.84$).

Similar contrast analysis was done to test the hypothesis if the unattended condition (UD) differed from the two attended ones (DD and FD), using contrast vector of [-1 -1 2]. Highly significant difference was found both in N100 amplitude ($F(1,9)=67.39$; $p<0.001$) and in N100 latency ($F(1,9)=11.15$; $p<0.01$). To get more detailed information, an individual condition-by-condition test was done to see in which stimulus type the change is most clear. This was done again with a contrast test, keeping [-1 -1 2] as the vector for the *condition* and by setting in turn each *stimulus type* to 1, e.g., [0 0 1 0 0 0 0 0] to test the third stimulus type in the pooled set. The results for testing N100 amplitude are shown in Table 4.1. Similar test to N100 latency didn't show significant changes in any other condition than the silent one ($F(1,9)=11.67$; $p<0.01$).

Table 4.1: F values for different stimulus types, unattended (UD) vs. attended conditions (DD and FD) * is for $p<0.05$, ** for $p<0.01$.

| Stimulus type | F(1,9) value | p-level |
|---------------|--------------|-----------|
| silent | 3.608 | 0.0900 |
| ± 500 | 0.1048 | 0.754 |
| ± 400 | 4.348 | 0.0667 |
| ± 250 | 12.85 | 0.00589** |
| ± 150 | 19.76 | 0.00161** |
| ± 80 | 10.42 | 0.0103* |
| ± 40 | 0.8846 | 0.372 |
| 0 | 19.25 | 0.00175** |

4.2.2 EEG contour maps

The contour maps of the different conditions are shown in Figure 4.7. The contour maps were plotted at N100 peak latency of electrode Cz. These are all-in-one maps, showing the total topographic EEG distribution on the scalp. Maximum view angle is 90°. As can be seen visually, there were no clear between-condition changes in the topographic distributions at least according to the group-average data. The most clear difference in the passive (UD) condition when compared to either attended task (DD or FD) was that the activation level was generally lower and thus the amplitudes shown by the contour map smaller.

4.3 Results of the MEG study

The event-related fields (ERFs) for MEG study were calculated similarly to the ERPs of the EEG study. As the stimuli were presented to the left ear, the strongest ERF amplitudes were shown in the right hemisphere. The progressive diminution of the ERFs in MEG study was very similar to EEG.

From the dipole fitting results, the dipole amplitude (moment) Q (in nAm) was chosen for inspection. Average results with SEM are shown in Figure 4.8. MEG dipole amplitudes show similar attenuation towards the narrower notch widths as the EEG ERP amplitudes. The dipole magnitudes were lowest for the unattended condition only with the three narrowest notch widths. However, the difference between the passive and the attended conditions in MEG failed to reach statistical significance. This could well be due to few number of subjects, high variance in dipole amplitudes and also in the shape of the "attenuation" in individual subjects (see Figure 4.9 and note especially the different scale on each subfigure). No dipole amplitude normalization or similar was attempted to overcome this.

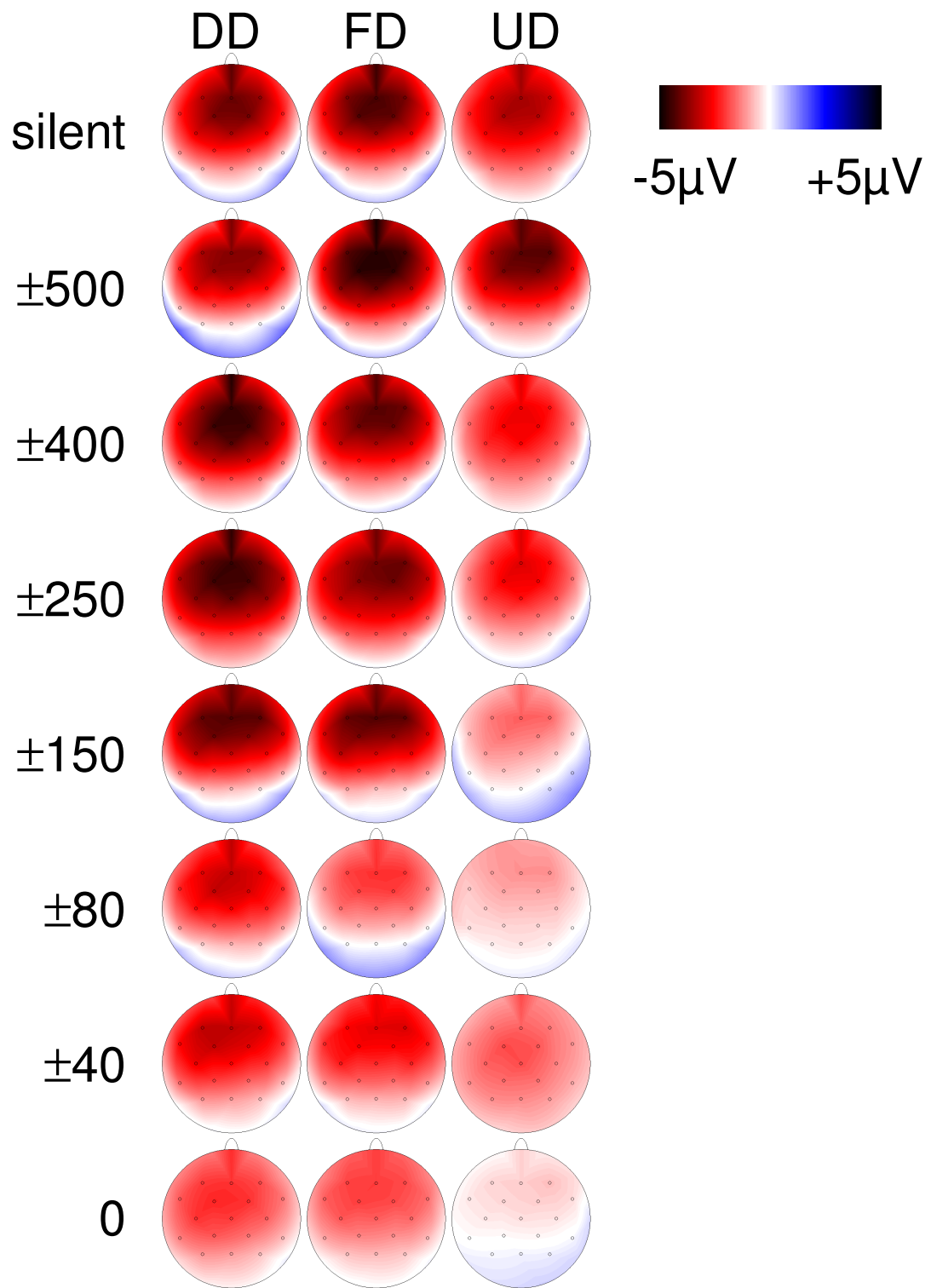


Figure 4.7: EEG contour maps of different conditions at N100 peak latency of electrode Cz. DD stands for duration discrimination task, FD for frequency discrimination and UD for unattended (passive) condition.

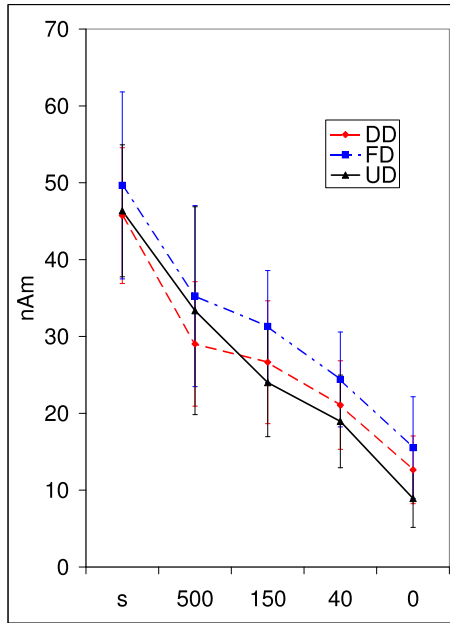


Figure 4.8: Average MEG dipole moments (N=4) with the standard error of the mean (SEM).

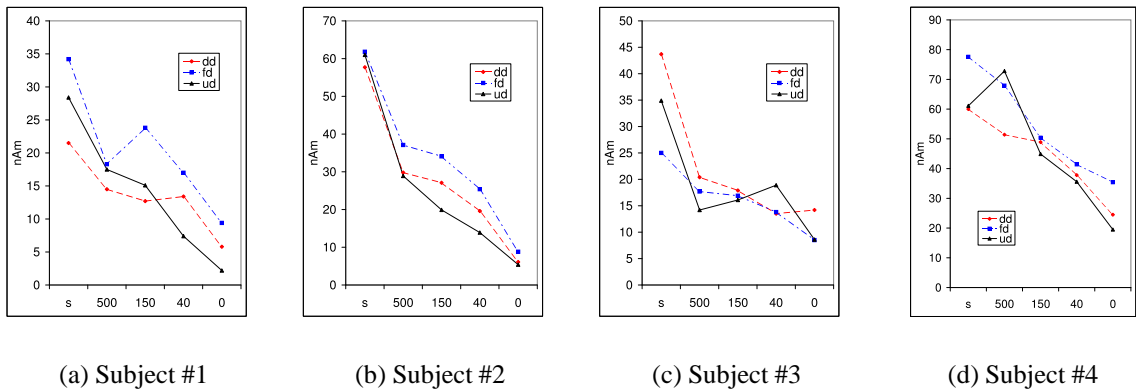


Figure 4.9: MEG dipole moments of individual subjects.

4.4 Behavioral task

Behavioral performance (hit rate) is shown in Figure 4.10. A hit was defined as a button press before the onset of the next stimuli (i.e., within a time window of 1.5–2.5 s). A late answer was regarded as a "false alarm", as was the case with answer to non-target stimuli. Results from both attended tasks (DD and FD) are highly similar, showing that the

difficulty level of both tasks was roughly equivalent. The number of target stimuli in each task was 14 (i.e. hits+misses=14 for each noise type). In the frequency discrimination task the number of false alarms was slightly higher than in the duration discrimination task.

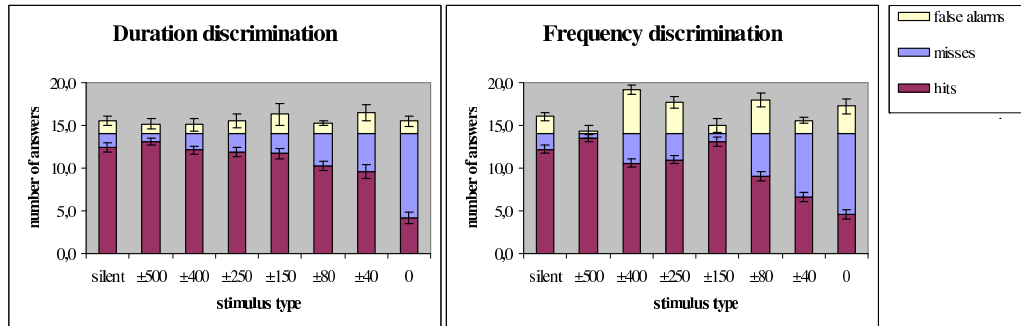


Figure 4.10: Behavioral task results (hit rate) from the EEG study. "False alarms" include answers to non-target stimuli and too long a response times (overlapping next stimulus). Standard error of the mean (SEM) of the response time is calculated from each subjects' average time, so the actual variance in response times is higher.

Reaction times are shown in Figure 4.11. The reaction times were generally longer the harder the task was and the narrower the notches were. ANOVA showed significant effect of the *stimulus type* ($F(7,49)=8.81$; $p<0.001$), but there was no significant effect of the *condition* (DD and FD) or in the interaction of those two factors.

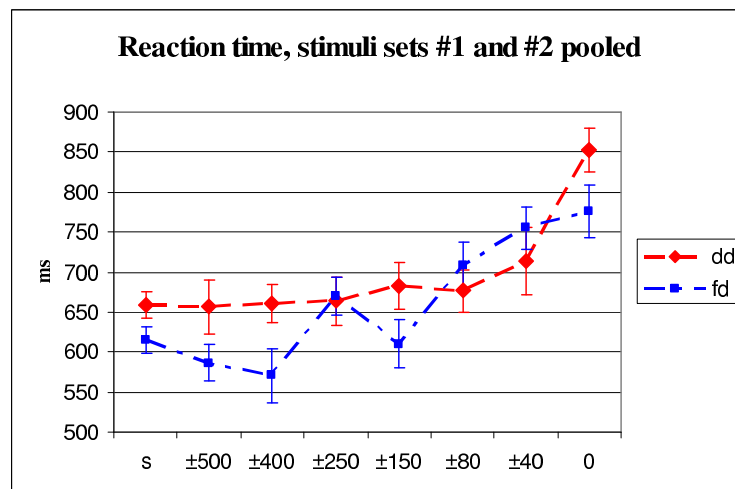


Figure 4.11: Reaction times from the EEG study. Reaction times with standard error of the mean (SEM) are plotted for both stimuli sets. DD stands for duration discrimination task, FD for frequency discrimination.

4.4.1 Hit rate vs. N100 peak amplitude

Behavioral performance followed quite closely the amplitudes of the N100 responses. Percentage of correctly detected deviant sounds (hit rate) diminished in a similar way than for example the N100 peak amplitude (see comparison in Figure 4.12). This is most evident in group average data, as there was quite much variance in individual subjects. Using this information, the neural responses could be used to predict the outcome of the behavioral task, at least to some amount. The linkage between the N100 peak amplitude and the detection of the stimulus been noted also by Parasuraman and Beatty (1980). The similarity between the neural responses and the behavioral results is clear also from other contexts, e.g. by noting the similarity between tuning curves obtained from single-neuron recordings and psychoacoustical tuning curves (see Section 2.1.2, page 10).

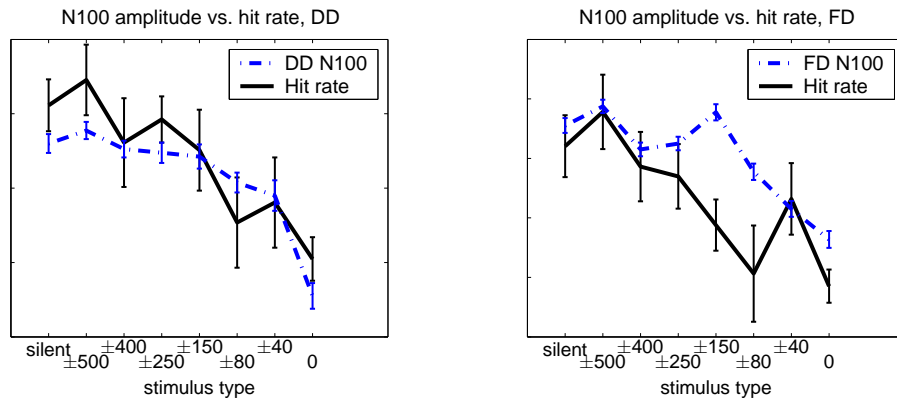


Figure 4.12: N100 peak amplitude from electrode Cz (solid black line) vs. behavioral task hit rate (dashed blue line). Plots are manually stretched to approximately same scale, but the scale units are not shown. Peak-to-peak amplitude unit was kept intact (in μV), and behavioral hit rate (in %) was scaled in all plots using coefficient of -3.5 and offset of -0.5 to approximately match the other scale.

As the effect seemed to be relevant in the group average data, the similarity between the correct answers and the neural response amplitude was tested on an individual level (see Figure 4.13). The correlation between the number of correctly detected deviants and the N100 peak amplitude was tested. Correlation coefficient r was found to be -0.3934. 200 observations comes from 2 stimuli sets, 2 attended conditions, 5 different stimulus types per condition and 10 subjects ($2*2*5*10=200$).

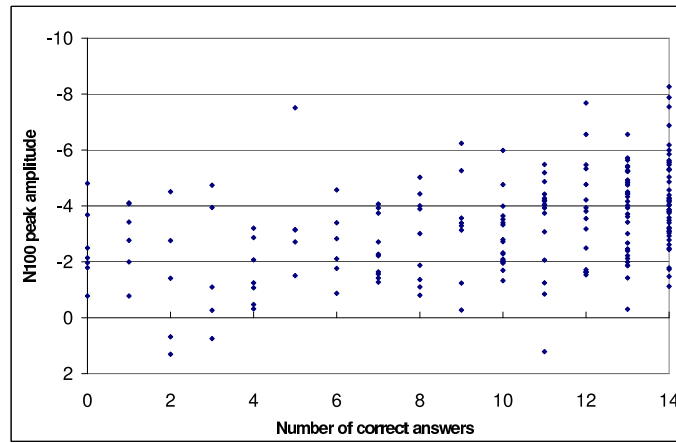


Figure 4.13: Scatterplot of hit rate and N100 peak amplitude.

4.4.2 Reaction time vs. N100 latency

Further, the N100 latency and the reaction times seemed to be linked, so their correlation was tested on an individual level as well (Figure 4.14). Correlation coefficient r was now 0.3386. This time there was only 193 observations (not 200 as before), because for some subjects, reaction time could not be calculated as there was no answer for certain stimulus types within one block.

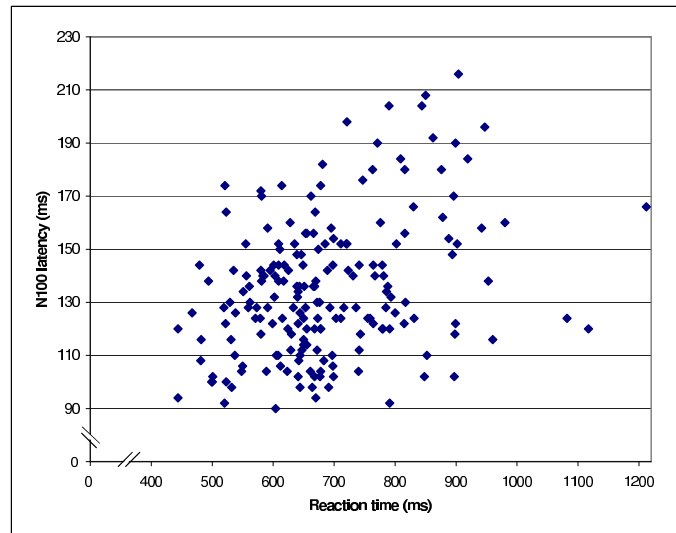


Figure 4.14: Scatterplot of N100 latency and the reaction time.

4.5 Simulation results

Simulated results of changing the tuning curve width are shown in Figure 4.15. The amplitude of simulated neural responses diminishes faster when the p value of $R_{oex}(p)$ is low and tuning curves of single neurons are wide. The mean activation level for the widest tuning curves starts from the highest value, but the activation level gradually diminishes to the lowest level with the thinnest notches. The level of activation does not decrease much when the tuning curves are sharp, as there are always some neurons responding to stimulus. In other words, with the sharpest tuning curves, the amplitudes seem to level out as a function of the notch width.

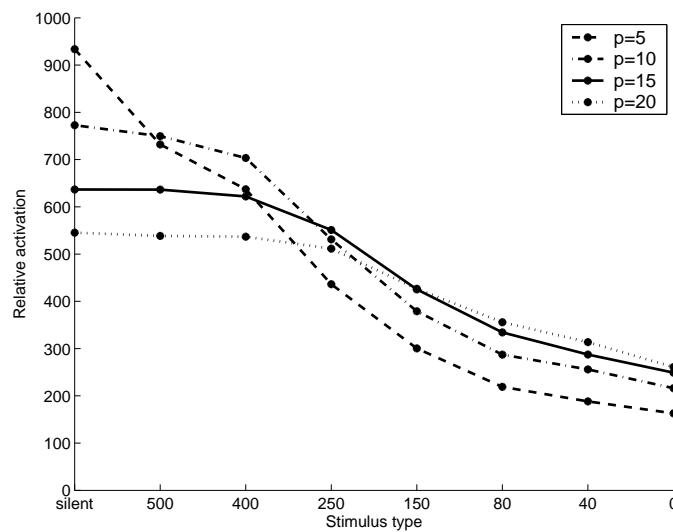


Figure 4.15: Modeling the effect of tuning curve sharpness change. The higher the p parameter value is, the sharper the tuning curve.

Results of simulated gain changes in tuning curves are shown in Figure 4.16. Based on this model, a constant gain change in tuning curves and thus increase in the probability of single neurons firing would simply increase the level of activation. The amount of increase is not constant in all conditions, rather the change in tuning curves induced by gain seems to have multiplicative effect also on the neural responses, depending on the level of the normal activation ($g=1.0$).

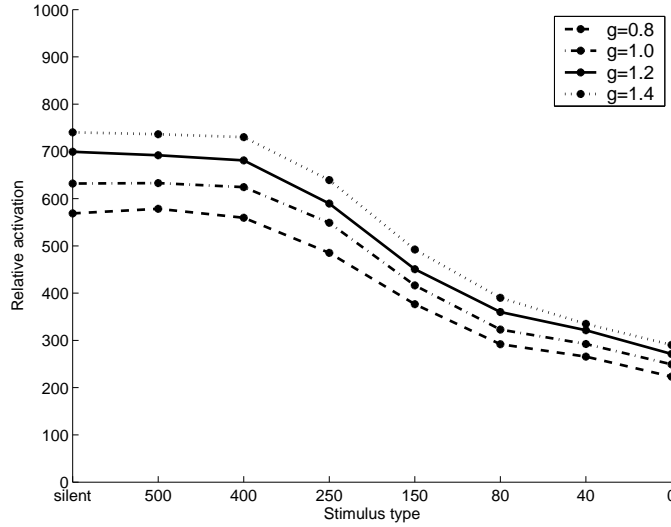


Figure 4.16: Modeling the effect of gain change.

4.5.1 Simulation results vs. the actual data

As the level of activation given by the model was in an arbitrary scale, the first step was to scale the data to the same level as the neural response amplitudes (about 2–5 μV). This was done with two parameters, coefficient α and offset β . The basic idea was to minimize error MS_e in

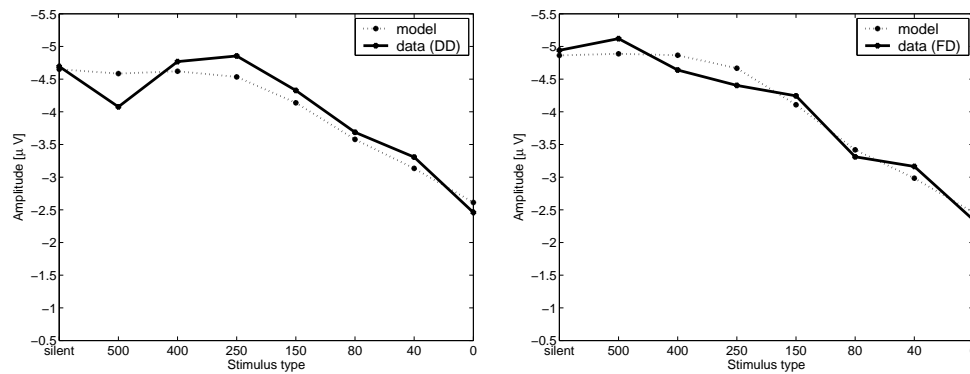
$$MS_e = \sum_{i=1}^n ((\alpha m_i + \beta) - d_{ud,i})^2 \quad (4.1)$$

where m_i are the values given by the simulation and $d_{ud,i}$ are the N100 peak amplitudes of the unattended (UD) condition at electrode Cz. Parameters for the initial fitting were $p=15$ for tuning curve sharpness and $g=1.0$ for the gain. The error e was minimized with $\alpha=-0.00678$ and $\beta=0.387$. These values were fixed for the further calculations. Additionally, the mean square error and a goodness-of-fit values were calculated. Goodness-of-fit was calculated by

$$g = 1 - \frac{\sum_{i=1}^n (b_i - \hat{b}_i)^2}{\sum_{i=1}^n b_i^2} \quad (4.2)$$

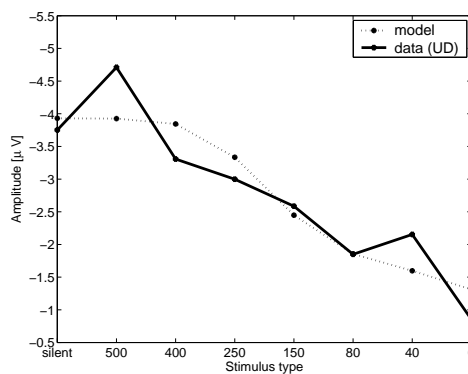
where b_i are the actual data values and \hat{b}_i are the simulation results. The same formula is typically used also in the evaluation of how well an ECD fits the actual measurement data in MEG (see Equation 61 in Hämäläinen et al., 1993). The closer the g is to 1 (or 100%), the better the model agrees with the measurement data.

Values α and β were fixed based on the best fit in UD condition, and the next step was to fit the data from the two attended conditions (DD and FD) to the simulation results by only adjusting the p and g parameters of the model. These were changed to take into account the change in tuning sharpness and change in gain, respectively. The best fit results are shown graphically in Figure 4.17. Additionally, it was tested how well only the other mechanism (sharpening vs. gain) could predict the measurement values. In these calculations, the g was 1.0 when changing only the p parameter (change in the sharpness), and p was 15 when changing only the g value (gain change). The mean square error and the goodness-of-fit values are shown in Table 4.2. As there were only few data points in this experiment, the goodness-of-fit values obtained here are close to 1.



(a) DD vs. simulation

(b) FD vs. simulation



(c) UD vs. simulation

Figure 4.17: Best fit results of the actual data vs. simulation.

Table 4.2: Results of fitting the simulation results to the real data.

| | Condition | g | p | mean square error | goodness-of-fit |
|------------------------------|-----------|-----|-----|-------------------|-----------------|
| Best fit | DD | 7.1 | 24 | 0.6974 | 99.64 % |
| | FD | 5.0 | 22 | 0.5049 | 99.81 % |
| | UD | 1.0 | 15 | 1.260 | 97.78 % |
| Sharpness change only | DD | 1.0 | 14 | 3.858 | 88.91 % |
| | FD | 1.0 | 13 | 3.543 | 90.77 % |
| | UD | 1.0 | 15 | 1.260 | 97.78 % |
| Gain change only | DD | 2.0 | 15 | 2.404 | 95.69 % |
| | FD | 2.0 | 15 | 1.687 | 97.91 % |
| | UD | 1.0 | 15 | 1.260 | 97.78 % |

Best fit values were obtained by taking into account both the change in the tuning curve sharpness and the change in gain. For this, both increase in gain (DD: $g=1.0 \Rightarrow 7.1$; FD: $g=1.0 \Rightarrow 5.0$) and sharpening of tuning (DD: $p=15 \Rightarrow 24$; FD: $p=15 \Rightarrow 22$) seemed to take place. Additionally, based on these calculations, the increase in gain explains better on its own the change in N100 amplitude in attended conditions than the sharpening of the tuning. Minimizing the mean square error when only tuning curve sharpness change takes place would suggest that the tuning curves would be actually *wider* in the attended conditions. This does not seem to be the case, if the gradual N100 amplitude suppression of actual data in attended conditions (Figure 4.5, p. 57) and the simulation results (Figure 4.15, p. 66) are compared visually. The straightforward minimization of the mean error only leads to situation, that for little different p value, the error is smaller, even though still substantial.

Chapter 5

Discussion

5.1 Neural response amplitude suppression by the masker stimuli

Suppression of the neural response amplitude with the smaller notches was expected, based on the previous results in Sams and Salmelin (1994). The closer the standard sine tone is to the noise masker edges in sound frequency, the greater the overlap between the neural populations that are activated by both sounds. In this study, the masker was bandstop filtered white noise. Decreasing the width of the bandstop filtered notch caused the masker to contain frequencies that activate the same neurons as the standard tone. This is especially true if both sounds fall within the same critical frequency band. As a result of this overlap, the neural response was smaller to the standard stimuli the narrower the notch was. Thus the fact that N100 shows this effect supports the previous reports showing that N100 is generated at least partially by the tonotopically organized auditory cortex neurons. Attentional effects have been previously shown to take place directly in the AC, e.g., by localization of the attention-sensitive neural generators (Rif et al., 1991; Woldorff et al., 1993) and according to 40-Hz transient responses (Tiitinen et al., 1993).

5.2 Attentional modulation of the neural responses

The EEG results showed most clearly the change of the neural responses in the attended conditions vs. the unattended condition. The N100 peak amplitudes from electrode Cz with some of the smallest bandstop filtered notches (± 250 Hz and below) were significantly smaller in the unattended condition than in the tasks where subject was asked to perform a discrimination based on the sine tones that were heard over the masker. Further, evaluation of MEG dipole fitting results showed a similar trend: in unattended task the gradual dipole amplitude diminution was slightly more pronounced as a function of narrowing of the noise notch widths than in the attended conditions.

Comparing the modeling results with the EEG data (Section 4.5.1, p. 67) would suggest that the effect of attention in the auditory system is more of an increase at the neural activity level (gain effect) than increase in the selectivity of the respective neurons (as measured in tuning curve sharpness). The results here are in accordance with previous studies in the auditory system showing increased neural activity during attention (e.g., Hillyard et al., 1973; Rif et al., 1991; Woldorff et al., 1993). The gain effect, as opposed to the selectivity increase, has been observed often also in the visual system (e.g., Treue and Trujillo, 1999; McAdams and Maunsell, 1999). Even though the gain effect is more pronounced in this study (seen as generally higher neural response amplitudes), the changes in N100 amplitude can not be explained by the gain effect only.

Even though there was a clear amplitude change in the attended vs. the unattended tasks using some window widths (± 250 , ± 150 , ± 80), the amplitudes seemed to converge to the same level in the lowest notch (± 40). Thus, it could be that there are limits to the attentional effect. The reason for this converging of the amplitudes in the lowest notch could even be physiological, i.e. it is simply not possible to discriminate different kinds of tones beyond some limit, when the masker and the sine tone frequencies overlap. Thus our brain won't produce any stronger neural responses after some lower threshold in frequency difference. However, as the hit rate didn't diminish to zero in the lowest notches, this was not the case at least in the attended conditions, as most of the subjects evidently heard the tone and were able to make the discrimination between the standard tone and

either the higher or the longer tone. Still, the statistical analysis showed significant difference in the unfiltered white noise ('0') condition between the unattended and the attended tasks.

A more logical explanation would be that the N100 amplitudes of using the ± 40 Hz notch window converged to the same level for some other unknown reason, but they should have been different. This way, the lower amplitudes in the unattended condition would form a more logical continuum, as the change would be evident for all notch widths of ± 250 Hz and below. This is, the ± 40 Hz is outlier due to the measurement noise. For example, by looking at the results from an electrode close by, Fz, the N100 amplitudes are generally in the same level, but the ± 40 Hz amplitude is lower than in Cz and fits better in the continuum. A follow-up experiment replicating the stimuli setup could be done to verify that the results of the ± 40 Hz stimulus type was really only due to noise.

As especially the N100 and P200 peaks seem to occur later for the attended tasks (Figure 4.6, p. 58), it could be that the neural sources reorganize in the cortex due to attention, causing asynchrony in their activation and thus different kind of summation in the scalp, which again can be seen as changes in the measured ERP peak amplitudes and latencies. Follow-up studies with e.g. MEG or fMRI (due to their better localization accuracy) could reveal with a modified test setup if this kind of reorganization should really happen. In any case, already according to this study, it seems that attention *does* change the neural responses to the auditory stimuli in some way, and this change is consistent in the evoked auditory responses measured. The maximum amplitudes of the neural responses, occurring in silent, ± 500 or in ± 400 condition, are basically at the same level for both attended and non-attended tasks. It is only with the narrower notches (± 250 Hz and smaller) that the changes take place.

The effects of attention were most prominent in the EEG experiment using the central electrodes Cz and Fz, where the amplitudes of the neural responses were also the largest. Qualitatively similar changes were found in ERPs of other electrodes as well, but the effect was much weaker. The scalp distribution of EEG potentials at N100 peak didn't show any special change during the attended conditions vs. the unattended one.

No significant difference in the neural responses was found between the two different attended tasks used, (1) duration discrimination and (2) frequency discrimination. The pre-study hypothesis was that during the frequency discrimination task, the effect would be even more evident. In this study, this kind of special selectivity increase was not found. It might be possible to show this with different attended tasks or different experimental setup, or with more thorough studies using only MEG, due to its better SNR and localization accuracy.

5.3 Behavioral task results and other notes

A notable correlation between the behavioral task results and the neural data was found, both in hit rate and in reaction times. This is interesting, especially when the time scale of the neural responses (≈ 100 - 170 ms) and behavioral tasks (≈ 500 - 1000 ms) were quite different.

It is important to note that the latencies of especially the N100 and P200 peaks seemed to be generally lower for the unattended, passive condition than for the two attended tasks. Thus, attention seems to delay the neural responses by a small amount. This could be explained by changes in the very early perception induced by attention, e.g. in accordance to Broadbent's classic early filter model (for a short review about some models of selective attention, see Cowan, 1988). In other words, it seems that attention changes some early perceptual stages which causes later peaking of N100, suggesting possibly a *top-down* feedback process. Because of the later, relative constant latency, the early auditory processing phases would seem most likely to be serial in nature, adding an extra stage to early processing of sound stimuli. On the other hand, the later peaking can also be explained by a parallel model, by stating that later peak is caused by the reordering of the neural processes that constitute the ERP component we call "N100". This is also supported by some models, which suggest quickly happening processes (less than 0.25 to 0.5 seconds) to be essentially parallel, and only the longer-lasting processes to be sequential (Cowan, 1988).

It is generally known, that the N100 peak does not consist of just a single source generator, but it has multiple neural sources that sum up together in the scalp (Jääskeläinen et al., 2004). Recording signals directly from the neurons could be used to investigate whether attention delays their maximal firing latency or just reshapes the area of cortical activation.

Notably, increased lateral inhibition in the auditory cortex might explain both the tuning effects and increased latency on its own. Lateral inhibition in the human auditory cortex has been recently suggested to have more important effect than habituation (Pantev et al., 2004). Lateral inhibition could work well in the tonotopically organized auditory cortex, where neurons responding to close-by frequencies are located close to each other. By increasing inhibition around the areas corresponding to the attended frequency, the neural response to the attended sound frequency would be more sharply tuned and robust than normally. Sharpening of the tuning due to inhibition has been evidenced in animal studies (e.g., Suga et al., 1997). Later latency of the response was noted also in monkey studies by Recanzone et al. (1993), where monkeys were trained to discriminate small frequency differences.

ERPs from the EEG experiment show that there is neural activity linked to the stimulus for much longer period of time in the attended tasks than in the passive condition. The ERPs of the unattended conditions quickly reached the baseline, whereas the ERPs of the discrimination tasks retained in the positive side longer (e.g. P200 peak was later). This suggests that some additional late processing of the stimuli takes place, probably fundamentally cognitive, but the exact effect and cause are unknown based on just this study. This probably reflects the P300 ERP component induced by attention, even though it was not specifically studied here. The P300 is known to be most prominent ERP component sensitive to cognitive processing, especially in discrimination tasks (see Herrmann and Knight, 2001). It is generally evoked by infrequent stimuli, but in this study it seems to be present also in the ERP of the frequent stimuli.

5.4 Final notes and ideas for further experiments

How is it possible for attention to increase our hearing sensitivity so that the change can be seen even in the underlying neural responses? Recruitment of completely new neural populations is one possibility, although not very likely to happen in such a short test period, at least on a large scale. For example, it took weeks for monkeys in a study by Recanzone et al. (1993) to show significant increase in the frequency discrimination performance and a clear change in the tonotopic organization. Based on these results, some kind of reshaping happening in the auditory responsive areas is still one possibility. One model to explain increased neural activity level in such a short time is so called *physiological memory* of the primary auditory cortex (Weinberger, 1998). By conditioning, auditory cortex changes were evident in guinea pigs already after few (5–10) trials. The changes were measured as frequency-specific receptive field changes, and they have been described to last for several weeks (Weinberger et al., 1993; Weinberger, 1998). In case of conditioning is studied, the motives of the subjects here could be considered. There was no direct reward or feedback after a correct answer in the attended tasks. However, as all subjects were paid, their motive was probably to please the experiment organizer and thus to perform as well as they possibly could.

Attention is likely to work in the early level of the human auditory pathway, based on the increased sensitivity it adds to many of our other senses besides hearing. This could be explained by e.g. some classic early attentional filter model (see Cowan, 1988). Early frequency filtering could happen in various ways. Direct modulation of the primary auditory cortex (PAC), also supported by this study, is one possibility. Some changes in the wiring of the PAC could be a partial cause for this selectivity increase, but the changes in the primary cortical areas are not the only option. As outer hair cells (OHCs) are one cause of our high frequency selectivity, it could be that attention is able to modulate the active feedback mechanism in our auditory system, and thus increase the effect of *cochlear amplifier* (see Section 2.1.6, p. 15), for example by increasing level of *prestin* protein (Lieberman et al., 2002; Géléoc and Holt, 2003). This hypothesis would require further studies in cellular level. Feedback mechanisms in some level of auditory system are in any case likely to "tune in" towards the attended sound frequency.

In subsequent studies on the same matter, the number of different bandstop filtered white noise types could be increased to have more fine-grained frequency resolution. By having more results, a more clear picture of the amount of effect as a function of notch width could be obtained. Alternatively, the selection of notch widths could be optimized in order to have a small set of stimuli which shows the effect clearly, and further concentrate on other kinds of changes. It could be verified if the effect occurs only in a certain frequency range, possibly close to the limits of critical band around the attended stimulus frequency. Using a shorter ISI might also reveal sharper tuning properties of the auditory system, as was one explanatory factor of results by Näätänen et al. (1988). However, based on the pilot studies here, this would require a redesign of the current test setup or the use of some other research method than the present EEG system. Then again, the use of long ISI is beneficial to induce high attentional load to the experimental subjects, as the limits of their echoic memory capacity temporally are nearly exceeded.

By using either the amplitude modulation or the slightly increased latency as the criteria, the results here could be adapted to clinical studies. The hypothesis is, that for patients with attentional dysfunctions, the attention effect shown in this study is not as clear as for the healthy control group. Proving this would, of course, require further studies with real patients. The discrimination tasks presented here require sustained attention, so only that will likely cause notable differences in the results by itself. On the other hand, as the attentional load required in the task is high, individuals with reduced vigilance or excess fatigue will show diminished effect as well.

Some further modeling could be done on how the frequency tuning curves change during attention. Also, it would be interesting to hypothesize and model on how the lateral inhibition works in the primary auditory cortex. Whether attention to certain attribute (e.g. frequency discrimination task) is able to modulate neural responses in a special way, still remains to be seen. This could be studied with some more clever research methods or different kind of tasks to the test subject.

Here, we focused on *how* the attention modulates the neural responses and did not specifically ask *where* the attentional changes took place. We only noted that the modulation

happened probably in the primary auditory cortex, as the ERP component N100, reported to be generated in the human PAC (Rif et al., 1991; Woldorff et al., 1993; Tiitinen et al., 1993), was modulated. It has been reported in both lesion and selective attention studies that there might be a center for attention in the frontal area of the brain (Wilkins et al., 1987; Rueckert and Grafman, 1996; Hopfinger et al., 2000; MacDonald et al., 2000). In future studies, the use of the functional magnetic resonance imaging (fMRI) would increase the spatial accuracy of the localization when searching for structures and networks of several regions involved in attentional top-down modulation. Additionally, the use of fMRI would allow us to extend the scope of the search to subcortical structures.

Bibliography

- Alho, K., Töttölä, K., Reinikainen, K., Sams, M., and Näätänen, R. (1987). Brain mechanism of selective listening reflected by event-related potentials. *Electroencephalography and Clinical Neurophysiology/Evoked Potentials Section*, 68:458–470.
- Allen, J. B. (2001). Nonlinear cochlear signal processing. In Jahn, A. and Santos-Sacchi, J., editors, *Physiology of the Ear, Second Edition*, chapter 19, pages 393–442. Singular Thompson, 401 West A Street, Suite 325 San Diego, CA 92101, 2nd edition.
- Ashmore, J. and Gale, J. (2000). The cochlea. *Current Biology*, 10:R325–R327.
- Barry, R. J., Johnstone, S. J., and Clarke, A. R. (2003). A review of electrophysiology in attention-deficit/hyperactivity disorder: II. Event-related potentials. *Clinical Neurophysiology*, 114:184–198.
- Belin, P., McAdams, S., Thivard, L., Smith, B., Savel, S., Zilbovicius, M., Samson, S., and Samson, Y. (2002). The neuroanatomical substrate of sound duration discrimination. *Neuropsychologia*, 40(12):1956–1964.
- Brugge, J. F. and Reale, R. A. (1985). Auditory cortex. In Peters, A. and Jones, E. G., editors, *Cerebral Cortex*, volume 4, pages 229–271. Plenum Press, New York.
- Budd, T. W., Barry, R. J., Gordon, E., Rennie, C., and Michie, P. T. (1998). Decrement of the N1 auditory event-related potential with stimulus repetition: habituation vs. refractoriness. *International Journal of Psychobiology*, 31(1):51–68.
- Buus, S., Florentine, M., and Poulsen, T. (1997). Temporal integration of loudness, loudness discrimination, and the form of the loudness function. *The Journal of the Acoustical Society of America*, 101(2):669–680.
- Carter, C. S., Mintun, M., Nichols, T., and Cohen, J. D. (1997). Anterior Cingulate Gyrus Dysfunction and Selective Attention Deficits in Schizophrenia: [15O]H₂O PET Study

- During Single-Trial Stroop Task Performance. *The American Journal of Psychiatry*, 154(12):1670–1675.
- Connor, C. E., Gallant, J. L., Preddie, D. C., and Van Essen, D. C. (1996). Responses in area V4 depend on the spatial relationship between stimulus and attention. *Journal of Neurophysiology*, 75(3):1306–1308.
- Connor, C. E., Preddie, D. C., Gallant, J. L., and Van Essen, D. C. (1997). Spatial attention effects in macaque area V4. *Journal of Neuroscience*, 17(9):3201–3214.
- Cowan, N. (1988). Evolving conceptions of memory storage, selective attention, and their mutual constraints within the human information-processing system. *Psychological Bulletin*, 104(2):163–191.
- Dubin, M. (2001). Brodmann areas. Retrieved December 9, 2004, from <http://spot.colorado.edu/~dubin/talks/brodmann/brodmann.html>.
- Galazyuk, A. V. and Feng, A. S. (1997). Encoding of sound duration by neurons in the auditory cortex of the little brown bat, *myotis lucifugus*. *Journal of Comparative Physiology A: Sensory, Neural, and Behavioral Physiology*, 180(4):301–311.
- García-Larrea, L., Lukaszewicz, A. C., and Mauguière, F. (1992). Revisiting the oddball paradigm. non-target vs neutral stimuli and the evaluation of ERP attentional effects. *Neuropsychologia*, 30(8):723–741.
- Géléoc, G. S. G. and Holt, J. R. (2003). Auditory amplification: outer hair cells *pres* the issue. *Trends in Neurosciences*, 26(3):115–117.
- Giard, M.-H., Fort, A., Mouchetant-Rostaing, Y., and Pernier, J. (2000). Neurophysiological mechanisms of auditory selective attention in humans. *Frontiers in Bioscience*, 5:D84–94.
- Giard, M. H., Lavikainen, J., Reinikainen, K., Perrin, F., Bertrand, O., Pernier, J., and Näätänen, R. (1995). Separate representation of stimulus frequency, intensity, and duration in auditory sensory memory: An event-related potential and dipole-model analysis. *Journal of Cognitive Neuroscience*, 7(2):133–143.
- Goldstein, E. B. (2002). *Sensation and Perception*. Wadsworth-Thomson Learning, 6th edition.
- Hämäläinen, M., Hari, R., Ilmoniemi, R. J., Knuutila, J., and Lounasmaa, O. V. (1993). Magnetoencephalography – theory, instrumentation, and applications to noninvasive studies of the working human brain. *Reviews of Modern Physics*, 65(2):413–497.

- Hari, R. (1999). Magnetoencephalography as a tool of clinical neurophysiology. In Niedermeyer, E. and Lopes da Silva, F., editors, *Electroencephalography: basic principles, clinical applications, and related fields*, chapter 60, pages 1107–1134. Lippincott Williams and Wilkins, 4th edition.
- Hari, R., Kaila, K., Katila, T., Tuomisto, T., and Varpula, T. (1982). Interstimulus interval dependence of the auditory vertex response and its magnetic counterpart: implications for their neural generation. *Electroencephalography and Clinical Neurophysiology*, 54(5):561–569.
- Henik, A. and Salo, R. (2004). Schizophrenia and the Stroop Effect. *Behavioral and Cognitive Neuroscience Reviews*, 3(1):42–59.
- Herrmann, C. S. and Knight, R. T. (2001). Mechanisms of human attention: event-related potentials and oscillations. *Neuroscience and Biobehavioral Reviews*, 25(6):465–476.
- Higashima, M., Nagasawa, T., Kawasaki, Y., Oka, T., Sakai, N., Tsukada, T., Komai, Y., and Koshino, Y. (2004). Event-related potentials elicited by non-target tones in an auditory oddball paradigm in schizophrenia. *International Journal of Psychophysiology*, 51:189–200.
- Hillyard, S. A., Hink, R. F., Schwent, V. L., and Picton, T. W. (1973). Electrical signs of selective attention in the human brain. *Science*, 182:177–180.
- Hopfinger, J. B., Buonocore, M. H., and Mangun, G. R. (2000). The neural mechanisms of top-down attentional control. *Nature Neuroscience*, 3(3):284–291.
- Hopfinger, J. B., Woldorff, M. G., Fletcher, E. M., and Mangun, G. R. (2001). Dissociating top-down attentional control from selective perception and action. *Neuropsychologia*, 39(12):1277–1291.
- Irino, T. and Patterson, R. D. (1996). A time-domain, level-dependant auditory filter: The gammachirp. *Journal of the Acoustical Society of America*, 101(1):412–419.
- Irino, T. and Patterson, R. D. (2001). A compressive gammachirp auditory filter for both physiological and psychophysical data. *Journal of the Acoustical Society of America*, 109(5):2008–2022.
- James, W. (1890). *The Principles of Psychology*. Holt, New York. Retrieved January 12, 2005, from <http://psychclassics.yorku.ca/James/Principles/>.
- Jääskeläinen, I. P., Ahveninen, J., Bonmassar, G., Dale, A. M., Ilmoniemi, R. J., Levänen, S., Lin, F.-H., May, P., Melcher, J., Stufflebeam, S., Tiitinen, H., and Belliveau,

- J. W. (2004). Human posterior auditory cortex gates novel sounds to consciousness. *Proceedings of the National Academy of Sciences*, 101(17):6809–6814.
- Kadia, S. C. and Wang, X. (2003). Spectral Integration in A1 of Awake Primates: Neurons With Single- and Multi-peaked Tuning Characteristics. *Journal of Neurophysiology*, 89(3):1603–1622.
- Karjalainen, M. (1999). Kommunikaatioakustiikka. Raportti 51, TKK, akustiikan ja äänenkäsittelytekniikan laboratorio.
- Kosaki, H., Hashikawa, T., He, J., and Jones, E. G. (1997). Tonotopic organization of auditory cortical fields delineated by parvalbumin immunoreactivity in macaque monkeys. *The Journal of Comparative Neurology*, 386(2):304–316.
- Koshino, Y., Nishio, M., Murata, T., Omori, M., Murata, I., Sakamoto, M., and Isaki, K. (1993). The influence of light drowsiness on the latency and amplitude of P300. *Clinical Electroencephalography*, 24(3):110–113.
- Kuikka, P., Pulliainen, V., and Hänninen, R. (2001). *Kliininen neuropsykologia*, chapter 10, pages 187–205. WSOY, 1st edition.
- Lang, H., Häkkinen, V., Larsen, T. A., Partanen, J., and Tolonen, U., editors (1994). *Sähköiset aivomme : keskushermoston neurofysiologiset tutkimukset*, chapter 2. Suomen kliinisen neurofysiologian yhdistys.
- Lange, K., Rosler, F., and Roder, B. (2003). Early processing stages are modulated when auditory stimuli are presented at an attended moment in time: An event-related potential study. *Psychophysiology*, 40(5):806–817.
- Lee, H.-J., Kim, L., Kim, Y.-K., Suh, K.-Y., Han, J., Park, M.-K., Park, K.-W., and Lee, D.-H. (2004). Auditory event-related potentials and psychological changes during sleep deprivation. *Neuropsychobiology*, 50(1):1–5.
- Levitt, H. (1971). Transformed up-down methods in psychoacoustics. *Journal of the Acoustical Society of America*, 49(2):467–477.
- Liberman, M. C., Gao, J., He, D. Z. Z., Wu, X., Jia, S., and Zuo, J. (2002). Prestin is required for electromotility of the outer hair cell and for the cochlear amplifier. *Nature*, 419:300–304.
- Ma, X. and Suga, N. (2001). Corticofugal modulation of duration-tuned neurons in the midbrain auditory nucleus in bats. *Proceedings of the National Academy of Sciences of the United States of America*, 98(24):14060–14065.

- MacDonald, A. W., Cohen, J. D., Stenger, V. A., and Carter, C. S. (2000). Dissociating the Role of the Dorsolateral Prefrontal and Anterior Cingulate Cortex in Cognitive Control. *Science*, 288(5472):1835–1838.
- Malmivuo, J. and Plonsey, R. (1995). *Bioelectromagnetism - Principles and Applications of Bioelectric and Biomagnetic Fields*. Oxford University Press. Retrieved December 9, 2004, from <http://butler.cc.tut.fi/~malmivuo/bem/bembook/>.
- McAdams, C. J. and Maunsell, J. H. R. (1999). Effects of attention on orientation-tuning functions of single neurons in macaque cortical area V4. *The Journal of Neuroscience*, 19(1):431–441.
- Moore, B. C. (1978). Psychophysical tuning curves measured in simultaneous and forward masking. *Journal of the Acoustical Society of America*, 63(2):524–532.
- Mosher, J. C., Baillet, S., and Leahy, R. M. (1999). EEG source localization and imaging using multiple signal classification approaches. *Journal of Clinical Neurophysiology*, 16(3):225–238.
- Murray, S. O. and Wojciulik, E. (2004). Attention increases neural selectivity in the human lateral occipital complex. *Nature Neuroscience*, 7(1):70–74.
- Näätänen, R., Sams, M., Alho, K., Paavilainen, P., Reinikainen, K., and Sokolov, E. N. (1988). Frequency and location specificity of the human vertex N1 wave. *Electroencephalography and clinical Neurophysiology*, 69(6):523–531.
- Niedermeyer, E. (1999). The normal EEG of the waking adult. In Niedermeyer, E. and Lopes da Silva, F., editors, *Electroencephalography: basic principles, clinical applications, and related fields*, chapter 9, pages 149–173. Lippincott Williams and Wilkins, 4th edition.
- Näätänen, R. (1982). Processing negativity: An evoked-potential reflection of selective attention. *Psychological Bulletin*, 3:605–640.
- Näätänen, R., Paavilainen, P., Tiitinen, H., Jiang, D., and Alho, K. (1993). Attention and mismatch negativity. *Psychophysiology*, 30(5):436–450.
- Oades, R. D., Dittmann-Balcar, A., Schepker, R., Eggers, C., and Zerbin, D. (1996). Auditory event-related potentials (ERPs) and mismatch negativity (MMN) in healthy children and those with attention-deficit or tourette/tic symptoms. *Biological Psychology*, 43:163–185.

- Pantev, C., Okamoto, H., Ross, B., Stoll, W., Ciurlia-Guy, E., Kakigi, R., and Kubo, T. (2004). Lateral inhibition and habituation of the human auditory cortex. *European Journal of Neuroscience*, 19(8):2337–2344.
- Parasuraman, R. and Beatty, J. (1980). Brain events underlying detection and recognition of weak sensory signals. *Science*.
- Rauschecker, J. P., Tian, B., and Hauser, M. (1995). Processing of complex sounds in the macaque nonprimary auditory cortex. *Science*, 268(5207):111–114.
- Recanzone, G., Schreiner, C., and Merzenich, M. (1993). Plasticity in the frequency representation of primary auditory cortex following discrimination training in adult owl monkeys. *The Journal of Neuroscience*, 13(1):87–103.
- Rif, J., Hari, J., Hämäläinen, M., and Sams, M. (1991). Auditory attention affects two different areas in the human supratemporal cortex. *Electroencephalography and Clinical Neurophysiology*, 79(6):464–472.
- Rueckert, L. and Grafman, J. (1996). Sustained attention deficits in patients with right frontal lesions. *Neuropsychologia*, 34(10):953–963.
- Sams, M. and Salmelin, R. (1994). Evidence of sharp frequency tuning in the human auditory cortex. *Hearing Research*, 75:67–74.
- Shipp, S. (2004). The brain circuitry of attention. *Trends in Cognitive Sciences*, 8(5):223–230.
- Solbakk, A.-K., Reinvang, I., Nielsen, C., and Sundet, K. (1999). ERP indicators of disturbed attention in mild closed head injury: A frontal lobe syndrome? *Psychophysiology*, 36(6):802–817.
- Speckmann, E.-J. and Elger, C. (1999). Introduction to the neurophysiological basis of the EEG and DC potentials. In Niedermeyer, E. and Lopes da Silva, F., editors, *Electroencephalography: basic principles, clinical applications, and related fields*, chapter 2, pages 25–27. Lippincott Williams and Wilkins, 4th edition.
- Spitzer, H., Desimone, R., and Moran, J. (1988). Increased attention enhances both behavioral and neuronal performance. *Science*, 240(4850):338–340.
- Steinmetz, P., Roy, A., Fitzgerald, P. J., Hsiao, S. S., Johnson, K. O., and Niebur, E. (2000). Attention modulates synchronized neuronal firing in primate somatosensory cortex. *Nature*, 404:188–191.

- Suga, N., Zhang, Y., and Yan, J. (1997). Sharpening of Frequency Tuning by Inhibition in the Thalamic Auditory Nucleus of the Mustached Bat. *Journal of Neurophysiology*, 77(4):2098–2114.
- Tiitinen, H., Sinkkonen, J., Reinikainen, K., Alho, K., Lavikainen, J., and Näätänen, R. (1993). Selective attention enhances the auditory 40-Hz transient response in humans. *Nature*, 364(6432):59–60.
- Tramo, M. J., Shah, G. D., and Braida, L. D. (2002). Functional role of auditory cortex in frequency processing and pitch perception. *Journal of Neurophysiology*, 87:122–139.
- Treue, S. and Trujillo, J. C. M. (1999). Feature-based attention influences motion processing gain in macaque visual cortex. *Nature*, 399(6739):575–579.
- Weinberger, N., Javid, R., and Lapan, B. (1993). Long-Term Retention of Learning-Induced Receptive-Field Plasticity in the Auditory Cortex. *Proceedings of the National Academy of Sciences of the United States of America*, 90(6):2394–2398.
- Weinberger, N. M. (1998). Physiological memory in primary auditory cortex: Characteristics and mechanisms. *Neurobiology of Learning and Memory*, 70:226–251.
- Wilkins, A. J., Shallice, T., and McCarthy, R. (1987). Frontal lesions and sustained attention. *Neuropsychologia*, 25(2):359–365.
- Woldorff, M. G., Gallen, C. C., Hampson, S. A., Hillyard, S. A., Pantev, C., Sobel, D., and Bloom, F. E. (1993). Modulation of Early Sensory Processing in Human Auditory Cortex During Auditory Selective Attention. *Proceedings of the National Academy of Sciences of the United States of America*, 90(18):8722–8726.
- Zwicker, E. and Terhardt, E. (1980). Analytical expressions for critical-band rate and critical bandwidth as a function of frequency. *Journal of the Acoustical Society of America*, 68(5):1523–1525.

Appendix A

Presentation scripts used in study

A.1 Example main presentation script for one stimulus type (d_1.sce)

```
scenario = "Effect of attention on neural tuning";
# in this phase 1 answer buttons
active_buttons=1;
button_codes=128;
target_button_codes=128;
write_codes=true; # write all codes to parallel port (for EEG acquisition)
pulse_width=100; # seems to be ok
response_matching = simple_matching; # don't stop trial on answer, there is one "correct" answer
default_monitor_sounds = false; # by default don't stop sounds
pcl_file = "read_volume.pcl"; # read volume info from file (att_tone.txt)
$noise_file="c:\\jaakko_noise\\noise_500_600s.wav";
$port_code_adder=60;
# FOR EEG:
$port_code_1='$port_code_adder+2';
$port_code_2='$port_code_adder+3';
$port_code_3='$port_code_adder+4';
$port_code_4='$port_code_adder+1';
# FOR MEG:
#$port_code_1=0;
#$port_code_2=0;
#$port_code_3=0;
#$port_code_4=?; # 1,2,4,8,16
$target_type_1=0;
$target_type_2=1;
$target_type_3=1;
$target_type_4=0;
# target_type pattern, frequency discrimination (fd) duration discrimination (dd)
# fd: 1 dd: 0 (1020 Hz, 100ms)
# 1 1 (1020 Hz, 150ms)
# 0 1 (1000 Hz, 150ms)
# 0 0 (1000 Hz, 100ms) STANDARD
# port_code_adder as follows:
#
# 40Hz noise gap = 0
# 80Hz noise gap = 10
# 100Hz noise gap = 20
# 150Hz noise gap = 30
# 250Hz noise gap = 40
# 400Hz noise gap = 50
# 500Hz noise gap = 60
# 0 Hz (whitenoise) = 70
# silence (no masker) = 80
#
# REAL volume read from files att_tone.txt and att_noise.txt
```

```

$att_noise=0.2; # attenuate 30dB by default
$att_tone=0.5; # attenuate 50dB by default
begin;
sound { wavfile { filename = $noise_file; };
attenuation = $att_noise;} whitenoise_300s;
#sound { wavfile { filename = "tone_980hz_200ms.wav"; };
# attenuation = $att_tone;} tone_980hz_200ms;
#sound { wavfile { filename = "tone_1000hz_1000ms.wav"; };
# attenuation = $att_tone;} tone_1000hz_1000ms;
sound { wavfile { filename = "tones\\tone_1000hz_100ms.wav"; };
attenuation = $att_tone;} tone_1000hz_100ms;
sound { wavfile { filename = "tones\\tone_1000hz_150ms.wav"; };
attenuation = $att_tone;} tone_1000hz_150ms;
sound { wavfile { filename = "tones\\tone_1020hz_100ms.wav"; };
attenuation = $att_tone;} tone_1020hz_100ms;
sound { wavfile { filename = "tones\\tone_1020hz_150ms.wav"; };
attenuation = $att_tone;} tone_1020hz_150ms;
picture { } default;
picture { bitmap { filename = "fixation3.bmp"; }; x=0; y=0;} fixation;
# start up the background noise (300sec)
# by default it will play till end, and
# the scenario will end
trial {
monitor_sounds = false;
trial_duration = stimuli_length;
trial_type = fixed;
sound whitenoise_300s;
code = $noise_file;
time = 0;
};
trial {
monitor_sounds = false;
trial_duration = 1000;
trial_type = fixed;
picture fixation;
};
# template has total of 140 or 160 trials, for where
# 10% (2*7=14 or 2*8=16 pcs) are different than standard stimuli (i.e. targets)
# 5% (7 or 8 pcs) are same as standard, but differ in one attribute which is not under attention
# 85% (119 or 136 pcs) are standard stimuli (1000 Hz, 100 ms)
TEMPLATE "noise_stim.sce";
# "empty" trial to stop the background noise and
# end the scenario
trial {
monitor_sounds = true;
trial_type = fixed;
trial_duration = 1;
};

```

A.2 Supplementary file for main script (noise_stim.sce)

```

# play the standard tone 5 times, disregard the results
# (no port code sent)
TEMPLATE "tones1b.tem" randomize {
sound_type ecode t_dura;
tone_1000hz_100ms "std_tone_disregard" '1500+$random_value*1000';
tone_1000hz_100ms "std_tone_disregard" '1500+$random_value*1000';
tone_1000hz_100ms "std_tone_disregard" '1500+$random_value*1000';
tone_1000hz_100ms "std_tone_disregard" '1500+$random_value*1000';
tone_1000hz_100ms "std_tone_disregard" '1500+$random_value*1000';
};
# template has total of 140 trials, for where
# 10% (2*7=14 pcs) are different than standard stimuli (i.e. targets)
# 5% (7 pcs) are same as standard, but differ in one attribute which is not under attention
# 85% (119 pcs) are standard stimuli (1000 Hz, 100 ms)
TEMPLATE "tones1.tem" randomize {
sound_type ecode t_dura portcode is_target;
# 7 pcs of 1020hz, 100ms
tone_1020hz_100ms "1020_100" '1500+$random_value*1000' '$port_code_1' '$target_type_1';
tone_1020hz_100ms "1020_100" '1500+$random_value*1000' '$port_code_1' '$target_type_1';
tone_1020hz_100ms "1020_100" '1500+$random_value*1000' '$port_code_1' '$target_type_1';
tone_1020hz_100ms "1020_100" '1500+$random_value*1000' '$port_code_1' '$target_type_1';
tone_1020hz_100ms "1020_100" '1500+$random_value*1000' '$port_code_1' '$target_type_1';
tone_1020hz_100ms "1020_100" '1500+$random_value*1000' '$port_code_1' '$target_type_1';
tone_1020hz_100ms "1020_100" '1500+$random_value*1000' '$port_code_1' '$target_type_1';
# 7 pcs of 1020hz, 150ms

```

```

tone_1020hz_150ms "1020_150" '1500+$random_value*1000' '$port_code_2' '$target_type_2';
tone_1020hz_150ms "1020_150" '1500+$random_value*1000' '$port_code_2' '$target_type_2';
tone_1020hz_150ms "1020_150" '1500+$random_value*1000' '$port_code_2' '$target_type_2';
tone_1020hz_150ms "1020_150" '1500+$random_value*1000' '$port_code_2' '$target_type_2';
tone_1020hz_150ms "1020_150" '1500+$random_value*1000' '$port_code_2' '$target_type_2';
tone_1020hz_150ms "1020_150" '1500+$random_value*1000' '$port_code_2' '$target_type_2';
# 7 pcs of 1000hz, 150ms
tone_1000hz_150ms "1000_150" '1500+$random_value*1000' '$port_code_3' '$target_type_3';
tone_1000hz_150ms "1000_150" '1500+$random_value*1000' '$port_code_3' '$target_type_3';
tone_1000hz_150ms "1000_150" '1500+$random_value*1000' '$port_code_3' '$target_type_3';
tone_1000hz_150ms "1000_150" '1500+$random_value*1000' '$port_code_3' '$target_type_3';
tone_1000hz_150ms "1000_150" '1500+$random_value*1000' '$port_code_3' '$target_type_3';
tone_1000hz_150ms "1000_150" '1500+$random_value*1000' '$port_code_3' '$target_type_3';
tone_1000hz_150ms "1000_150" '1500+$random_value*1000' '$port_code_3' '$target_type_3';
# 119 pcs of 1000hz, 100ms
tone_1000hz_100ms "1000_100" '1500+$random_value*1000' '$port_code_4' '$target_type_4';
tone_1000hz_100ms "1000_100" '1500+$random_value*1000' '$port_code_4' '$target_type_4';
tone_1000hz_100ms "1000_100" '1500+$random_value*1000' '$port_code_4' '$target_type_4';
tone_1000hz_100ms "1000_100" '1500+$random_value*1000' '$port_code_4' '$target_type_4';
tone_1000hz_100ms "1000_100" '1500+$random_value*1000' '$port_code_4' '$target_type_4';
tone_1000hz_100ms "1000_100" '1500+$random_value*1000' '$port_code_4' '$target_type_4';
[...];
tone_1000hz_100ms "1000_100" '1500+$random_value*1000' '$port_code_4' '$target_type_4';
tone_1000hz_100ms "1000_100" '1500+$random_value*1000' '$port_code_4' '$target_type_4';
tone_1000hz_100ms "1000_100" '1500+$random_value*1000' '$port_code_4' '$target_type_4';
};

```

A.3 Supplementary file for main script (read_volume.pcl)

```

# reads volume info from file
double att_tone;
input_file in = new input_file;
in.open( "att_tone.txt" );
att_tone=in.get_double();
#tone_1000hz_100ms.set_attenuation(att_tone);
tone_1000hz_100ms.set_attenuation(att_tone);
tone_1000hz_150ms.set_attenuation(att_tone);
tone_1020hz_100ms.set_attenuation(att_tone);
tone_1020hz_150ms.set_attenuation(att_tone);

double att_noise;
input_file in2 = new input_file;
in2.open( "att_noise.txt" );
att_noise=in2.get_double();
whitenoise_300s.set_attenuation(att_noise);

double pan_global;
input_file in3 = new input_file;
in3.open( "set_pan.txt" );
pan_global=in3.get_double();
# set pan to left speaker only
whitenoise_300s.set_pan(pan_global);
tone_1000hz_100ms.set_pan(pan_global);
tone_1000hz_150ms.set_pan(pan_global);
tone_1020hz_100ms.set_pan(pan_global);
tone_1020hz_150ms.set_pan(pan_global);

if (in.last_succeeded() && in2.last_succeeded() && in3.last_succeeded()) then
    term.print("Reading att_tone.txt ok\nUsing value att_tone="+string(att_tone)+"\n");
    term.print("Reading att_noise.txt ok\nUsing value att_noise="+string(att_noise)+"\n");
    term.print("Reading set_pan.txt ok\nUsing value pan_global="+string(pan_global)+"\n");
    # run rest of trials if volume reading OK
    loop
        int i = 1
    until
        i > trials.count()
    begin
        trials[i].present();
        i = i + 1
    end
elseif (in.last_succeeded() != true) then
    term.print( "Reading volume from att_tone.txt failed!" );
elseif (in2.last_succeeded() != true) then
    term.print( "Reading volume from att_noise_start.txt failed!" );
else
    term.print( "Reading volume from set_pan.txt failed!" );
end;
in.close();
in2.close();
in3.close();

```

A.4 Volume adjust part, main script (adjust_volume.sce)

```
scenario = "Sound adjust";
pcl_file = "adjust_volume.pcl";
# this script adjusts the sound volume
# of tones, with noise in the background

active_buttons=1;
button_codes=128;
# by default don't stop sounds
default_monitor_sounds = false;

begin;

# attenuation values are REALLY read from files
# att_tone.txt and att_noise_start.txt
# in PCL file - these are just to set
# the entry level attenuation
$att_noise=0.69;
$att_tone=0.69;

sound { wavefile { filename = "c:\\jaakko_noise\\noise_600s.wav"; };
attenuation = $att_noise;} whitenoise_300s;
sound { wavefile { filename = "tones\\tone_1000hz_100ms.wav"; };
attenuation = $att_tone;} tone_1000hz_std;
picture { } default;

trial {
  monitor_sounds = false;
  trial_duration = 1000; # wait 1sec before playing beep
  trial_type = fixed;

  sound whitenoise_300s;
  time = 0;
  code="noise";
} noise;

trial {
  monitor_sounds = false;
  # let's just take 900ms so subject has 700ms to answer
  trial_duration = 900;
  trial_type=first_response;

  picture {
    text { caption = "Change volume with keypad (num lock turned on)\n
'4' - 'down' group, decrease SNR, decrease noise attenuation by 2dB (att_noise -= 0.02)
'6' - 'up' group, increase SNR, increase noise attenuation by 2dB (att_noise += 0.02)
'5' - 'down' group, decrease SNR, decrease noise attenuation by 1dB (att_noise -= 0.01)
'8' - 'up' group, increase SNR, increase noise attenuation by 1dB (att_noise += 0.01)
'0' - end volume adjust"; font_size = 8;} text_instructions;
    x=0; y=-200;
    text { caption = "Ask subject to press button whenever beep is heard\n\n\n\n\n\n\n";
font_size = 18; } text1;
    x = 0; y = 150;
    text { caption = "Last 5 answers after volume change:\n\n"; font_size = 18; } text2;
    x = 0; y = -20;
    text { caption = " "; font_size = 30; } text3;
    x = 0; y = -50;
  } pic1;
  time=0;

  #$att_tone=whitenoise_300s.attenuation;
  sound tone_1000hz_std;
  time=0;
  target_button = 1;
  code="beep";
  duration=200;
  /*picture {
    text { caption = "[beep]"; font_size = 10; } text2;
    x = 0; y = 80;
  } pic2;
  time=1;
  duration=200;*/

} trial1;

# "empty" trial to stop the background noise and
# end the scenario
trial {
  monitor_sounds=true;
  trial_type = fixed;
  trial_duration = 1;
  nothing { } ;
  code="stop_noise";
} stop_noise;

/*
trial {
  trial_duration = 5000;

  picture {
    text { caption = "attenuation $att_tone"; font_size = 24; };
    x = 0; y = 0;
  };
  code = "att_tone=$att_tone";
};
*/
```

A.5 Supplementary file for volume adjust script

(adjust_volume.pcl)

```
# reads volume info from file
double att_tone;
input_file in = new input_file;
in.open( "att_tone.txt" );
att_tone=in.get_double();
tone_1000hz_std.set_attenuation(att_tone);

double att_noise;
input_file in2 = new input_file;
in2.open( "att_noise_start.txt" );
att_noise=in2.get_double();
whitenoise_300s.set_attenuation(att_noise);

double pan_global;
input_file in3 = new input_file;
in3.open( "set_pan.txt" );
pan_global=in3.get_double();
# set pan to left speaker only
whitenoise_300s.set_pan(pan_global);
tone_1000hz_std.set_pan(pan_global);

if ( in.last_succeeded() && in2.last_succeeded() && in3.last_succeeded() ) then
  term.print( "Reading att_tone.txt ok\nUsing att_tone="+string(att_tone)+"\n" );
  term.print( "Reading att_noise_start.txt ok\nUsing att_noise="+string(att_noise)+"\n" );
  term.print( "Reading set_pan.txt ok\nUsing pan_global="+string(pan_global)+"\n" );
  # run rest of trials if volume reading OK
  loop
    int i = 1
  until
    i > trials.count()
  begin
    trials[i].present();
    i = i + 1
  end
elseif ( in.last_succeeded() != true ) then
  term.print( "Reading volume from att_tone.txt failed!" );
elseif ( in2.last_succeeded() != true ) then
  term.print( "Reading volume from att_noise_start.txt failed!" );
else
  term.print( "Reading volume from set_pan.txt failed!" );
end;
in.close();
in2.close();
in3.close();

string input="";
double att_change=0.0;
#double att_noise=0.45; # attenuate 20dB by default
#double att_tone=0.74; # attenuate 30dB by default
int num4s;
int num6s;
int num5s;
int num8s;
int num0s;

int last_n_hits;
int last_n_incorrects;
int last_n_false_alarms;
int last_n_misses;
int last_answer_type;
string last_answers=" ";

sub
  int number_of_chars(string input_string, string search_string)
# subroutine to return number of occurrences
# inside a string
#
# notice: search_string should be only
# one characters in length..
#
begin
  int no_chars=0;
  loop
    int startpos=1;
    string new_string=input_string;
```

```

until
    startpos==0
begin
    startpos=new_string.find(search_string);
    if startpos>0 then
        no_chars=no_chars+1;
        if startpos==new_string.count() then
            new_string="";
            startpos=0;
        else
            new_string=new_string.substring(startpos+1,new_string.count()-startpos);
        end
    end
end;
return no_chars
end;

#att_tone=workspace.get_double_variable("att_tone");
whitenoise_300s.present();
triall.present();
loop
    int i = 0;
    last_n_hits=0;
    last_n_incorrects=0;
    last_n_false_alarms=0;
    last_n_misses=0;
    last_answer_type=-1;
until
    i == 1
begin
    system_keyboard.set_max_length(10); # take max 10 keyboard presses
    system_keyboard.set_time_out( random(2000,8000) ); # wait 2-8 secs for input
    input = system_keyboard.get_input();
    #triall.set_duration(random(0,4000));
    # adjust volume using following buttons
    # (preferably on keypad in right side of keyboard,
    # numlock state doesn't seem to matter)
    #
    #
    #      8
    # 4      5      6
    #
    # 4-decrease tone volume by 2dB
    # 6-increase tone volume by 2dB
    # 5-decrease tone volume by 1dB
    # 8-increase tone volume by 1dB
    #
    # 0-end volume adjust
    #
    /*
    num4s=input.find("4");
    num6s=input.find("6");
    num5s=input.find("5");
    num8s=input.find("8");
    numqs=input.find("q");
    */

    num4s=number_of_chars(input,"4");
    num6s=number_of_chars(input,"6");
    num5s=number_of_chars(input,"5");
    num8s=number_of_chars(input,"8");
    num0s=number_of_chars(input,"0");

att_change=0.0;
att_change=-double(num4s)*0.02+double(num6s)*0.02
            -double(num5s)*0.01+double(num8s)*0.01;
    if num0s>0 then #end volume adjust
        i=1;
        stop_noise.present();
end;
att_noise=att_noise+att_change;
if att_noise>1.0 then att_noise=1.0 end;
if att_noise<0.0 then att_noise=0.0 end;
whitenoise_300s.set_attenuation(att_noise);
# line below commented out because it caused
# tone to be presented twice..
# (possibly because of triall.present()
#tone_1000hz_200ms.present();

string att_text=string(att_noise);
#text1.set_caption(input);
string rval = "total_response_count: " +
    string( response_manager.total_response_count() ) +
    "\ntotal_response_count(1): " +
    string( response_manager.total_response_count( 1 ) ) +
    "\ntotal_hits: " +
    string( response_manager.total_hits() ) +
    "\ntotal_incorrects: " +
    string( response_manager.total_incorrects() ) +
    "\ntotal_false_alarms: " +
    string( response_manager.total_false_alarms() ) +
    "\ntotal_misses: " +
    string( response_manager.total_misses() );

```

```

text1.set_caption( "Ask subject to press button whenever beep is heard\n
  att_noise="+att_text+"\n"+rval);
text1.redraw();
if response_manager.total_incorrects() != last_n_incorrects then
  last_answer_type=0;
  last_n_incorrects=response_manager.total_incorrects();
elseif response_manager.total_false_alarms() != last_n_false_alarms then
  last_answer_type=0;
  last_n_false_alarms=response_manager.total_false_alarms();
elseif response_manager.total_misses() != last_n_misses then
  last_answer_type=0;
  last_n_misses=response_manager.total_misses();
elseif response_manager.total_hits() != last_n_hits then
  last_answer_type=1;
  last_n_hits=response_manager.total_hits();
else
  last_answer_type=-1;
end;
if last_answer_type==0 then
# last answer = -
# -if there was no answer (miss), even one false
# alarm or answer was incorrect
  last_answers=last_answers.substring(2,4)+"-";
elseif last_answer_type==1 then
# last answer = +
# -only if last answer was correct and answer
# was only one (i.e. no false alarms in same run)
  last_answers=last_answers.substring(2,4)+"+";
end;
if att_change != 0.0 then
  last_answers=" ";
end;
text3.set_caption( last_answers );
text3.redraw();
#pic1.present();
if att_change != 0.0 then
  stop_noise.present();
  if i==0 then noise.present() end;
end;
if i==0 then
  trial1.present();
end;
end;
# write att_tone variable to special file,
# overwriting the old one
output_file out = new output_file;
#out.open( "att_tone.txt" );
#out.print(att_tone);
#out.close();
#term.print("Writing volume to att_tone.txt\nUsing value att_tone="+string(att_tone));
out.open( "att_noise.txt" );
out.print(att_noise);
out.close();
term.print("Writing volume to att_noise.txt\nUsing value att_noise="+string(att_noise));
# workspace.set_variable("att_tone",att_tone);

```